APR1400-F-M-TR-12001-NP
Revision 0

PLUS7 Fuel Design for the APR1400

Non-Proprietary

November 2012

KEPCO KHNP

PLUS7 Fuel Design for the APR1400

November 2012

ABSTRACT

Eight Westinghouse type PWRs, eleven Combustion Engineering type OPR1000s, and four CANDU type PHWRs are currently operating in the Republic of Korea. Additionally, one OPR1000s will start operation sequentially by 2013 and four APR1400s are under construction and four more APR1400s will be constructed.

KEPCO NF had jointly developed PLUS7 fuel from 1999 to 2002 with Westinghouse to improve the fuel performance relative to Guardian fuel. Four lead test assemblies (LTAs) were loaded in an OPR1000 nuclear power plant (Ulchin unit 3) and irradiated for three cycles from 2002 to 2007. The LTAs were confirmed to have been irradiated within the design limits through the pool-side examinations at the end of each cycle operation. Additionally, four commercial surveillance assemblies (CSAs) were examined in Yonggwang unit 5 for three cycles from 2006 to 2010. The in-pile performance of PLUS7 fuel was confirmed through the LTAs and CSAs. Based on the successful in-reactor performance of the LTAs and CSAs, more than 2,300 PLUS7 fuel assemblies have been supplied to OPR1000 nuclear power plants from 2006.

This topical report describes the design evaluation of PLUS7 fuel and the results of its in-reactor performance. The designs of PLUS7 fuel assembly and its components are evaluated in order to verify the mechanical integrity of the PLUS7 fuel during the in-reactor operations. The results of the design evaluations confirmed that all the out-of-pile and in-reactor mechanical integrity-related design criteria on the PLUS7 fuel are satisfied.

REVISION HISTORY

Revision	Date	Page	Description
0	November 2012	All	Original issue

LIST OF ACRONYMS

AOO	Anticipated Operational Occurrences
APR1400	Advanced Power Reactor 1400
ASME	American Society of Mechanical Engineers
BOC	Beginning of Cycle
CEA	Control Element Assembly
CEDM	Control Element Drive Mechanism
CHF	Critical Heat Flux
CSA	Commercial Surveillance Assembly
DCD	Design Control Document
DFBN	Debris Filter Bottom Nozzle
DNB	Departure from Nucleate Boiling
DNBR	Departure from Nucleate Boiling Ratio
ECT	Eddy Current Test
FACTS	Fuel Assembly Compatibility Test System
FDF	Fatigue Damage Factor
KSNP	Korean Standard Nuclear Power Plants
LOCA	Loss Of Coolant Accident
LTA	Lead Test Assembly
LVDT	Linear Variable Differential Transducer
OPR1000	Optimized Power Reactor 1000
PSE	Pool Side Examination
RCS	Reactor Coolant System
SSE	Safe Shutdown Earthquake
VIPER	Vibration Investigation and Pressure drop Experimental Research

TABLE OF CONTENTS

LIST OF TABLES

LIST OF FIGURES

1. INTRODUCTION

PLUS7 fuel was jointly developed from 1999 through 2002 with Westinghouse to enhance the fuel performance relative to Guardian fuel. In the process of the design, various out-of-pile mechanical, thermal, hydraulic, and vibration characteristic tests were performed.

For the in-pile tests, four lead test assemblies (LTAs) were loaded in an OPR1000 nuclear power plant in the Republic of Korea and irradiated from 2002 through 2007. Additionally, four commercial surveillance assemblies (CSAs) were examined in Yonggwang unit 5 for three cycles from 2006 to 2010. The in-pile performance of PLUS7 fuel was confirmed through the LTAs and CSAs. Based on the successful in-reactor performance of the LTAs and CSAs, more than 2,300 PLUS7 fuel assemblies have been supplied to OPR1000 nuclear power plants since 2006. PLUS7 fuel will also be supplied to APR1400 nuclear power plants from the initial cores.

PLUS7 fuel has the following advanced design features with respect to Guardian fuel:

- High burnup performance
  Batch average burnup increase from 45,000 to 55,000 MWD/MTU

- High thermal performance
  Overpower margin increase by more than 10%

- High mechanical strength
  Mid grid dynamic buckling strength increase by 45%

- Improved economy
  Enhanced uranium utilization (optimized H/U ratio) and neutron economy

- Improved fretting wear resistance
  Increased grid-to-rod fretting wear resistance with the conformal grid springs and dimples

- Multi-devices for debris filtering
  Improved debris filtering efficiency with a small-hole bottom nozzle and the protective grid

- Enhanced fuel production
  Standardized design and manufacturing processes

This report describes the design features, evaluation results, and in-reactor performance results of PLUS7 fuel.

In Chapter 2, the mechanical design features, design criteria and evaluation results of PLUS7 fuel assembly and components are described.

Chapter 3 covers the design and the evaluation results of the PLUS7 fuel rods with ZIRLO™ cladding up to 60,000 MWD/MTU.

In Chapter 4, the in-reactor performance of PLUS7 LTAs and CSAs are described based on the measured data from the pool-side examinations.

In Chapter 5, commercial operating experiences of PLUS7 fuel are described.

In the appendices, the summary of out-of-pile test results, the commercial operating experiences, the scram data verification, and the wear performance analysis for PLUS7 fuel are described.

2. FUEL ASSEMBLY AND COMPONENTS DESIGN

2.1 Overview

In this chapter, the design features and evaluation results of the PLUS7 fuel assembly are described. The evaluation results show that the PLUS7 fuel assembly maintains high burnup performance, thermal performance, mechanical performance, and the structural integrity needed for the in-reactor operations.

2.2 Fuel Assembly

2.2.1 Design Features

The PLUS7 fuel assembly is composed of a reconstitutable top nozzle, a debris filtering bottom nozzle with small holes, a debris filtering protective grid, nine mid grids with mixing vanes, a vaneless top grid, a vaneless bottom grid, four guide thimbles, an instrument tube, and 236 fuel rods inserted into the cells of each grid, as shown in Figure 2-1. Table 2-1 shows the comparison of design features of PLUS7 fuel and Guardian fuel.

Figure 2-2 shows that the PLUS7 fuel rod adopts ZIRLO cladding and a variable pitch plenum spring to secure high burnup performance. The PLUS7 fuel rod diameter is reduced by [ ] TS relative to the Guardian fuel rod, which reduces the rod-induced pressure drop and improves the uranium utilization. The axial blankets at the top and the bottom of the fuel stack region reduce the axial leakage of neutrons.

As shown in Figure 2-3, the PLUS7 mid-grids adopt mixing vanes to increase the overpower margin by more than 10 % compared with Guardian fuel. The grid straps are in a straight shape to enhance the buckling strength. PLUS7 uses the conformal spring and dimple to reduce the grid-to-rod fretting wear. The conformal spring and dimple make grid-to-rod area contacts instead of the point contact in Guardian fuel. The springs and dimples are designed to minimize the grid-induced pressure drop, as shown in Figure 2-4.

As shown in Figure 2-5, the PLUS7 top and bottom grids have straight-shaped straps to enhance the buckling strength. The pressure drop of the top and the bottom grids is reduced by designing the dimple in the horizontal direction. These grids adopt Inconel material to maintain a sufficient rod supporting force during the fuel life-time since Inconel has the property of low irradiation growth and relaxation.

Figure 2-6 shows that the protective grid connected to the top of the bottom nozzle divide the round flow hole into four and the slotted flow holes into two. This feature reduces the size of debris passing through the bottom nozzle. Moreover, the debris passing through the bottom nozzle flow holes and the inner straps of the protective grid will be captured by the dimples of the protective grid. The protective grid contains four dimples in each grid cell that provide a co-planar contact with long end plug of the fuel rod.

Figure 2-7 shows the reconstitutable top nozzle of PLUS7 fuel. The PLUS7 top nozzle components are not dismantled when the inner extension tube is disconnected from the guide thimble flange during the fuel assembly reconstitution process (integral design concept). In comparison, the Guardian top nozzle requires the installation of a temporary post to prevent dismantling of the top

nozzle components. This PLUS7 top nozzle design makes the fuel reconstitution work easier and less time-consuming.

As shown in Figure 2-8, the flow hole of the PLUS7 bottom nozzle is about half size of the Guardian's flow hole in order to enhance the debris-filtering efficiency. To minimize the pressure drop, the bottom nozzle is designed with round holes and slotted holes.

The configurations of the guide thimbles in the Guardian fuel and PLUS7 fuel are shown in Figure 2-9. To improve the manufacturability, the PLUS7 guide thimbles have two steps of tube diameters rather than three steps in the Guardian guide thimbles. However, there are no difference in the CEA insertability between PLUS7 fuel and Guardian fuel since inner and outer diameters and flow hole dimensions of the guide thimbles are identical.

All the dimensions of the PLUS7 instrument tube are the same as those of the Guardian.

2.2.2 Design Basis, Criteria and Evaluation

2.2.2.1 Structural Integrity

(1) Basis

The objectives of the fuel system safety are to provide assurance that (a) the fuel system is not damaged as a result of normal operation and anticipated operational occurrences (AOOs), (b) fuel system damage is never so severe as to prevent control rod insertion when it is required, (c) the number of fuel rod failures is not underestimated for postulated accidents, and (d) coolability is always maintained.

(2) Criteria

The fuel assembly shall maintain the structural integrity under any load occurring at all operating conditions during the entire lifetime.

For the normal operation and upset AOO conditions, the stress limits for the fuel assembly and its components are given below:

$$P_m \leq S_m$$
$$P_m + P_b \leq 1.5 \cdot S_m$$

Worst case abnormal loads during the postulated accidents are represented by seismic and LOCA loads. For these conditions, the stress limits for the fuel assembly and its components are given below:

$$P_m \leq S_m'$$
$$P_m + P_b \leq 1.5 \cdot S_m'$$

Where,
P_m = calculated primary membrane stress
P_b = calculated primary bending stress
S_m = allowable design stress intensity defined in the ASME Section III
S_u = minimum ultimate tensile strength at the unirradiated condition
S_m' = allowable design strength for the accident conditions (a smaller value of 2.4 S_m and 0.7 S_u)

(3) Evaluation

The structural integrity of the PLUS7 components is verified in Section 2.3 for all conditions. The evaluation results of the seismic and LOCA load for specific plant is addressed in chapter 4 of DCD.

2.2.2.2 Rod-to-Top Nozzle Axial Clearance

(1) Basis

If a fuel rod were to be fully constrained axially by contact with top and bottom nozzles, large axial load could be generated. This load could result in fuel rod bowing, overstressing of guide thimbles, or overstressing of guide thimble joints to nozzles.

(2) Criteria

The axial clearance between the fuel rod and top nozzle shall be maintained during the fuel lifetime.

(3) Evaluation

Based on the calculation of the axial gap between the fuel rod and top nozzle considering their irradiation growths, the axial clearance is maintained during the fuel lifetime. The PLUS7 PSE results confirmed the sufficient gap after three cycles of irradiation as shown in the Section 4.3.

2.2.2.3 Hydraulic Stability

(1) Basis

Since the fuel assembly liftoff may cause the fuel assembly and incore structure failure, the fuel assembly shall not be lifted off during the normal operation. The fuel assembly and fuel rod vibration causing the fuel failure shall not occur over the full range of flow rates of the plant.

(2) Criteria

- The fuel assembly shall not be lifted off during normal operation.
- Fuel rod vibration causing the fuel failure shall not occur over the full range of flow rates.
- The fuel rod vibration caused by the cross-flow between the fuel assemblies shall not result in fretting wear-induced cladding failure.

(3) Evaluation

The fuel assembly was confirmed not to be lifted off over the full range of flow rates, based on the fuel assembly lift-off tests at the FACTS loop test facility, as described in Appendix A.2.10 herein.

The PLUS7 fuel assembly vibration tests were performed at the FACTS loop test facility to evaluate its vibration characteristics (see Appendix A.2.1). The test results showed that PLUS7 fuel maintained dynamic stability and did not generate abnormal fluid-induced vibration in the reactor operating flow range, as shown in Figure 2-10.

Five hundred hours of endurance tests were performed in the VIPER high temperature loop having two kinds of fuel assemblies, PLUS7 fuel and Guardian fuel. This test is to evaluate the grid-to-rod fretting wear-induced failure that may be caused by the cross-flow between the two fuel assemblies.

Based on these test results, it was confirmed that the cross flow-induced vibration did not produce the grid-to-rod fretting wear-induced failure (see Appendix A.2.3).

Hydraulic stability of PLUS7 fuel assembly was also confirmed by successful operating experience (see Section 5). There was no fuel rod fretting failure for the LTA and commercially supplied PLUS7 fuel assemblies since 2002.

2.2.2.4 Shipping and Handling Loads

(1) Basis

The fuel assembly shall withstand loads encountered during normal shipping and handling conditions.

(2) Criteria

- The fuel assembly shall meet the stress criteria of the normal operation with an axial load of 4g acceleration and a lateral load of 6g acceleration that may occur during the shipping.
- The fuel assembly shall meet the stress criteria of the normal operation with the maximum load of 4g acceleration that may occur during the handling.

(3) Evaluation

The shift of fuel rods and the deformation of the grid springs do not occur during fuel assembly shipping because the grid springs have initial pre-loads greater than an axial load of 4g acceleration and a lateral load of 6g acceleration.

Grids are not deformed during fuel assembly shipping because the grid impact strength measured from the tests is found to be larger than the lateral load on the grid surface generated by 6g acceleration (see Appendix A.2.4).

It was evaluated that the stress acting on the fuel assembly was less than the stress allowable for the normal operation even when the load of 4g acceleration of fuel assembly mass was applied to the bottom nozzle as shown Section 2.3.1.2.

2.2.2.5 Mechanical Compatibility

(1) Basis

Fuel Assembly should properly interface with core components and the internal structure.

(2) Criteria

The fuel assembly shall be loaded without any interference with the reactor internals and the adjacent fuel assemblies. It also shall maintain mechanical compatibility with core components (control element assembly and neutron source rods).

(3) Evaluation

There is no impact on the mechanical compatibility because the PLUS7 designs are same as the Guardian at the interface with reactor internals and core components. Compatibility has been proved through the extensive operating experiences since 2002.

2.3 Fuel Assembly Components

2.3.1 Bottom Nozzle

2.3.1.1 Description

As shown in Figure 2-11, the bottom nozzle is composed of an adapter plate, four legs including skirt plates, and a cylindrical instrument guide. The bottom nozzle is attached to the four guide thimbles by thimble screws that penetrate through the adapter plate and mate with threaded end plugs of the guide thimbles. The thimble screws are locked in place by crimping on the underside of the adapter plate to prevent loosening.

The adapter plate of the bottom nozzle together with the protective grid can protect the fuel rods from debris entering the fuel assembly. The adapter plate consists of 188 round flow holes and 372 slotted flow holes, preventing the inflow of debris and minimizing the pressure drop of the bottom nozzle. The skirt plates and legs are welded to the adapter plate.

The instrument guide to guide instrument into the reactor core is fixed on the underside of the adapter plate at its center by a spot weld.

2.3.1.2 Design Basis, Criteria and Evaluation

(1) Structural support of the fuel assembly

1) Basis

The bottom nozzle integrity is maintained for lateral and vertical loads from normal and abnormal shipping, handling, and operating conditions.

2) Criteria

The bottom nozzle shall withstand lateral and vertical loads without exceeding the stress limits of Section 2.2.2.1.

3) Evaluation

The finite element analysis was performed to verify the mechanical integrity of the bottom nozzle for the loads arising from the fuel assembly shipping and handling as well as normal operation, AOOs and postulated accidents.

Figure 2-12 shows the finite element analysis model of the bottom nozzle. The load acting on the bottom nozzle at postulated accidents was conservatively assumed as [ ].[TS] As shown in the Table 2-2, it was found that all mechanical integrity design criteria were satisfied.

(2) Prevention of fuel rod ejection

1) Basis

The fuel rod shall not be ejected out of fuel assembly.

2) Criteria

The bottom nozzle shall be designed fuel rods not to be ejected through the nozzle.

3) Evaluation

The bottom nozzle design provides optimal offset in the centerline of the fuel rod array and the nozzle's primary flow hole array. This offset prevents fuel rod ejection.

(3) Compatibility with the lower support structure

1) Basis

The bottom nozzle can mate with the lower support structure without interference.

2) Criteria

The bottom nozzle shall be acceptable with the lower internal by mating between the bottom nozzle and the lower support structure.

3) Evaluation

The geometrical compatibility between the bottom nozzle and the reactor lower internals was evaluated considering the worst dimension tolerances of the bottom nozzle and the reactor lower support structure. It was evaluated that the bottom nozzle maintained compatibility with the reactor lower internals.

(4) Compatibility with the instrument guide

1) Basis

Proper alignment with the in-core instrument will assure reliable function of core monitoring and protection.

2) Criteria

The bottom nozzle shall be dimensionally compatible with the in-core instrument while providing adequate cooling.

3) Evaluation

The bottom nozzle design employs a cylindrical, thick-walled instrument guide that directs the in-core instrument through the bottom nozzle plenum region, as shown in Figure 2-11. The inside diameter of the guide matches the outside diameter of the instrument. Chamfering is provided on the inner diameter at the guide's lower end for the lead-in of the instrument.

2.3.2 Top Nozzle

2.3.2.1 Description

As shown in Figure 2-13 and Figure 2-14, the top nozzle is composed of an adapter plate, four outer guide posts, a holddown plate, four helical holddown springs, and an instrument housing.

The outer guide posts are threaded externally at their lower ends for connection to the adapter plate and welded to the underside of the adapter plate against unlocking. The outer guide post provides a groove on its outside for crimping against unlocking.

The inner extension is inserted through the outer guide post, threaded into the guide thimble flange and crimped with outer guide post.

The holddown plate accommodates the fuel handling tool to the fuel assembly. The holddown plate is a key component of the top nozzle that prevent the fuel assembly lift-off by the holddown spring force occurring when the insert tube of the upper structure holds it down (Figures 2-7 and 2-13).

The instrument housing is attached at the center of the adapter plate by a threaded joint, and it accommodates and protects the in-core instrument.

2.3.2.2 Design Basis, Criteria and Evaluation

(1) Structural support of the fuel assembly

1) Basis

The top nozzle integrity is maintained for lateral and vertical loads from normal and abnormal shipping, handling, and operating conditions.

2) Criteria

The top nozzle shall withstand lateral and vertical loads without exceeding the stress limits of Section 2.2.2.1.

3) Evaluation

Finite element analysis was performed to verify the mechanical integrity of the top nozzle for the loads from the fuel assembly shipping and handling as well as normal operation, AOOs and postulated accidents.

Figures 2-15 and 2-16 show the finite element analysis model of the top nozzle components. The load acting on the top nozzle at postulated accidents was conservatively assumed as [ ].[TS] As shown in the Table 2-3, it was found that all mechanical integrity design criteria were satisfied.

(2) Prevention of fuel rod ejection

1) Basis

The fuel rod shall not be ejected out of fuel assembly.

2) Criteria

The top nozzle shall be designed fuel rods not to be ejected through the nozzle.

3) Evaluation

The top nozzle design provides that ligaments are oriented above fuel rod centerlines preventing from fuel rod ejection and that the flow holes are offset laterally from the fuel rod horizontal position.

(3) Compatibility with the upper guide structure

1) Basis

The top nozzle can mate with the upper guide structure without interference.

2) Criteria

The top nozzle shall be acceptable with the upper internal by mating between the top nozzle and the upper guide structure.

3) Evaluation

The geometrical compatibility between the top nozzle and the reactor upper internals was evaluated, considering the worst dimensional tolerances of the top nozzle and the reactor upper guide structure. It was evaluated that the top nozzle maintained compatibility with the reactor upper internals.

(4) Remote reconstitutability

1) Basis

The fuel assembly design requires all necessary features to allow remote reconstitution at the plant site by removal of the top nozzle.

2) Criteria

The components of the top nozzle and fuel assembly must interface with each other such that smooth remote removal and replacement of the top nozzle can be performed. All parts removed during the reconstitution must be captured to preclude the loss of parts in the reactor. Adequate clearance must be provided after removal of the top nozzle to allow the removal of the fuel rods.

3) Evaluation

The top nozzle is disengaged from the fuel assembly by removing the four inner extensions and lifting the top nozzle off the guide thimble flanges. A sliding fit between the inner diameter of the outer guide post and the outer diameter of the inner extension is provided for smooth removal or replacement process.

(5) Compatibility with handling equipment

1) Basis

The top nozzle design must assure that proper handling and storage of new and irradiated fuel assemblies can be performed.

2) Criteria

The top nozzle design must ensure that the fuel assembly can be installed in fuel storage racks, fuel transfer equipment, fuel elevators, and in the core. All components of the top nozzle must be designed for proper fit-up with plant handling equipment.

3) Evaluation

All available information on the handling tools and procedures has been reviewed. The containment handling tool grapple was found to provide the most limiting fit with the top nozzle holddown plate. These interface dimensions of the top nozzle related the handling tools are identical to those of Guardian fuel.

2.3.3 Holddown Spring

2.3.3.1 Description

The holddown spring is designed to provide a sufficient holddown force for the fuel assembly in order not to lift off during normal operation. As shown in Figure 2-13, the holddown coil spring of Inconel-718 surrounds the outer guide post and generates the holddown force.

2.3.3.2 Design Basis, Criteria and Evaluation

(1) Holddown force in normal operation

1) Basis

Fuel assembly lift-off during normal operating conditions can result in fuel assembly or core support structural damage. If lift-off occurs during normal operation, large amplitude fuel assembly oscillations could ensue. These oscillations can cause impact forces on the core structures and fuel assembly.

2) Criteria

The fuel assembly shall not lift off the core support structure during the normal operation.

3) Evaluation

As explained in Section 2.2.2.3 and shown in Table 2-4, the holddown spring was shown to have a sufficient design margin against fuel assembly lift-off. The fuel assembly lift-off tests at the FACTS loop showed that the fuel assembly did not lift off (see Appendix A.2.10).

(2) Holddown spring maximum deflection range and solid condition

1) Basis

Load of solid spring may cause improper load distribution through the top nozzle, and may have an adverse effect on the spring itself. The load of solid spring on the fuel assembly can cause extensive structural damage and subsequent fuel failure.

2) Criteria

The clearance between the holddown working height and spring solid height shall be maintained under normal operation.

3) Evaluation

The holddown working height was calculated based on the maximum fuel assembly growth. It was evaluated that the holddown working height is greater than the solid spring height.

(3) Holddown spring stress and fatigue

1) Basis

The spring shear stress shall meet the ASME Boiler and Pressure Vessel Code. The fatigue properties must be considered to preclude fatigue failure by vibration induced alternating stress.

2) Criteria

The spring shear stress for normal operation except lift-off shall be less than 0.8 S_m. The alternating shear stress resulting from coil vibration shall not exceed the endurance limit. The maximum shear stress resulting from the alternating stress, plus the mean shear stress, shall not exceed the shear yield stress.

3) Evaluation

A functional analysis of the fuel assembly holddown spring was performed to optimize the geometric configuration of the spring based on both holddown spring static stress and fatigue considerations. As a result of calculating the shear stresses, the maximum shear stress of the holddown spring was respectively calculated to be [ ]^{TS} at cold, [ ]^{TS} at hot. The results are less than the allowable design criteria which are [ ]^{TS} at cold, [ ]^{TS} at hot.

2.3.4 Guide Thimble and Instrument Tube

2.3.4.1 Description

As the structural components of the fuel assembly skeleton, four guide thimbles are located toward the corners of the square envelope and an instrument tube located at the center of the fuel assembly. The guide thimbles and the instrument tube guide the control element assembly, the neutron source rods, and the in-core instrument into the fuel assembly (See Figure 2-1).

As shown in Figure 2-17, the lower section of the guide thimble tube has a smaller diameter than the upper section. This design feature provides for hydraulic deceleration of CEAs during SCRAM to reduce impact forces on the upper guide structure. Two flow holes of guide thimbles accommodate cooling of the CEAs and the neutron source rods.

The upper portion of the guide thimble tube is welded to the internally threaded flange, which is attached to the top nozzle by an externally threaded inner extension inserted into the outer guide post. The internally threaded end plug is welded to the lower portion of the guide thimbles and the guide thimble screw is inserted into the end plug from the underside of the bottom nozzle, connecting the guide thimble tube to the bottom nozzle.

Two pairs of inward dimples, offset in a radial direction by 90° are formed on the instrument tube at each mid-span elevation. The 40 dimples formed axially along the instrument tube support the in-core instrument laterally when inserted into the instrument tube. The coolant flows through one flow hole of the instrument tube, cooling the in-core instrument.

2.3.4.2 Design Basis, Criteria and Evaluation

(1) Structural support of the fuel assembly

1) Basis

The guide thimble maintains its structural integrity for lateral and vertical loads from normal and abnormal shipping, handling, and operating conditions.

2) Criteria

The design criteria of guide thimble and instrument tube are same as the structural integrity design criteria of the fuel assembly described in Section 2.2.2.1.

3) Evaluation

The maximum stress on the guide thimble tube is applied by the axial hydraulic force and the holddown spring force. As a result of calculating the stress, the maximum stress of guide thimble tube is less than allowable design criteria as shown in the Table 2-5.

The control rod drop did not generate a severe impact on the upper guide structure and the acting stress was far below the stress design limit. The kinetic energy of the CEA during SCRAM was reduced by the hydraulic damping in the dashpot of the guide thimble and by the CEA spring.

The circumferential stress acting on the guide thimble tube from the pressure difference between inner and outer guide thimble tube around the dashpot region was evaluated to satisfy the stress design limit.

Assuming that the CEA drop occurs once a day conservatively, the guide thimble tube stress was calculated to be so small that the fatigue-induced guide thimble tube failure does not occur.

(2) CEA drop time

1) Basis

CEA shall shut down the reactor in time and be inserted fully without damage to the fuel assembly, CEA, or the upper guide structure.

2) Criteria

The geometrical shape of the guide thimble tube shall meet the control rod drop time limit.

3) Evaluation

The CEA drop time depends on the geometrical configurations (the inner diameter of the guide thimble tube, the number of flow holes and their diameters, the control rod diameter), the CEA weight, and the fuel assembly pressure drop. The results of CEA SCRAM analysis show that the CEA design meets the drop time and displacement limits, as shown in Figure 2-18. In addition, it is verified that SCRAM analysis provides reasonable CEA drop time data, as described in Appendix C.

2.3.5 Grid

2.3.5.1 Description

The PLUS7 grids are composed of a top grid minimizing fuel rod bow due to fuel rod irradiation growth, a bottom grid preventing fuel rod failure due to fretting wear at high burnup, a protective grid enhancing the debris filtering efficiency, and nine mid grids with mixing vanes to improve thermal performance as a result of better coolant mixing. The design feature of each grid is described as follows.

(1) Top and bottom grids

Top and bottom grids are brazed among the inner straps, outer straps and sleeves, and have horizontal dimples in each grid cell to minimize pressure drops. Top and bottom grid have an anti-snag design to minimize adverse assembly interactions during core loading and unloading.

The spring force of the top grid is designed small enough to minimize the rod bow due to fuel rod irradiation growth. The spring force of the bottom grid is designed large enough to support the fuel rods sufficiently up to the target design burnup. The PLUS7 top and bottom Inconel grids are shown in Figures 2-5 and 2-19.

(2) Protective grid

The PLUS7 protective grid is located directly above the small-hole bottom nozzle for additional debris filtering. The protective grid also reduces the flow induced fuel rod fretting wear by supporting the end region of the fuel rod with the bottom grid.

The protective grid contains four dimples in each grid cell that provide a co-planar contact with the fuel rod bottom end plug. These dimples are combined with the long solid end plug and the small-hole bottom nozzle to provide multi-debris filtering capability (see Figures 2-6 and 2-20). As shown in Figure 2-6, the protective grid straps divide the round holes of the bottom nozzle into four equal parts and the slotted holes of the bottom nozzle into two equal parts. Hence, debris in the reactor core can be filtered at first from the flow inlet of the small-hole bottom nozzle and then the debris passing through the bottom nozzle can be filtered next at the flow outlet of the bottom nozzle by the protective grid straps. In addition, the debris passing through the flow outlet of bottom nozzle will be captured by the protective grid dimples (triple protection concept). The debris captured by the protective grid cannot cause a fuel rod failure since the debris is to contact the long solid end plug instead of the cladding of the fuel rod.

Four washers are welded to the underside of the protective grid cells containing the guide thimbles. Then, the protective grid is attached to the bottom nozzle by the guide thimble screws through the washers.

(3) Mixing Vane Mid Grid

The PLUS7 mid grid has mixing vanes to increase the overpower margin by more than 10% (see Figures 2-3 and 2-4). The fluid-induced fuel assembly vibration may occur when hydraulic force balance in the fuel assembly is not achieved due to the asymmetrical mixing vane pattern of the mid grid. The mixing vane pattern of the PLUS7 mid grid is optimized to have hydraulic force balance.

The mid grid, like the top and the bottom grids, is designed to decrease the possibility of grid hang-up during the loading and unloading of fuel assembly.

As shown in Figures 2-4 and 2-21, the mid grid has conformal grid springs and dimples creating area contacts with the fuel rods, which can help prevent grid-to-rod fretting wear-induced fuel

failure. The conformal shapes increase the fretting wear-induced fuel rod perforation time significantly since the area contact will result in less wear depth than the point or line contact even when the same wear volume is made.

Also, the seismic-resistance of the fuel assembly is largely improved due to a large increase in the buckling strength of the mid-grids due to the straight-shaped grid strap.

2.3.5.2 Design Basis, Criteria and Evaluation

(1) Fuel Rod Support

1) Basis

The grid shall support the fuel rod axially and laterally.

2) Criteria

The spring force of the bottom grid at EOL shall be a minimum of [ ].[TS]

3) Evaluation

Based on the operating experiences of the PWR fuels, when the EOL residual spring force of the bottom grid is less than [ ],[TS] the grid-to-rod fretting wear can occur. Therefore, the design criteria for the spring force of the PLUS7 bottom gird at EOL is conservatively set to [ ].[TS] The evaluation results of the bottom grid spring forces of the PLUS7 fuel show that the PLUS7 fuel meets the design criteria of [ ][TS] at EOL.

(2) Shipping and Handling

1) Basis

The fuel should be designed to withstand shipping and handling loads without damage
2) Criteria

The grid shall withstand 4g axial and 6g lateral accelerations without allowing the fuel rods to shift or the grid to permanently deform during the shipping and handling.

3) Evaluation

The grid should withstand 4g axial and 6g lateral accelerations without allowing the fuel rods to shift or the grid to permanently deform under the loads resulting from the design level of axial and lateral accelerations during the fuel assembly shipping and fuel assembly handling.

The frictional load associated with the spring force of the PLUS7 grids on fuel rod is greater than the axial load of 4g acceleration so that the fuel rods should not to be shifted from the grids. The grid spring force is larger than the fuel rod lateral load by 6g acceleration. Therefore, the fuel rod lateral movement was evaluated to have been restrained.

The grid buckling test results indicated that the buckling strength was greater than the lateral load of 6g acceleration generated by the fuel rods' weight of the grid-to-grid span length (see Appendix A.2.4). Therefore, the permanent deformation of the grid assembly was evaluated not to occur.

(3) Fuel Rod Fretting Wear

1) Basis

The fuel rods should not fail due to the grid-to-rod fretting wear caused by the fuel assembly-induced or the fuel rod-induced vibration during normal operation.

2) Criteria

The fuel rod should not fail due to fretting wear during fuel lifetime.

3) Evaluation

The fuel rods must not fail due to the grid-to-rod fretting wear caused by the fuel assembly-induced or the fuel rod-induced vibration during normal operation. The grid-to-rod fretting wear resistance performance can be verified by the following three kinds of verification tests:

- Fluid-induced fuel assembly vibration test
- Fluid-induced high frequency vibration test of the grid strap
- 500-hour long-term wear-resistance test

The mixing vanes of the PLUS7 grids were arranged symmetrically to have the hydraulic balance for preventing the fluid-induced fuel assembly vibration. As shown in Figure 2-10, the PLUS7 fuel assembly vibration is very small over the range of flow rates of the plants. According to the fluid-induced high frequency vibration test of the PLUS7 grid strap, the grid strap high frequency-induced fretting wear was evaluated not to occur over the range of flow rates of the plant since the PLUS7 grid strap generated low amplitude of high frequency vibration as shown in Figure 2-22 (see Appendix A.2.2).

The 500-hour long-term wear-resistance test results showed that the PLUS7 fuel did not generate the fretting wear-induced fuel failure for the fuel lifetime (see Appendices A.2.3 and D). Fuel rod fretting wear performance of PLUS7 fuel assembly was verified by successful operating experience without any fuel rod fretting wear failure for the fuel lifetime (see Appendix A.2.3, B and D).

(4) Fuel Rod Bow

1) Basis

An excessive grid spring force may restrain the fuel rods from slipping, which may generate the fuel rod bow, making the fuel rod channel spacing smaller and subsequently overheating the fuel rods. Therefore, the grids shall accommodate the fuel rod growth caused by the thermal expansion and neutron irradiation without inducing unacceptable fuel rod bow.

2) Criteria

The grid shall not permit or cause rod bowing that exceeds the allowable limits for channel closure for the fuel assembly lifetime.

3) Evaluation

The fuel rod bow is used to determine if the Departure from Nucleate Boiling Ratio (DNBR) penalty is to be imposed or not. The DNBR penalty is not imposed if the reduction of the fuel rod channel

spacing due to the fuel rod bow is less than [ ]^{TS} of the initial fuel rod channel spacing. As seen in the in-reactor irradiation test results in Section 4.4, the minimum fuel rod channel spacing measured after the three cycles operation is [ ],^{TS} while the [ ]^{TS} of the initial fuel rod channel spacing is [ ].^{TS} Therefore, PLUS7 fuel was evaluated to meet the fuel rod bow-related design criteria for the fuel lifetime.

(5) Mid-Grid Buckling Strength

1) Basis

Core coolability and safe shutdown of the reactor should be maintained under the most limiting load on the mid grid assembly.

2) Criteria

The grids must provide a coolable geometry and allow the control rod insertion for the postulated accidents, such as seismic and LOCA.

3) Evaluation

The evaluation of this criterion is addressed in Chapter 4 of DCD.

(6) Grid Width

1) Basis

The grid width will grow due to the neutron irradiation as the fuel burnup increases. This grid irradiation growth should not affect the fuel loading and unloading operation in the reactor core.

2) Criteria

An adequate space between the fuel assemblies should be maintained to load and unload the fuel assembly safely for the fuel lifetime.

3) Evaluation

With taking account of the increase in the grid width due to the neutron irradiation in the reactor core, an adequate space between the fuel assemblies should be maintained to load and unload the fuel assembly safely after irradiation. Also a proper guide chamfer should be provided on the outer grid strap to prevent the fuel failure caused by interferences between adjacent fuel assemblies during fuel handling.

The pool-side examination (PSE) results of PLUS7 fuels confirmed that an adequate space between the fuel assemblies could be maintained after the three cycle irradiation (see Section 4.5). Furthermore, the designs of the grid guide tab, grid guide vane, and grid corner shape of PLUS7 fuel were based on the previous designs used successfully in commercial nuclear power plants. Therefore, there should be no fuel assembly interference-induced fuel failure (see Appendix A.2.7).

2.3.6 Joint and Connection

2.3.6.1 Description

(1) Top nozzle/guide thimble

As shown in Figure 2-14, the top nozzle/guide thimble are assembled such that the inner extension tube is inserted into the outer guide post and then threaded into the guide thimble flange, and the upper head of the inner extension tube is crimped on the upper part of the outer guide post to prevent un-torquing due to vibration.

(2) Top grid/guide thimble /instrument tube

As shown in Figure 2-23, the top grid/guide thimble/instrument tube are assembled so that the sleeves of zirconium alloy located at the upper and the lower sides of the Inconel top grid are spot welded to the guide thimble tube and the instrument tube at four points positioned at intervals of 90° to fix the position of the Inconel top grid.

(3) Mid grid/guide thimble /instrument tube

As shown in Figure 2-23, the mid grid/guide thimble/instrument tube are assembled so that the sleeves of zirconium alloy laser-welded at the lower sides of the mid grid are spot welded to the guide thimble tube and the instrument tube at four points positioned at intervals of 90° to fix the position of the mid grid.

(4) Bottom grid/guide thimble tube/instrument tube

As shown in Figure 2-24, the bottom grid/guide thimble /instrument tube are assembled so that the sleeves of zirconium alloy located at the upper and the lower sides of the bottom grid are spot welded to the guide thimble and the instrument tube at four points positioned at intervals of 90° to fix the position of the Inconel bottom grid.

(5) Bottom nozzle/protective grid/guide thimble tube

As shown in Figure 2-25, the bottom nozzle/protective grid/guide thimble are assembled so that the protective grid having welded washers are inserted between the bottom nozzle and the guide thimble end plugs, and then the guide thimble screws inserted from the lower side of the bottom nozzle are threaded into the guide thimble end plugs.

2.3.6.2 Design Basis, Criteria and Evaluation

(1) Top nozzle/guide thimble

1) Basis

The top nozzle/guide thimble joint and connections shall not be damaged under the loads of normal operation and AOOs.

2) Criteria

Under the loads of normal operation and AOOs, the top nozzle/guide thimble joint and connections shall not be damaged and must meet the following design criteria:

$P_m \leq$ a smaller value of $0.9\ S_y$ and $2/3\ S_u$
$\tau \leq 0.6\ S_y$

Where,
P_m = membrane stress intensity
τ = primary shear stress
S_u = minimum ultimate tensile strength at unirradiated condition
S_y = minimum yield strength at unirradiated condition

3) Evaluation

The largest load acting on the top nozzle/guide thimble joint and connections is a preload caused by a torque occurring during the screw connection process. As a result of calculating the stress, the stress of the preload is less than allowable design criteria.

(2) Grid/guide thimble/instrument tube

1) Basis

Dimensional stability of the fuel assembly must be maintained under operating, shipping, and handling conditions. The joint must remain intact under operating, shipping, and handling conditions. Since the spot-welds are not expected to yield significantly before failure, the design limits are based on failure loads.

2) Criteria

Under the loads of normal operation and AOOs, the grid/guide thimble /instrument tube joint and connections shall not be damaged.

3) Evaluation

The largest load acting on the grid/guide thimble welding point is a slip load at the fuel rod/grid interface caused by the difference in their thermal expansion. As a result of calculating the stress, it was evaluated to be far less than the weld strength of the grid/guide thimble connection measured by the test.

(3) Bottom nozzle/guide thimble

1) Basis

Fuel assembly dimensional stability must be maintained under shipping, handling, operating, and accident conditions. The lifting force requirement ensures that the joint can withstand the maximum possible force exerted on the fuel assembly by the fuel handling equipment during removal from the core.

2) Criteria

Under the loads of normal operation and AOOs, the bottom nozzle/guide thimble joint and connections shall not be damaged and must meet the following design criteria:

$P_m \leq$ a smaller value of $0.9\ S_y$ and $2/3\ S_u$
$\tau \leq 0.6\ S_y$

Where,
P_m = membrane stress intensity

τ = primary shear stress
S_u = minimum ultimate tensile strength at unirradiated condition
S_y = minimum yield strength at unirradiated condition

3) Evaluation

The largest load acting on the bottom nozzle/guide thimble joint and connections is a preload caused by a torque occurring during the screw connection process. As a result of calculating the stress, the stress of the preload is less than allowable design criteria.

Table 2-1 Comparison of Design Features of PLUS7 Fuel and Guardian Fuel

Fuel Components	
Overall assembly height, inches	
Fuel assembly weight, lbs	
Number of grids	
Fuel Rod	
Pellet diameter, inches	
Cladding I.D., inches	
Cladding O.D., inches	
Cladding Material	
Plenum Spring	
Fuel rod length, inches	
Axial Blanket	
Mid Grid	
Mixing Vane	
Strap Shape	
Spring/Dimple Shape	
Number / material	
Top/Bottom Grid	
Mixing Vane	
Strap Shape	
Spring/Dimple Shape	
Material	
Top Nozzle	
Reconstitution	
Holddown Spring Material	
Bottom Nozzle	
Flow Hole shape	
Reconstitution	
Protective Grid	
Material	
Guide Thimble	
Number of Diameter Steps	
Material	
Instrument Tube	
Material	

Table 2-2 PLUS7 Bottom Nozzle Stress Summary

TS

Table 2-3 PLUS7 Top Nozzle Stress Summary

TS

Table 2-4 PLUS7 Holddown Margin at Hot Condition

TS

Table 2-5 PLUS7 Guide Thimble Tube Stress Summary

TS

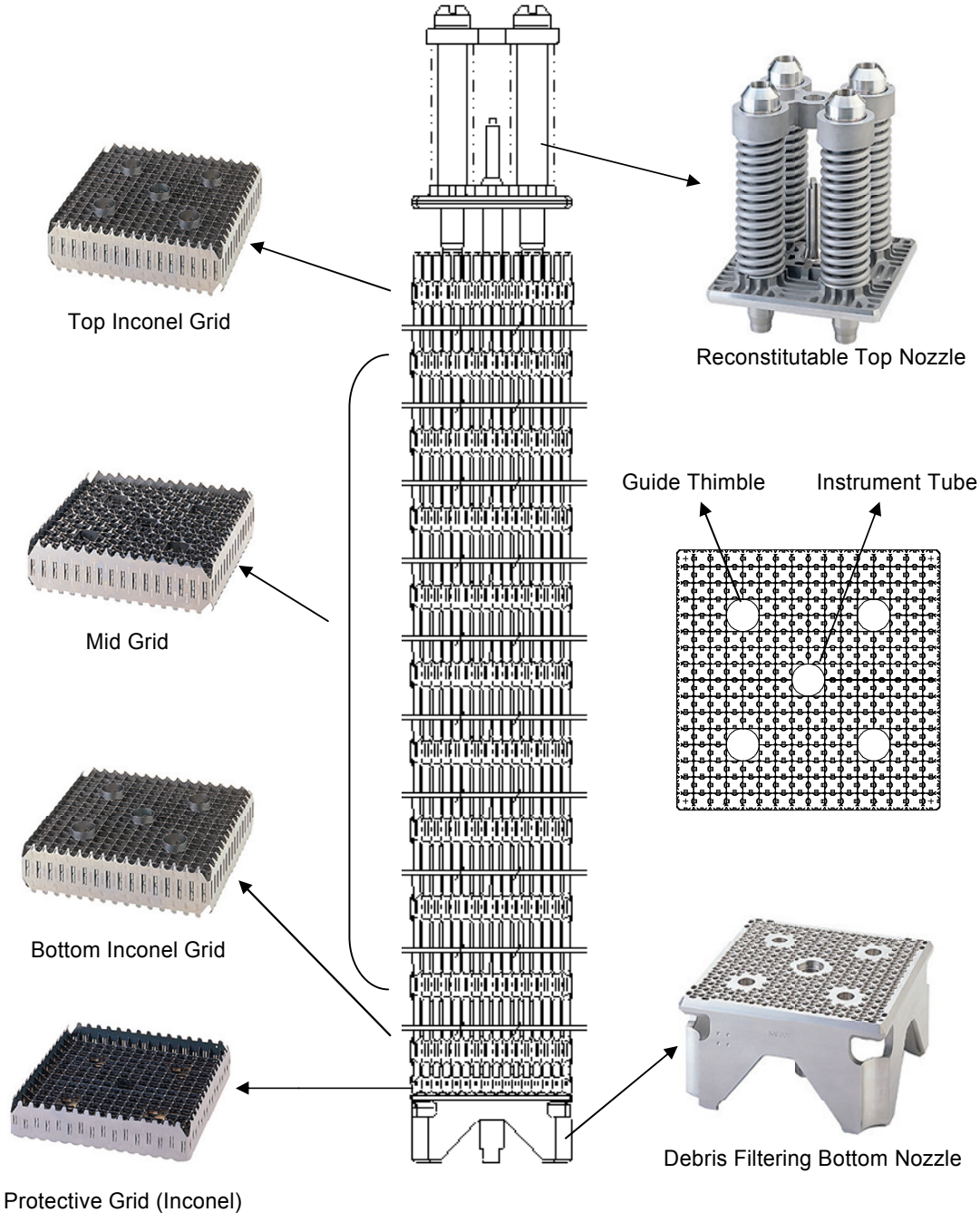

Figure 2-1 PLUS7 Fuel Assembly Configuration

TS

Figure 2-2 Comparison of Fuel Rod Designs

TS

Figure 2-3 Mid Grid Designs

TS

Figure 2-4 Spring and Dimple Configurations of PLUS7 Mid Grid

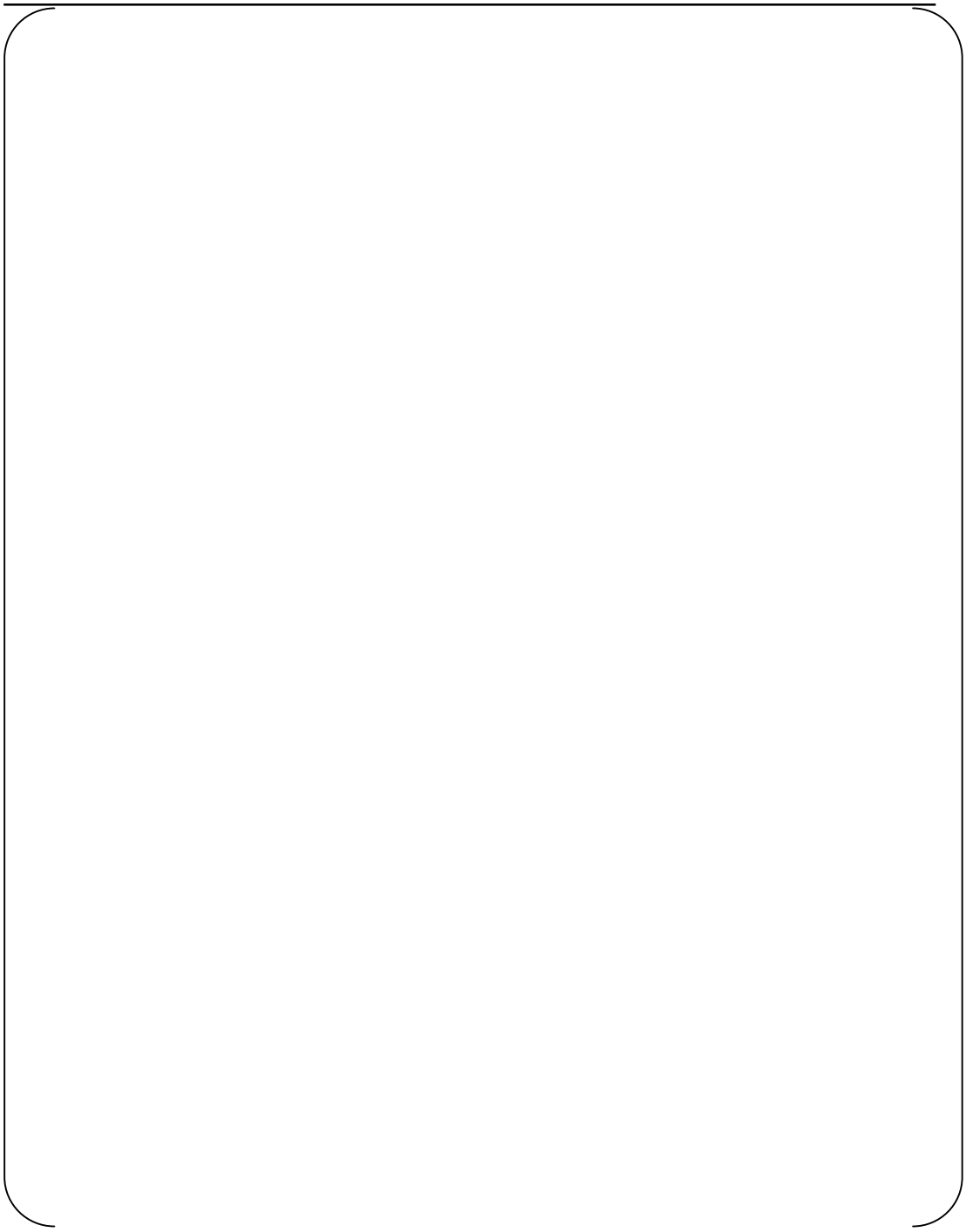

TS

Figure 2-5 Comparison of Top and Bottom Grids

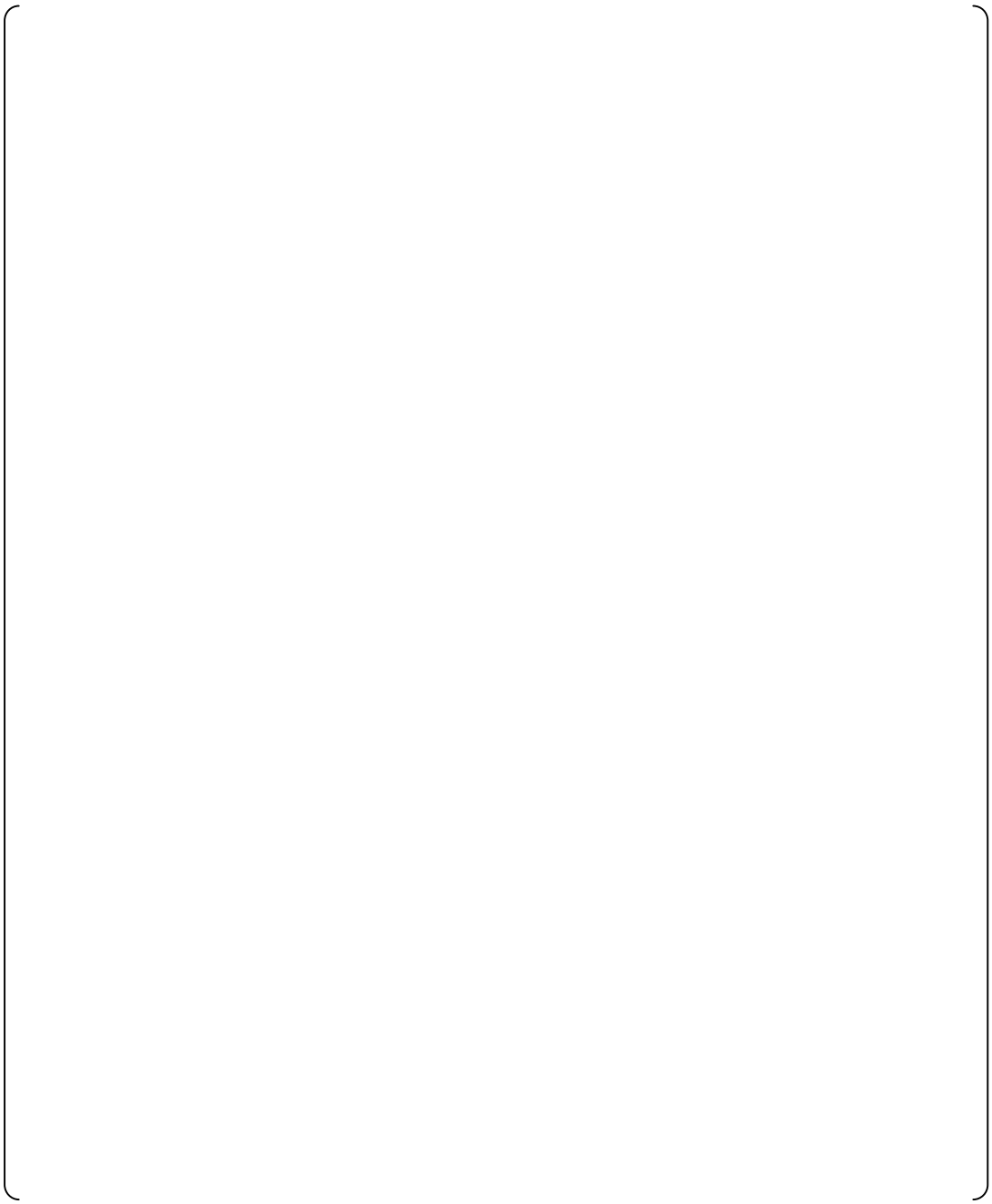

Figure 2-6 Debris Filtering Design of PLUS7

<Before Constituting Inner Extension>

[ ] TS

Figure 2-7 Reconstitutable Design of PLUS7 Top Nozzle

TS

Figure 2-8 Comparison of Bottom Nozzles

TS

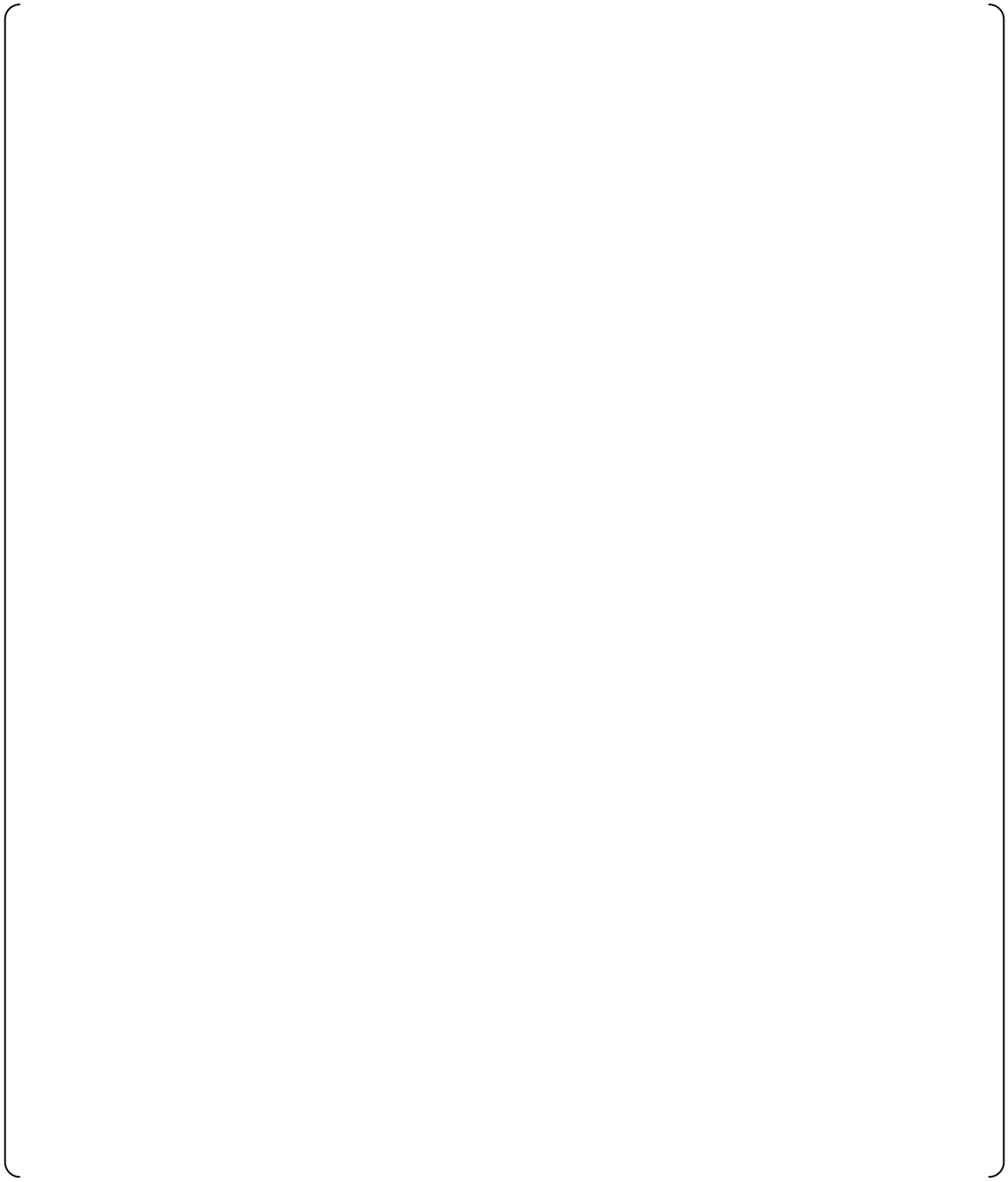

Figure 2-9 Comparison of Guide Thimbles

TS

Figure 2-10 Vibration Test Results of PLUS7 Fuel Assembly

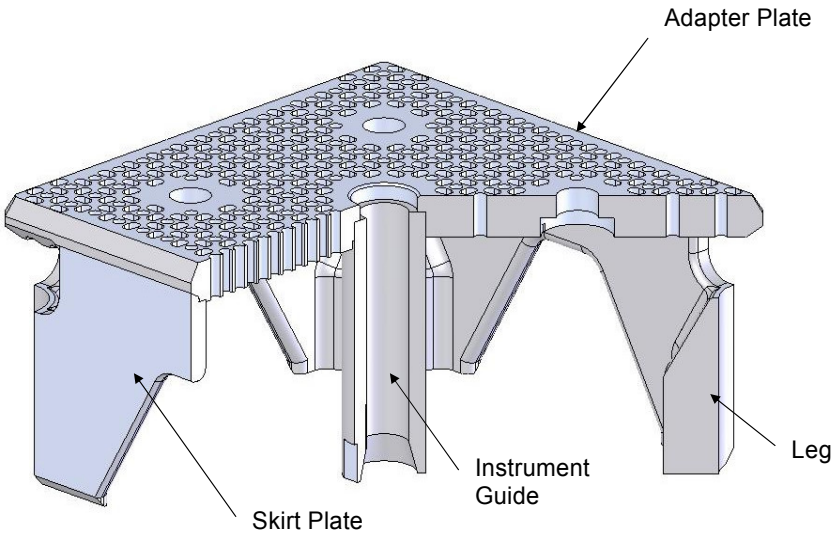

Figure 2-11 PLUS7 Bottom Nozzle

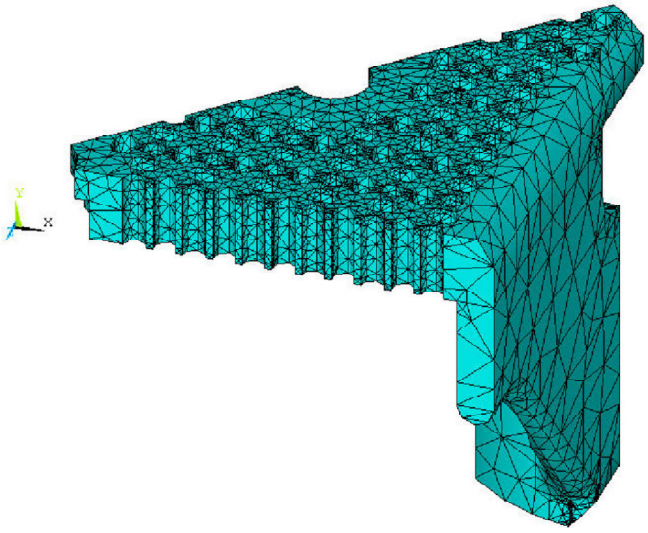

Figure 2-12 1/8 Bottom Nozzle Finite Element Model

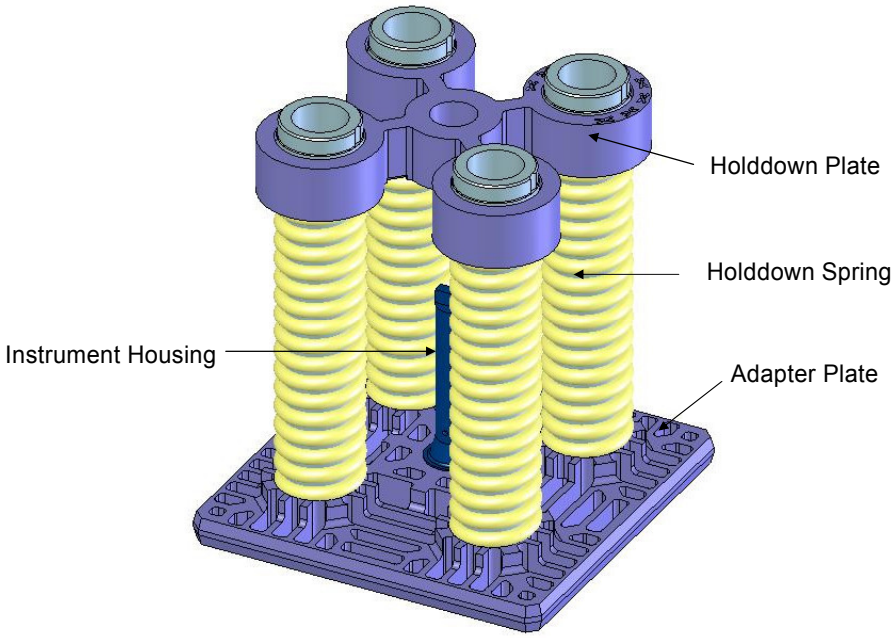

[ ] TS

Figure 2-13 PLUS7 Top Nozzle

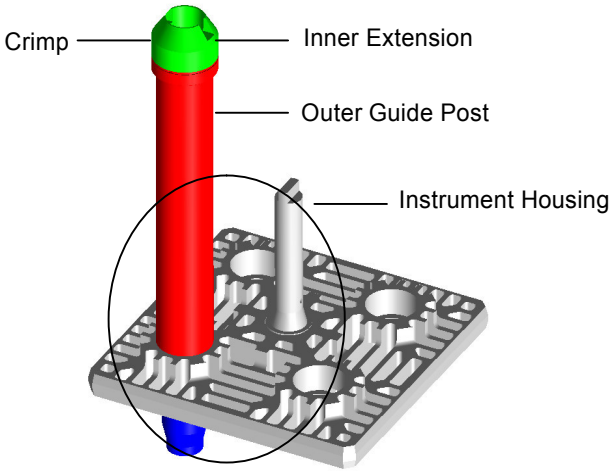

TS

Figure 2-14 PLUS7 Top Nozzle/Guide Thimble Joint & Connection

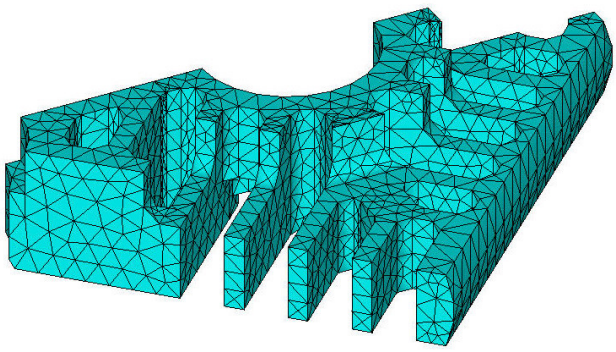

Figure 2-15 1/8 Top Nozzle Adapter Plate Finite Element Model

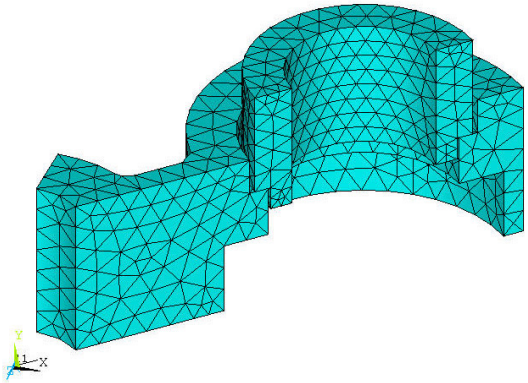

Figure 2-16 1/8 Top Nozzle Holddown Plate Finite Element Model

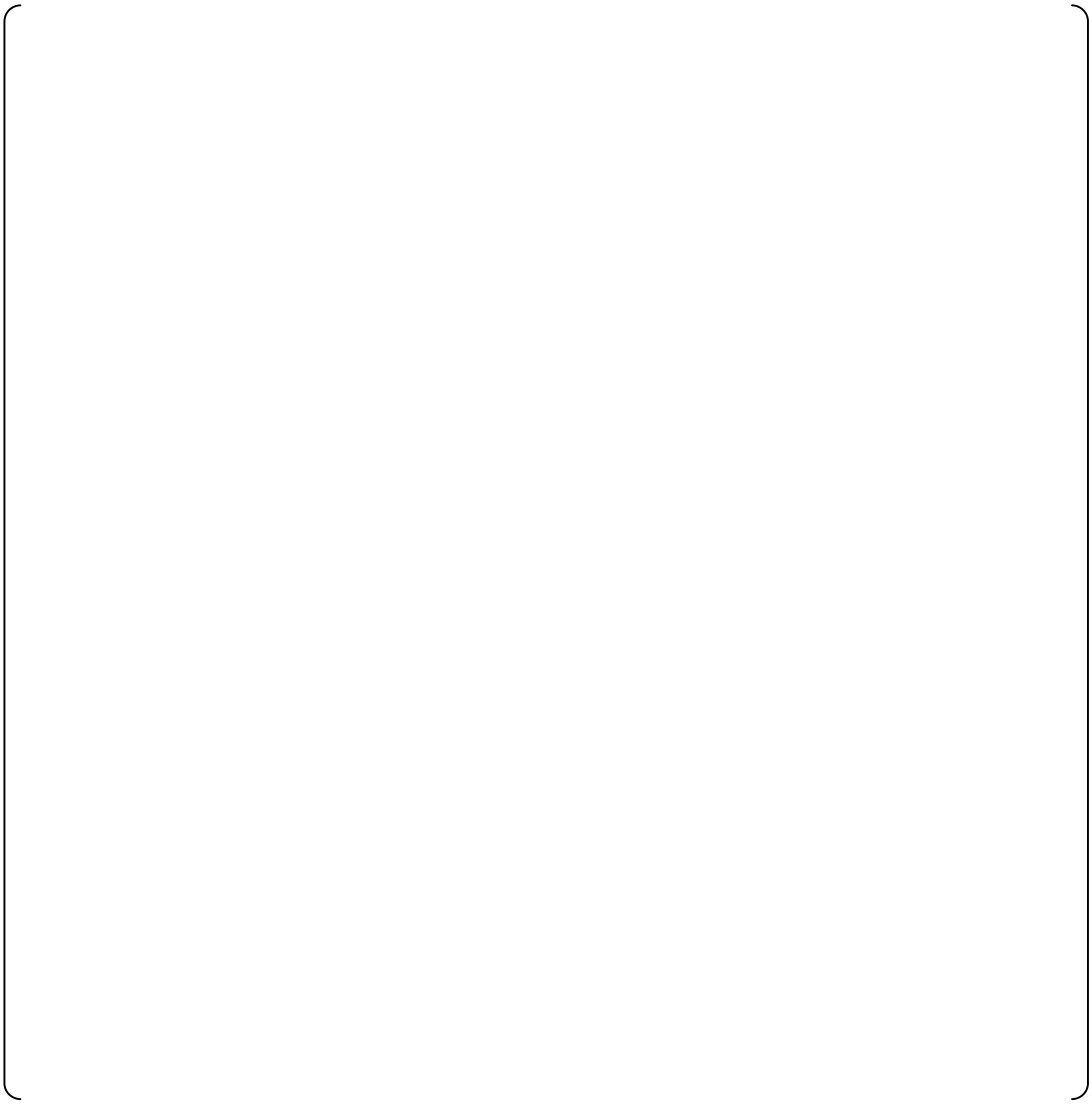

TS

Figure 2-17 PLUS7 Guide Thimble and Instrument Tube

TS

Figure 2-18 CEA Drop Time

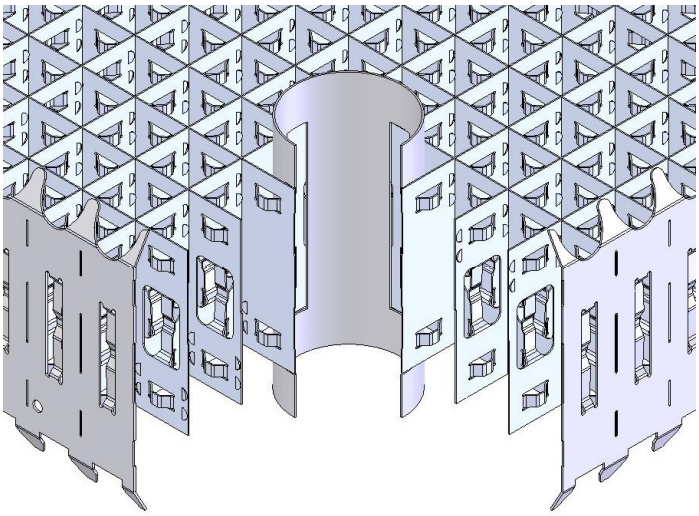

Figure 2-19 PLUS7 Top and Bottom Grid

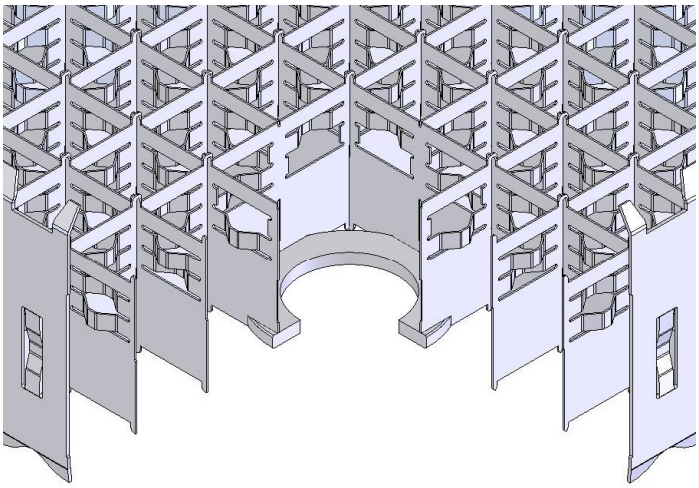

Figure 2-20 PLUS7 Protective Grid

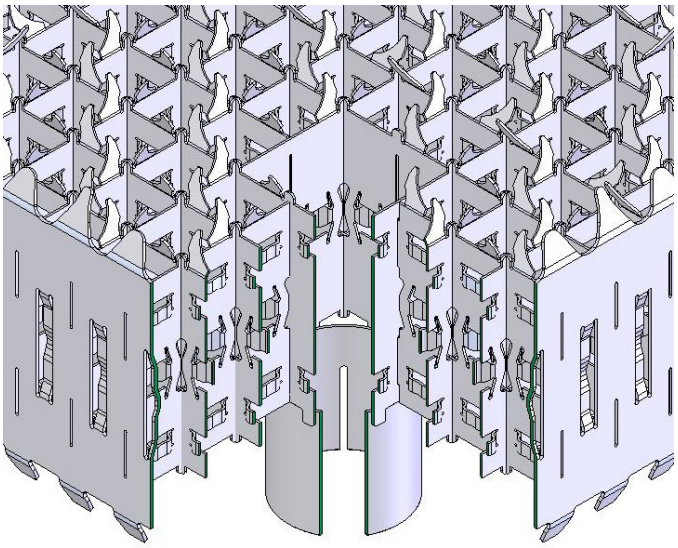

Figure 2-21 PLUS7 Mid Grid

TS

Figure 2-22 PLUS7 Mid Grid High Frequency Vibration Test Results

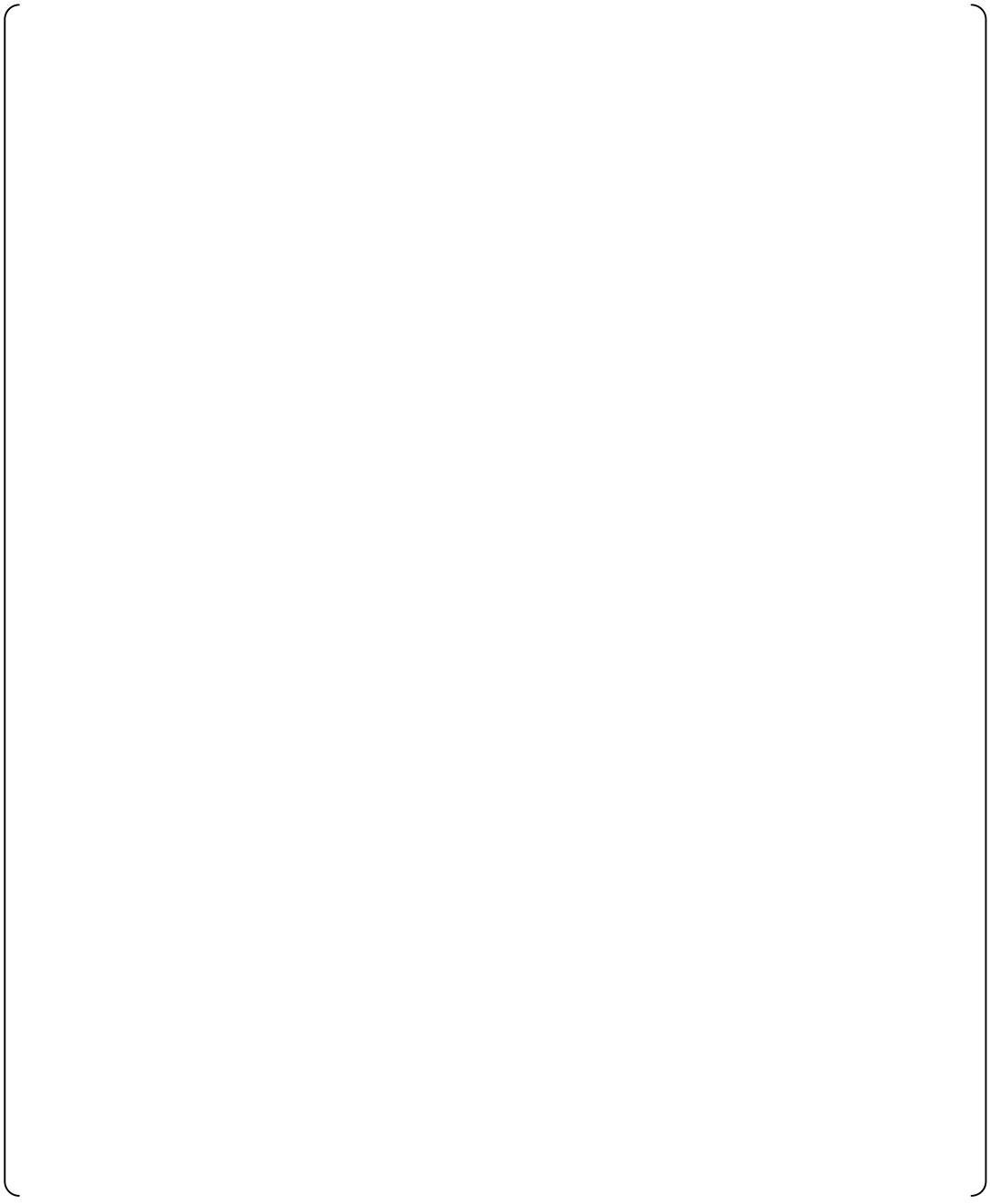

Figure 2-23 PLUS7 Grid/Guide Thimble and Instrument Tube Joint & Connection

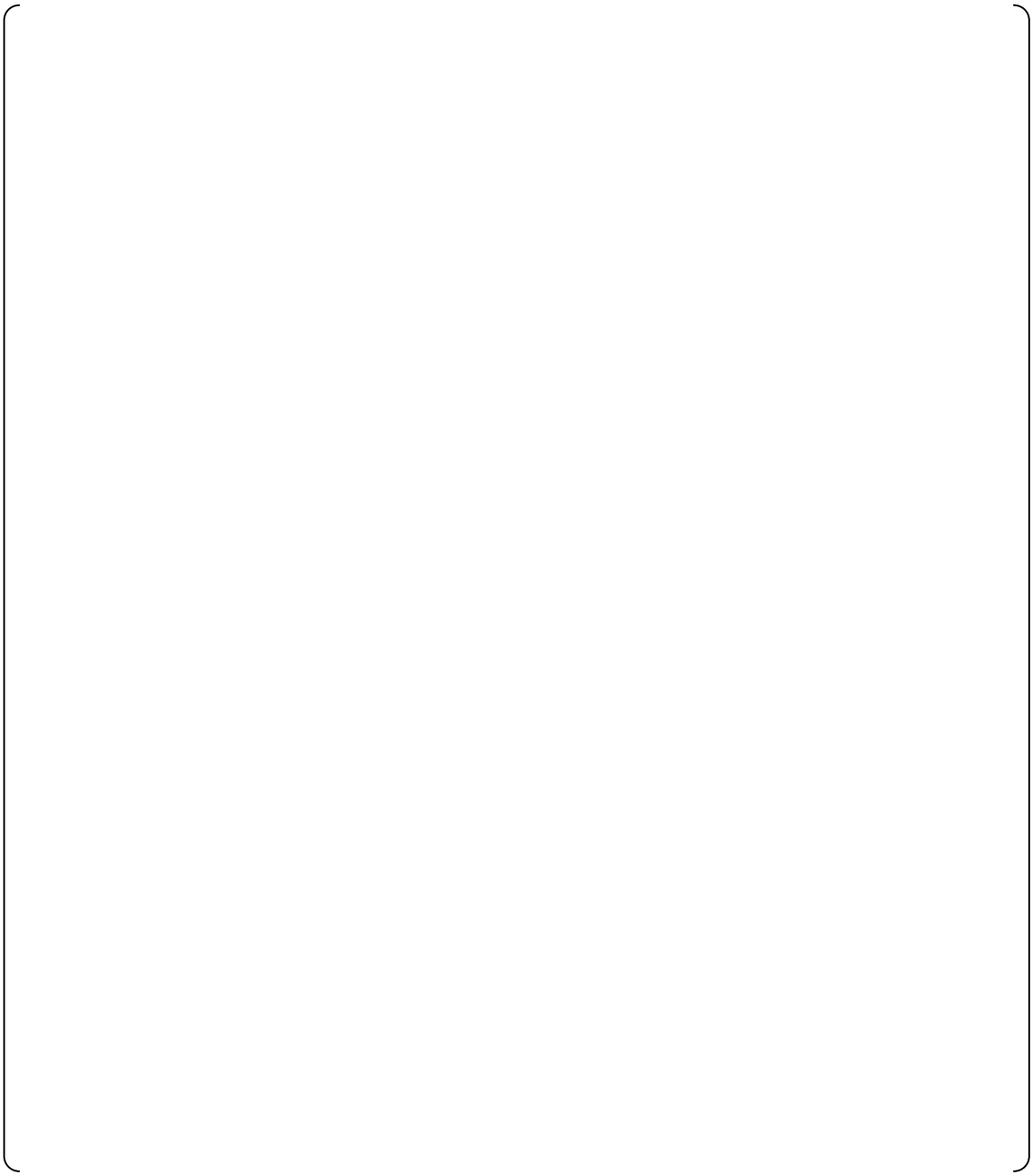

TS

Figure 2-24 PLUS7 Bottom Grid/Guide Thimble and Instrument Tube Joint & Connection

TS

Figure 2-25 PLUS7 Bottom Nozzle and P-Grid/Guide Thimble Joint & Connection

3. FUEL ROD DESIGN

3.1 Overview

The PLUS7 fuel had been developed to improve the fuel performance against the Guardian fuel. Table 3-1 shows the design differences between the PLUS7 fuel rod and the Guardian fuel rod. The key design features of the PLUS7 fuel rod with respect to the Guardian fuel rod are summarized as follows:

- Decrease in the fuel rod diameter from [ ] [TS] to reduce the fuel rod-induced pressure drop and to enhance neutron economy
- Axial blankets (low enriched UO_2) at the top and bottom of the fuel stack region of the UO_2 fuel rod to reduce neutron leakage
- Gadolinia (Gd_2O_3-UO_2) fuel rod as a burnable absorber
- Reduction of initial helium gas pressure in the fuel rod from [ ] [TS]
- Lower volume variable pitch plenum spring to increase void volume
- ZIRLO cladding to improve corrosion-resistance

The fuel rods consist of slightly enriched UO_2 cylindrical ceramic pellets and a round wire helical type 302 stainless steel compression spring, both encapsulated within a cladding and seal welded with Zircaloy-4 end caps. The fuel rods are internally pre-pressurized with helium during assembly. The pellets are dished at both ends in order to better accommodate thermal expansion and fuel swelling. The nominal density of the UO_2 pellets is [ ], [TS] which corresponds to [ ] [TS] of 10.96 g/cm^3, the theoretical density of UO_2.

The cladding tube is Westinghouse's 1% niobium-tin-iron zirconium based alloy, ZIRLO, having a microstructure comprising second phase precipitates homogeneous distributed throughout the zirconium matrix. The upper end cap has external features to allow remote underwater fuel rod handling during repair and reconstitution work. The lower end cap has an external tip which is seized by the gripper during fuel rod loading. It is round to minimize chances of damage to the grid dimples, springs, or straps during installation or removal of the rod. Compression spring located at the top of the fuel pellet column maintains the column in its proper position during handling and shipping.

3.2 Design Basis, Criteria and Evaluation

During normal operation, AOOs and postulated accidents, the analyses are performed to satisfy the design criteria to avoid fuel rod damage/failure as appropriate. The fuel rod design criteria include cladding stress, cladding strain, cladding fatigue, cladding corrosion/hydriding, fuel rod bowing, rod internal pressure, internal hydriding, cladding collapse, overheating of cladding, overheating of fuel pellet, excessive fuel enthalpy, pellet-to-cladding interaction, bursting, cladding embrittlement, violent expulsion of fuel, generalized cladding melting and fuel rod ballooning.

Each fuel rod design criterion is evaluated up to the peak rod average burnup of 60,000 MWD/MTU. The fuel rod integrity analyses of the PLUS7 fuel rod are performed using the fuel rod design codes considering the ZIRLO cladding.

3.2.1 Cladding Stress

(1) Basis

A fuel system will not be damaged due to excessive stress under normal operation including AOOs.

(2) Criteria

The stress acting on the cladding may cause fuel cladding failure. In order to prevent cladding failure due to excessive stress, the following criteria are considered.

- The primary tensile stresses in the cladding and end cap welds shall not exceed [ ] [ ] of the material at the applicable temperature during normal operation and AOOs.

- The primary compressive stresses in the cladding and end cap welds shall not exceed the [ ] of the material at the applicable temperature during normal operation and AOOs.

Even though the cladding yield strength increases due to the fast neutron flux during irradiation, the unirradiated cladding yield strength is conservatively used as the cladding stress design criterion.

(3) Evaluation

The method used to perform the stress analysis accounts for power dependent and time dependent changes (e.g., fuel rod void volume, fission gas release and gas temperature, differential cladding pressure, cladding creep and thermal expansion) that can affect stresses in the fuel rod cladding. The same analytical techniques are used for the evaluation of the PLUS7 design as for other Westinghouse CE PWR fuel designs [3-1].

The primary membrane cladding stress is resulted from the external load caused by the pressure difference between the system pressure and the rod internal pressure. The resulting differential pressures for the various operation conditions are used for primary stress, along with conservative-case cladding and end cap dimensions considering manufacturing tolerances. The calculated stresses are then compared to stress limits.

The results of the evaluation indicate that the primary tensile and compressive stresses in the cladding and end cap welds are within the allowable limits as shown in Table 3-2.

3.2.2 Cladding Strain

(1) Basis

Fuel system will not be damaged due to excessive strain under normal operation including AOOs.

(2) Criteria

In order to prevent fuel failure due to excessive strain, the following criteria are considered.

- At any time during the fuel rod lifetime, the plastic circumferential tensile cladding strain shall not exceed [ ] based on the beginning-of-life (BOL) cladding dimensions. This criterion is applicable to normal operating conditions and following a single AOO.

- For axial average fuel rod burnup greater than 52,000 MWD/MTU, the total (elastic plus plastic) circumferential cladding strain increment produced as a result of a single AOO shall not exceed [ ].[TS]

(3) Evaluation

The method used to evaluate the strain accounts for power dependent and time dependent changes (e.g., fuel rod void volume, fission gas release and gas temperature, differential cladding pressure, cladding creep and thermal expansion) that can produce strain in the fuel rod cladding. In addition, the strain analysis accounts for both long term, normal operating condition, and short term, transient condition. The methods used for the evaluation of the PLUS7 fuel cladding strain are the same as those of Westinghouse CE PWR fuel designs.

Under normal operating and transient operational conditions, the circumferential cladding strains are calculated using conservative rod internal pressures.

For the present application, the predicted plastic strain is [ ],[TS] and the total (elastic plus plastic) circumferential cladding strain increment produced as a result of a single AOO is [ ].[TS] As the calculated strains are less than [ ],[TS] the design criteria are satisfied.

3.2.3 Cladding Fatigue

(1) Basis

Fuel system will not be damaged due to excessive fatigue under normal operation including AOOs.

(2) Criteria

For the number and types of transients which occur during normal operation, end-of-life (EOL) cumulative fatigue damage factor in the cladding shall be less than [ ].[TS]

A fatigue analysis for the ZIRLO cladding is performed using the Langer-O'Donnell fatigue design curve. A safety factor of 2 on the stress or a safety factor of 20 on the number of cycles is imposed on this curve conservatively.

(3) Evaluation

Fatigue damage factor is calculated under daily power cycling. Its calculation accounts for power dependent and time dependent phenomena (e.g., fuel rod void volume, fission gas release and gas temperature, cladding creep and thermal expansion) that can produce cyclic straining of the fuel rod cladding. The cladding is assumed to conform to the predicted diameter of the pellet during periods of contact (i.e., elastic compression and hot pressing of the pellet are conservatively ignored). [ ][TS] is assumed throughout life. [ ][TS] are also represented.

The cumulative fatigue damage factor is determined by summing the ratios of the number of cycles in a given strain range to the permitted number in that range. The permitted number of cycles in any strain range is based on the Langer-O'Donnell fatigue design curve.

The fatigue design criterion is satisfied because the predicted fatigue damage factor is [ ].[TS]

3.2.4 Cladding Oxidation and Hydriding

(1) Basis

Fuel system will not be damaged due to excessive oxidation under normal operation including AOOs.

(2) Criteria

The best estimate cladding oxide thickness shall be less than [ ] [TS] during normal operation and AOOs.

The best estimate hydrogen content absorbed in cladding shall not exceed [ ] [TS] at end-of-life (EOL) during normal operation and AOOs.

(3) Evaluation

The cladding oxide thickness and hydrogen content of the PLUS7 fuel rod is evaluated by the same methods as are used for Westinghouse PWR fuel rod designs. The best estimate oxide thickness and hydrogen content at the end of irradiation are calculated with PAD corrosion model [3-2] during normal operation. Since cladding oxide thickness and hydrogen content do not increase during AOOs due to short time, oxide thickness and hydrogen content will not increase during AOOs.

The maximum cladding thickness and hydrogen content up to rod average burnup of 60,000 MWD/MTU are [ ] [TS] and [ ], [TS] respectively. The criteria of cladding oxide thickness and hydrogen content are satisfied.

3.2.5 Fuel Rod Internal Pressure

(1) Basis

Fuel system will not be damaged due to excessive rod internal pressure under normal operation.

(2) Criteria

- Liftoff Pressure

The fuel rod internal hot gas pressure shall not exceed the pressure that would cause an outward cladding creep rate exceeding fuel radial growth rate anywhere along the length of the rod.

- DNB Propagation

The fuel rod internal hot gas pressure shall be limited to below a value which could cause extensive departure from nucleate boiling (DNB) propagation to occur during transient and accident conditions. If the additional fuel failures due to excessive DNB propagation occur, the radiological dose consequences of DNB failures shall remain within the specified limits.

- Hydride Reorientation Pressure

The fuel rod internal hot gas pressure shall not exceed the pressure that causes hydride reorientation in cladding.

(3) Evaluation

The maximum rod internal pressures are evaluated using the FATES3B [3-3 and 3-4] in the same manners as are used for other Westinghouse CE PWR fuel rod designs. Maximum rod internal pressure is calculated using conservative biasing of nominal fuel rod data and will usually include additional uncertainty in the power levels representing each successive cycle of projected residency in the reactor core. The main parameters and rod power histories considered in representative fuel rod internal pressure are summarized in Table 3-3 and Figure 3-1, respectively.

- Liftoff Pressure

Critical pressure limits are determined by FATES3B fuel performance code based on the no clad liftoff pressure criterion. The critical pressure limit is the internal hot gas pressure where outward tensile creep of the cladding would just equal the fuel pellet swelling. Thus, fuel-clad gap separation due to pressure induced creep does not occur at or below this critical pressure limit.

The evaluation shows that the maximum rod internal pressures are [ ]^{TS} and [ ]^{TS} for the UO_2 rod and Gd_2O_3-UO_2 rod, respectively. Therefore, no clad liftoff criterion is satisfied since the calculated gas pressures are less than critical pressure limit.

- DNB Propagation

The methods used for the evaluation of cladding high temperature creep strain are the same as those of Westinghouse CE PWR fuel designs described in Reference 3-5. The time-dependent DNB transient local properties are obtained from the appropriate transient analysis methodology for any given plant. These inputs include time, heat flux, quality, mass flow, system pressure, rod internal pressure, and fuel rod initial geometry. To evaluate the potential for DNB propagation, the limiting DNB transients and internal pressure of [ ]^{TS} are used.

The results indicate that the clad strains induced by high temperature creep for limiting transients are less than [ ].^{TS} This amount of strain does not induce DNB propagation to adjacent fuel rods.

- Hydride Reorientation Pressure

The potential for hydride reorientation due to operation with internal pressure exceeding system pressure is evaluated.

The evaluation shows that hydride reorientation does not occur if the rod internal pressure is below [ ].^{TS} This assures that radial hydride reorientation will not occur for APR1400 fuel.

3.2.6 Internal Hydriding

(1) Basis

Fuel system will not be damaged due to excessive hydriding.

(2) Criteria

Primary hydriding is prevented by maintaining the level of moisture very low during the pellet manufacturing. The moisture content shall remain below the limit of [ ]^{TS} (hydrogen from all sources for fuel pellets).

(3) Evaluation

The hydrogen levels in the fuel pellet are maintained at very lower than the design criterion through manufacturing controls. Current PLUS7 fuel pellets have a total hydrogen content of less than [ ] [ ][TS] at 95% confidence. As a result of these controls, the failures due to internal hydriding have not experienced for PLUS7 fuel. [TS]

3.2.7 Cladding Collapse

(1) Basis

Fuel rod failure will not occur due to cladding collapse.

(2) Criteria

The radial buckling of the cladding in any fuel rod or burnable absorber rod shall not occur during reactor operation.

(3) Evaluation

The method used to evaluate the cladding collapse accounts for power dependent and time dependent changes (e.g., differential cladding pressures, cladding temperature, cladding flux, and oxide buildup) that can affect the ovalization of the cladding during operation. The same methods are used for the evaluation of the PLUS7 fuel rod designs as for other Westinghouse CE PWR fuel designs [3-6].

The rod internal pressure increases with fission gas accumulation in the pellet-cladding gap as burnup increases. However, to maximize the compressive cladding stress, the minimum rod internal pressure used in the cladding collapse analysis does not count the fission gas release.

The evaluation results of the cladding collapse in the active region indicate that the cladding collapse does not occur for both UO_2 rod and Gd_2O_3-UO_2 rod during entire fuel lifetime of 37,390 hours. The evaluation of cladding collapse in the plenum region demonstrated that PLUS7 plenum spring design provides sufficient radial support to the cladding to preclude collapse.

3.2.8 Overheating of Cladding

(1) Basis

Fuel rod failure will not occur due to the overheating of cladding under normal operation including AOOs.

(2) Criteria

There should be a 95-percent probability at the 95-percent confidence level that a hot fuel rod in the reactor core will not experience a DNB during normal operation or AOOs. For postulated accidents, the rods that experience DNB are assumed to fail for radiological dose calculation purposes.

(3) Evaluation

The evaluation for overheating cladding is addressed in plant specific transient and accident analysis (Chapter 15 of DCD).

3.2.9 Overheating of Fuel Pellets

1) Basis

Fuel rod failure will not occur due to the overheating of fuel pellets under normal operation including AOOs.

(2) Criteria

During normal operating and AOOs, the fuel centerline temperature shall not exceed the melting temperature accounting for degradation due to burnup and addition of burnable absorbers.

The fuel rod is considered to be failed [ ] [TS] during postulated accidents. In the event of fuel failure, the radiological consequences of fuel failure must be accounted in the dose calculations.

The melting temperature of UO_2 is taken to be 5,080°F (unirradiated) and to decrease 58°F per 10,000 MWD/MTU fuel burnup. For Gd_2O_3-UO_2 burnable absorber fuel rod, the melting temperature decreases additionally [ ] [TS] per weight percent of Gd_2O_3.

(3) Evaluation

The temperature of the fuel pellet is evaluated by the same methods as are used for Westinghouse CE PWR fuel designs.

The powers to fuel melting are calculated as a function of rod burnup. To preclude fuel melting, the peak local power experienced in normal operation and AOOs should be less than the power to fuel melting for rod burnup which is sufficient to ensure that the fuel centerline temperatures remain below the melting temperature at all burnups. Design evaluations for normal operation and AOOs have shown that fuel melting will not occur for achievable local powers up to rod average burnup of 60,000 MWD/MTU.

The linear heat rate corresponding to centerline melt of Gd_2O_3-UO_2 rod is always less than that of UO_2 rod. However, the low power of Gd_2O_3-UO_2 rod compared to UO_2 rods ensures that UO_2 rods remain limiting for centerline melt.

3.2.10 Excessive Fuel Enthalpy

(1) Basis
The number of fuel rod failures is not underestimated for postulated accidents.

(2) Criteria

The total number of fuel rods that must be considered in the radiological assessment is equal to the sum of all of the fuel rods failing each of the criteria below.

1. The high cladding temperature failure criteria for zero power conditions is a peak radial average fuel enthalpy greater than 170 cal/g for fuel rods with an internal rod pressure at or below

system pressure and 150 cal/g for fuel rods with an internal rod pressure exceeding system pressure. For intermediate (greater than 5% rated thermal power) and full power conditions, fuel cladding failure is presumed if local heat flux exceeds thermal design limits (DNBR).

2. The PCMI failure criteria is a change in radial average fuel enthalpy greater than the corrosion-dependent limit depicted in Figure B-1 in the NRC standard review plan, Revision 3.

(3) Evaluation

The evaluation for excessive fuel enthalpy is addressed in plant specific transient and accident analysis (Chapter 15 of DCD).

3.2.11 Pellet-to-Cladding Interaction (PCI)

(1) Basis

Fuel rod failure will not occur due to pellet cladding interaction(PCI) under normal operation including AOOs.

(2) Criteria

The following two related criteria are considered for normal operation and AOOs.

- The total (elastic plus plastic) strain during a single AOO shall not exceed 1%.

- Fuel melting does not occur.

(3) Evaluation

Evaluations on the cladding strain and fuel centerline melting are described in Sections 3.2.2 and 3.2.9, respectively. Based on such evaluation results, it can be concluded that the criteria regarding the pellet-to-cladding interaction are satisfied.

3.2.12 Bursting

(1) Basis

Fuel rod failures are permitted during postulated accidents, but they will be accounted for in the dose analysis.

(2) Criteria

To meet the requirements of 10 CFR 50.46, as it relates to ECCS performance evaluation, the ECCS evaluation model should include a calculation of the swelling and rupture of the cladding resulting. Regulatory Guide (RG) 1.157 provides guidelines for performing a realistic model to calculate the degree of cladding swelling and rupture.

(3) Evaluation

The evaluation of this criterion is addressed in plant specific transient and accident analysis (Chapter 15 of DCD).

3.2.13 Cladding Embrittlement

(1) Basis

Core geometry shall be such that the core remains amenable to cooling under postulated accidents.

(2) Criteria

The ECCS performance analysis must satisfy the fuel design criteria specified within 10 CFR 50.46(b). These criteria ensure a coolable core geometry by preserving adequate post-quench ductility in the fuel rod cladding. The current criteria require that (1) the peak cladding temperature remains below 2200 ^{O}F and (2) the peak cladding oxidation remains below 17 percent ECR.

(3) Evaluation

The evaluation of this criterion is addressed in plant specific transient and accident analysis (Chapter 15 of DCD).

3.2.14 Violent Expulsion of Fuel

(1) Basis

Coolability is always maintained.

(2) Criteria

1. Peak radial average fuel enthalpy must remain below 230 cal/g.
2. Peak fuel temperature must remain below incipient fuel melting conditions.
3. Mechanical energy generated as a result of (1) non-molten fuel-to-coolant interaction and (2) fuel rod burst must be addressed with respect to reactor pressure boundary, reactor internals, and fuel assembly structural integrity.
4. No loss of coolable geometry due to (1) fuel pellet and cladding fragmentation and dispersal and (2) fuel rod ballooning.

(3) Evaluation

The evaluation of this criterion is addressed in plant specific transient and accident analysis (Chapter 15 of DCD).

3.2.15 Generalized Cladding Melting

Generalized (i.e., nonlocal) melting of the cladding could result in the loss of rod-bundle fuel geometry. Criteria for cladding embrittlement in Section 3.2.13 above are more stringent than melting criteria. Therefore, additional specific criteria are not used.

3.2.16 Fuel Rod Ballooning

(1) Basis

Coolability is always maintained.

(2) Criteria

To meet the requirements of 10 CFR 50.46 as it relates to ECCS performance during accidents, the analysis of the core flow distribution must account for burst strain and flow blockage caused by ballooning (swelling) of the cladding. Those non-LOCA accidents that result in clad ballooning should examine the possibility of DNB propagation.

(3) Evaluation

The burst strain and flow blockage caused by ballooning (swelling) of the cladding are taken into account in the plant-specific LOCA analyses (Chapter 15 of DCD). The possibility of ballooning and DNB propagation is examined in the plant-specific non-LOCA analyses (Chapter 15 of DCD).

3.3 Fuel Performance Codes for Design Evaluation

The PLUS7 fuel rod is evaluated using the USNRC approved Westinghouse fuel rod design codes. The FATES3B[3-3 and 3-4] is used for the fuel rod integrity evaluations under normal operating and operational transient conditions. Since FATES3B does not have the capability to evaluate cladding corrosion behavior, the PAD code corrosion model [3-2] is used for corrosion calculation.

3.3.1 Applicability of FATES3B to PLUS7 Fuel

The FATES3B fuel performance code is generically applicable to PWR fuel. The various versions of FATES have historically been evaluated against an extensive variety of fuel rod design and power histories. The code applicability extends to all zircaloy clad UO_2 fuel pellets currently used in PWRs because the data base for FATES3B model development and for overall code verification includes a broad range of fuel designs and irradiation histories [3-3]. In conclusion, FATES3B is generically applicable for the PLUS7 fuel designs.

3.3.2 Applicability of PAD Code Corrosion Model to PLUS7 Fuel

The PAD corrosion model for ZIRLO cladding has been developed based on in-reactor corrosion data from [ ], [TS] which was licensed by NRC.

It has been well known that the corrosion behaviors of cladding are strongly dependent on plant operating conditions. The operating conditions involve linear heat generation rate, coolant inlet/outlet temperatures, and coolant chemistry. In order to confirm the applicability of corrosion model to APR1400 power plant, the key operating conditions [ ] [TS] and APR1400 power plant are compared in Table 3-4. In addition, the operating conditions of several representative Westinghouse type power plants in which ZIRLO cladding is applied are listed in Table 3-4.

As shown in Table 3-4, the plant operating of the APR1400 plant are within the operating experience of Westinghouse type plants as well as [ ].[TS] Therefore, the PAD code corrosion model can be applied to cladding oxide layer thickness calculations for the PLUS7 fuel design.

3.4 Conclusion

The PLUS7 fuel rod design is verified to maintain the rod integrity up to rod average burnup of 60,000 MWD/MTU based on the thermal performance and mechanical integrity evaluation results obtained by the design methodologies and design codes.

Table 3-1 Comparison of PLUS7 Fuel Rod with Guardian Fuel Rod

Parameter	
UO_2 Pellet	
Diameter, inches	
Length, inches	
Density (%TD)	
Enrichment(w/o U-235)	
Dish Configuration	
Chamfer	
Roughness, inches	
Gd_2O_3-UO_2 Pellet	
Diameter, inches	
Length, inches	
Density (%TD)	
Enrichment(w/o U-235)	
Gd_2O_3 Weight%	
Dish Configuration	
Chamfer	
Axial Blanket	
Configuration	
Enrichment (w/o U-235)	
Diameter, inches	
Pellet Length, inches	
Total Length, inches	
Axial Cutback	
Configuration	
Enrichment (w/o U-235)	
Diameter, inches	
Pellet Length, inches	
Total Length, inches	
Cladding	
Material	
Outer Diameter, inches	
Inner Diameter, inches	
Thickness, inches	
Roughness, inches	
UO_2 and Gd_2O_3-UO_2 Fuel Rod	
Stack Length, inches	
Pellet-to-Cladding Gap, inches	
Initial Helium Pressure, psig	
Plenum Length, inches	
Plenum Spring	
Plenum Spring Volume, in^3	
Plenum Volume, in^3	
Upper End Cap Length, inches	
Lower End Cap Length, inches	
Fuel Rod Length, inches	
Fuel Rod Pitch, inches	
Rod Internal Void Volume, in^3	

TS

Table 3-2 Cladding Stress Evaluation Results

TS

Table 3-3 Main Design Parameters Used for PLUS7 Fuel Rod Performance Analysis

TS

Table 3-4 Operating Conditions of APR1400 and Westinghouse Type Plants

TS

* M) Modified pH Control ** C) Coordinated pH Control

TS

Figure 3-1 Rod Power History Used for PLUS7 Fuel Rod Performance Analysis

4. IN-REACTOR PERFORMANCE OF PLUS7 FUEL

Four PLUS7 lead test assemblies (LTAs) were loaded into the fifth cycle of Ulchin unit 3 (UCN-3) to verify in-reactor performance. Figure 4-1 shows the fuel rods configuration of the PLUS7 LTAs and the fuel loading patterns from the fifth to the seventh cycles of UCN-3 where the four PLUS7 LTAs were loaded.

The inlet temperature of the UCN-3 reactor core is [ ]^{TS} at 100% power and the average power of the reactor core is [ ].^{TS} The effective full power days, the fuel assembly average burnup, and maximum fuel rod burnup of the LTAs are as shown in Table 4-1.

At the end of cycles 5, 6, and 7 of UCN-3, pool-side examinations (PSEs) of the LTAs were conducted. Among the four LTAs, the LTA of U3HA06 was only selected for the full-scope PSE since the four LTAs were manufactured with the same specifications and were loaded symmetrically in the reactor core. In addition, the U3HA03 LTA was examined for some additional information.

Since PSE results of the four PLUS7 LTAs confirmed that the PLUS7 fuel assembly and the fuel rod satisfied all the design criteria, PLUS7 fuel started its commercial supply to all OPR1000 reactors in Korea, starting from Ulchin unit 4 (UCN-4) cycle 6. Additionally, two twice burned assemblies and two thrice burned assemblies in Yonggwang unit 5 (YGN-5) cycle 5 were selected to be commercial surveillance assemblies (CSAs). At the end of cycles 5, 6, and 7 of YGN-5, PSEs of the CSAs were conducted. CSAs of KY5H605 and KY5H615 were burned during cycles 5, 6, and 7; KY5H520 and KY5H630 were burned during cycles 5 and 6. PSE results of the CSAs confirmed that the PLUS7 fuel assembly and the fuel rod satisfied all the design criteria.

Fuel assembly irradiation growth, fuel assembly bow and twist, rod-to-top nozzle axial clearance (shoulder gap), fuel rod bow, spacer grid width and cladding oxide thickness were measured during the PSE. The PSE results and evaluations for the LTAs are described in below sections.

4.1 Fuel Assembly Irradiation Growth

4.1.1 Measurement Method

A visual image recording technique with an underwater camera was used to measure the length change of irradiation-induced fuel assembly. Each length from the bottom nozzle to each grid and to the top nozzle was measured at the end of cycles.

4.1.2 Measurement Results and Evaluation

The irradiation-induced fuel assembly growth is used for evaluating the compatibility with the reactor internals and the interference between the top nozzle and the fuel rods. Fuel assembly growth is calculated by the differences between the initial fuel assembly length and the lengths after the first, second, and third cycle burnup. Table 4-2 and Figure 4-3 show the measurement value of the irradiation-induced fuel assembly length changes and an allowable design limit for maintaining the compatibility with the reactor internals. The maximum irradiation-induced growths of LTAs measured after the first, second, and third cycle burnup are [ ],^{TS} respectively. This shows that there is no effect of the PLUS7 fuel assembly irradiation growth on the reactor internals integrity since a sufficient margin exists for the PLUS7 assembly growth against the allowable design limit of [ ]^{TS} for the compatibility maintenance. The effect of the

assembly growth on the interference between the top nozzle and the fuel rod is described in Section 4.3.

4.2 Fuel Assembly Bow and Twist

4.2.1 Measurement Method

The assembly bow is measured from two adjacent faces of the assemblies. At first the line is installed on the right-hand side of the assembly. Then, the assembly bow is obtained for one face, measuring distance from the line to the adjacent assembly face. After rotating the assembly 90°, the assembly bow is obtained for the other face using the same method.

The assembly twist can be obtained by measuring the twist angle of the top nozzle with reference to the bottom nozzle or by measuring the twist angle of the bottom nozzle with reference to the top nozzle. In detail, two lines are installed on the right-hand side of the assembly at the front and back rows, respectively, and then the assembly twist angle is obtained by measuring an angle between the plane made by two lines and the adjacent face of the top and bottom nozzles.

4.2.2 Measurement Results and Evaluation

For U3HA03 and U3HA06 after three cycles of irradiation, the maximum assembly bows are [ ] [ ], respectively, and the maximum twist angles are [ ], respectively. Therefore, the PLUS7 LTAs have no impact on the CEA insertion and withdrawal, and the compatibility with the reactor internals, or on the fuel assembly unloading and loading.

4.3 Rod-to-Top Nozzle Axial Clearance (Shoulder Gap)

4.3.1 Measurement Method

The shoulder gap, which is defined as the distance between the lower surface of the top nozzle and the upper end of the fuel rod top end plug, is determined by the difference in the irradiation growth between the fuel rod and the fuel assembly. The shoulder gaps were measured for U3HA03 and U3HA06.

4.3.2 Measurement Results and Evaluation

The measured shoulder gap is used to check whether the interference between the fuel rod and the top/bottom nozzles occurs or not, and if it maintains a positive (+) value for the entire fuel lifetime. Table 4-3 and Figure 4-4 show the minimum measured shoulder gaps for U3HA03 and U3HA06 at the end of each cycle. After the burnup of three cycles, the measured minimum shoulder gaps are [ ] for U3HA03 and U3HA06, respectively. Therefore, as shown in this table and figure, the positive (+) value of the criteria for the shoulder gap is sufficiently satisfied.

4.4 Fuel Rod Bow

4.4.1 Measurement Method

To evaluate the PLUS7 fuel rod bow, peripheral rods of the U3HA03 and U3HA06 LTAs were selected and the rod-to-rod distances were measured at the middle of the adjacent grids.

4.4.2 Measurement Results and Evaluation

The fuel rod bow is used to check whether the DNBR penalty is to be imposed or not. The DNBR penalty is not imposed if the reduction of the fuel rod channel spacing due to the fuel rod bow is less than [ ] [TS] of the initial fuel rod channel spacing. Table 4-4 and Figure 4-5 shows the initial rod-to-rod spacing and the minimum measured rod-to-rod spacing for the U3HA03 and U3HA06 LTAs. The LTAs least fuel rod channel spacing measured at the end of their first, second, and third cycles' burnup are [ ],[TS] respectively, which sufficiently satisfy the criteria of [ ] [TS] of the initial fuel rod channel spacing.

4.5 Grid Width

4.5.1 Measurement Method

Using the Linear Variable Differential Transformer (LVDT), the grid widths were measured at four faces of nine mid-grids.

4.5.2 Measurement Results and Evaluation

The excessive growth of grid width caused by the neutron irradiation may have an impact on the fuel assembly unloading and loading. Hence, the neutron irradiation-dependent grid width is limited to less than the fuel assembly pitch to facilitate the assembly unloading and loading. The maximum grid widths were measured at the ninth grids. Table 4-5 and Figure 4-6 show the grid widths measured at the end of each cycle.

After the first, second, and third cycles of burnup, the measured grid widths of LTAs were [ ],[TS] [ ],[TS] respectively. The PLUS7 fuel assembly has a sufficient margin compared to the fuel assembly pitch [ ],[TS] so it was evaluated that the PLUS7 LTAs had no impact on the fuel assembly unloading and loading due to the irradiation growth of the grid.

4.6 Cladding Oxide Thickness

4.6.1 Measurement Method

The oxide layer thickness for fuel rods was measured by the Eddy Current Test (ECT). The measurements of oxide thickness were carried out for fuel rods up to rod average burnup of [ ] [TS] MWD/MTU.

4.6.2 Measurement Results and Evaluation

The measured oxide layer thicknesses of PLUS7 fuel rods with ZIRLO cladding along rod average burnup are shown in Figure 4-7. The maximum of the measured oxide thickness is about [ ],[TS] which is less than the oxide thickness design limit of [ ].[TS] Therefore, the performance of the PLUS7 fuel rod against cladding corrosion is confirmed.

Table 4-1 Burnup Data of PLUS7 LTAs

TS

Table 4-2 Irradiation Growths of the PLUS7 LTAs

TS

Table 4-3 Shoulder Gaps of the PLUS7 LTAs

TS

Table 4-4 Rod-to-Rod Gaps of the PLUS7 LTAs

TS

Table 4-5 Grid Widths of the PLUS7 LTAs

[ ] TS

TS

Figure 4-1 Configuration of Fuel Rods in PLUS7 LTAs

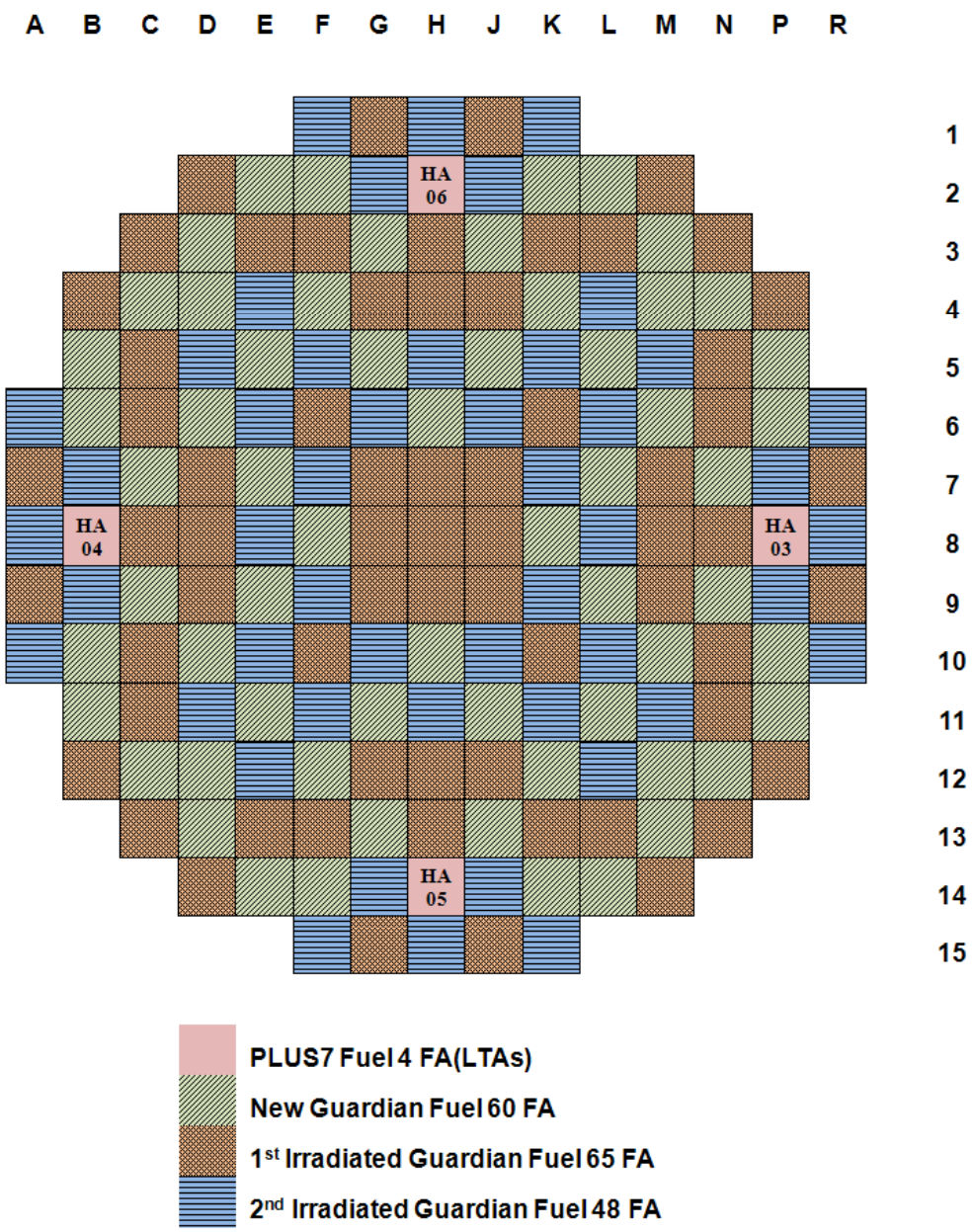

(a) The core of loading pattern of the UCN-3 5th cycle

Figure 4-2 Core Loading Pattern with PLUS7 LTAs

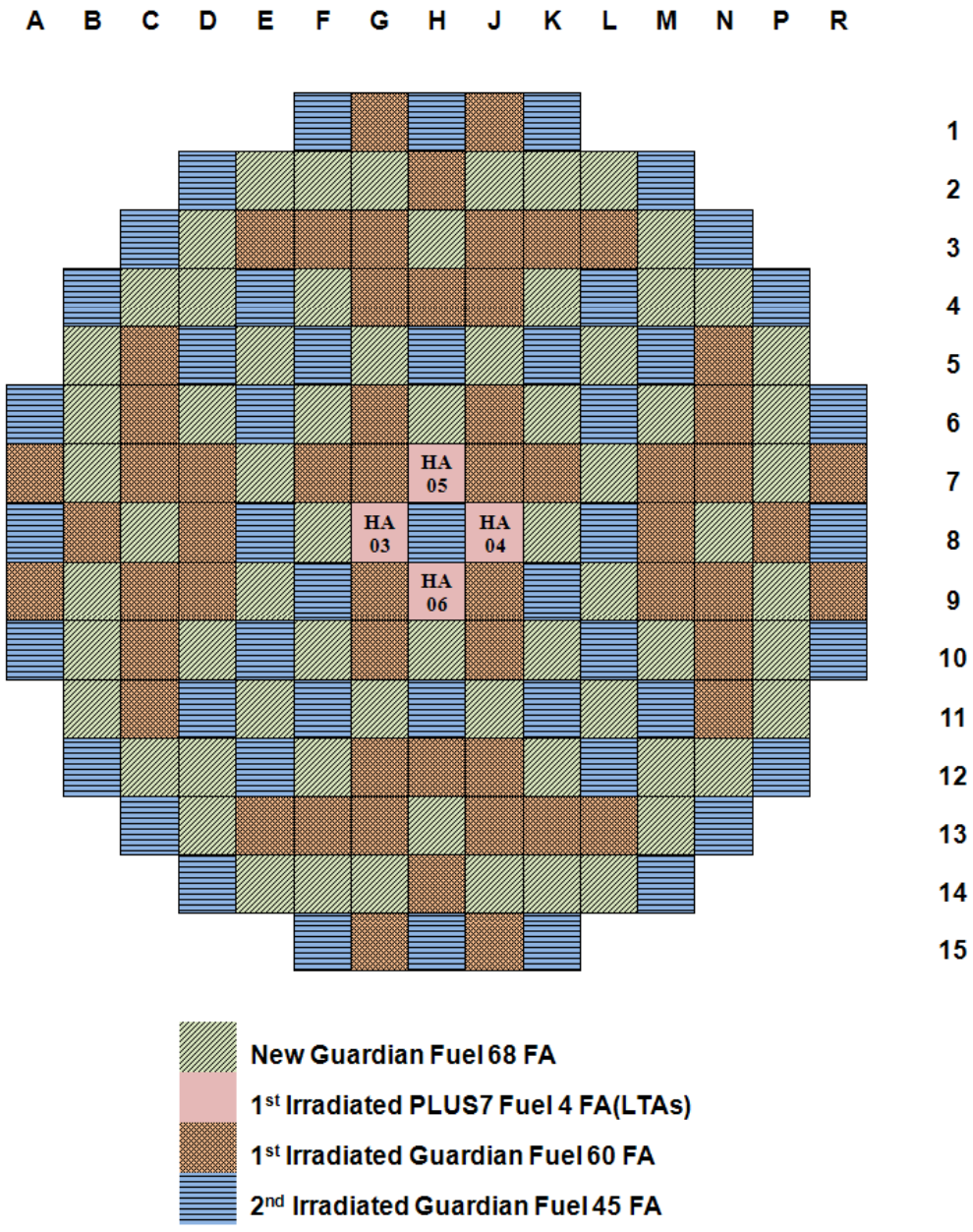

(b) The core of loading pattern of the UCN-3 6th cycle

Figure 4-2 Core Loading Pattern with PLUS7 LTAs (Continued)

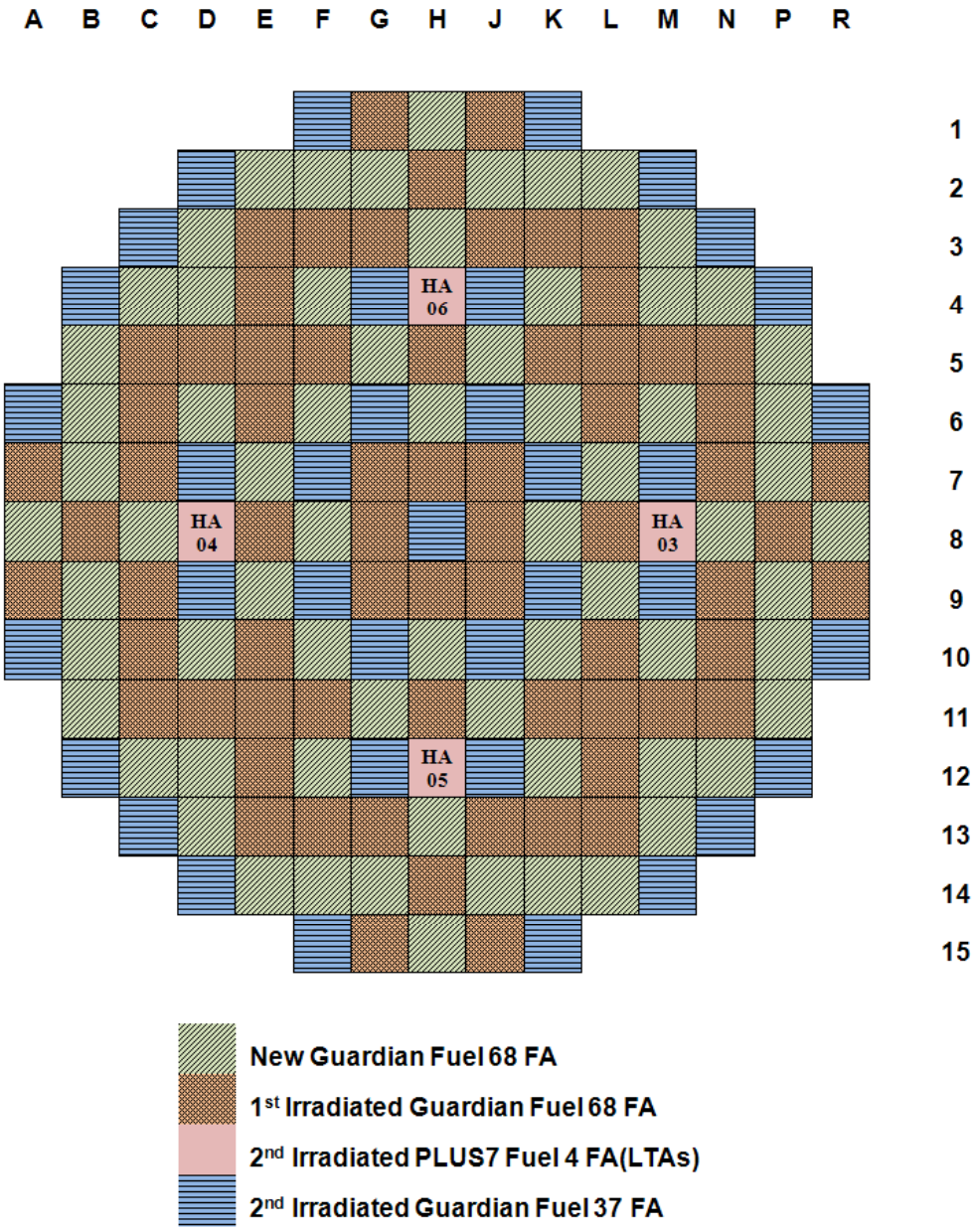

(c) The core of loading pattern of the UCN-3 7th cycle

Figure 4-2 Core Loading Pattern with PLUS7 LTAs (Continued)

TS

Figure 4-3 Measured Irradiation Growths of PLUS7 LTAs

TS

Figure 4-4 Measured Rod-to-Top Nozzle Clearances of PLUS7 LTAs

TS

Figure 4-5 Measured Rod-to-Rod Gaps of PLUS7 LTAs

TS

Figure 4-6 Measured Grid Widths of PLUS7 LTAs

TS

Figure 4-7 Measured Cladding Oxide Layer Thickness of PLUS7 LTAs

5. COMMERCIAL OPERATING EXPERIENCES OF PLUS7 FUEL

KNF has developed advanced PWR fuel for the OPR 1000s, PLUS7, because Guardian fuel for the OPR 1000s was not enough to meet Korean customers' requirements, such as sufficient overpower margin to employ full low leakage loading patterns as well as safe implementation of power uprating, elimination of fuel failure attributable to grid-to-rod fretting wear and debris, better fuel economics, fuel integrity maintenance even at high burnup beyond the current licensed burnup of 60,000 MWD/MTU. For these purposes, PLUS7 fuel development activities, such as fuel assembly and its components design, their manufacturing technology, out-of-pile mechanical /thermal/hydraulic/vibration characteristic tests, were performed from 1999 to 2001 as shown in Figure 5-1.

Four PLUS7 lead test assemblies (LTAs) were loaded into the fifth cycle of Ulchin unit 3 in December of 2002. The first commercial operation of PLUS7 fuel started in Ulchin-4 Cycle 6 in 2006 (Refer to Sec B.1). More than 2,300 PLUS7 fuel assemblies had been loaded in all OPR 1000 NPPs in Korea (Yonggwang-3, 4, 5 & 6, Ulchin-3, 4, 5 & 6) by 2012 (see Table 5-1). All OPR 1000s have equilibrium cores with PLUS7 fuel now. Shin-Kori unit 1&2 and Shin-Wolsung units 1&2 are scheduled to load PLUS7 fuel from their second cycles. PLUS7 fuels will be loaded into APR 1400s from the initial cores.

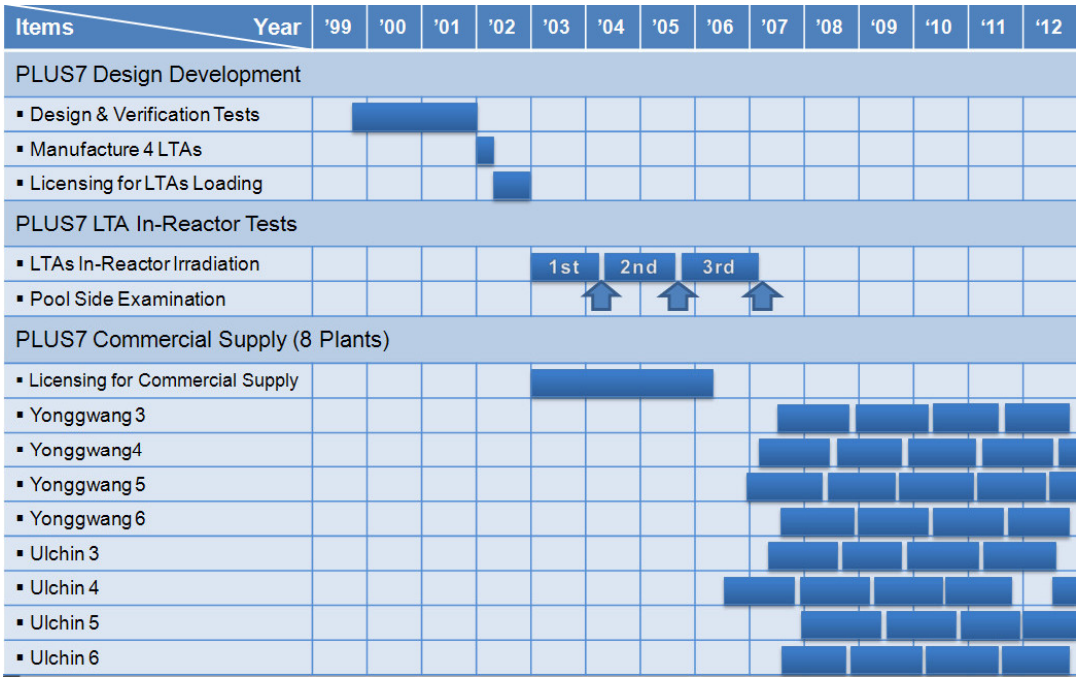

Figure 5-1 Development & Commercial Supply Status of PLUS7

Table 5-1 Commercial Loading of PLUS7 up to 2012

TS

6. CONCLUSION

PLUS7 fuel has been developed to improve fuel performance relative to Guardian fuel. The integrity and safety evaluation results for fuel assembly and fuel rods are summarized as follows.

- Fuel assembly and its components design

The performance of the PLUS7 fuel assembly and its components was evaluated. The evaluation results showed that the PLUS7 fuel assembly met all the design criteria related to the in-reactor mechanical integrity. It was confirmed that the PLUS7 fuel assembly and its components were irradiated within the design limit based on the in-reactor performance data measured for the PLUS7 fuels.

- Fuel rod design

The thermal performance and mechanical integrity of the PLUS7 fuel rods adopting ZIRLO cladding were evaluated up to the maximum fuel rod average burnup of 60,000 MWD/MTU. The results confirmed that the PLUS7 fuel rod satisfied all the design criteria related to the rod thermal performance and mechanical integrity. It was confirmed that the PLUS7 fuel rods have been irradiated within the design limit based on the in-reactor performance data measured for the fuel rods in PLUS7 fuels.

7. REFERENCES

3-1 WCAP-16500-P-A, Rev.0 “CE 16x16 Next Generation Fuel Core Reference Report,” August 2007.

3-2 WCAP-15063-P-A, Rev.1, with Errata, “Westinghouse Improved Performance Analysis and Design Model (PAD4.0),” July 2000.

3-3 CEN-161(B)-P Supplement 1-P-A, “Improvements to Fuel Evaluation Model,” January 1992.

3-4 CENPD-404-P-A, Rev.0 “Implementation of ZIRLO™ Cladding Material in CE Nuclear Power Fuel Assembly Designs,” November 2001.

3-5 CEN-372-P-A, “Fuel Rod Maximum Allowable Gas Pressure,” May 1990.

3-6 CENPD-187-P-A, “CEPAN Method of Analyzing Creep Collapse of Oval Cladding,” Combustion Engineering, Inc., April 1976; Supplement 1-P-A, June 1977.

3-7 APR1400-F-C-TR-12002-P, Rev.0, “KCE-1 Critical Heat Flux Correlation for PLUS7 Thermal Design,” November 2012.

Appendix A

Summary of PLUS7 Fuel Assembly Tests

November 2012

TABLE OF CONTENTS

LIST OF TABLES

LIST OF FIGURES

A.1.0 INTRODUCTION

The following tests were conducted to verify the hydraulic and mechanical characteristics of the PLUS7 fuel assembly:

Test Item	Test Objectives	Facility
1. Fuel Assembly Vibration Test	To determine the flow induced fuel assembly vibration characteristics	FACTS
2. High Frequency Vibration Test	To determine the high frequency vibration (HFV) characteristics of mid grid designs	VISTA
3. Fuel Rod Fretting Wear Test	To evaluate the fuel rod fretting wear	VIPER
4. Mid Grid Crush Test	To obtain dynamic strength and stiffness	Grid Impact Tester
5. Top Nozzle Mechanical Test	To obtain strain levels and displacements of the adapter plate and holddown plate at selected locations as a function of axial loading	FA Test Facility
6. DFBN Mechanical Test	To obtain fuel assembly mechanical characteristics	FA Test Facility
7. Grid Hang-up Test	To confirm FA to FA grid hang-up performance	FA to FA test
8. FACTS Hydraulic Pressure Drop Test	To measure the fuel assembly and component pressure drop	FACTS
9. Grid Spring Test	To determine the inner and outer cell spring load deflection characteristics of grid assemblies.	Grid Spring Tester
10. Fuel Assembly Lift-off Test	To determine the flow rates at which the fuel assembly lifts off	FACTS

A.2.0 SUMMARY OF TESTS

A.2.1 Fuel Assembly Vibration Test (FACTS)

1.0 Introduction and Objectives

The objective of this test is to confirm that the PLUS7 design is not susceptible to high resonance flow-induced assembly vibration over a range of plant operating flow rates. This is assessed by reviewing the vibration spectra from displacement transducers (see Figure A.2.1-1) and the instrumented fuel rod accelerometers for the presence of abnormal, flow-dependent, resonant vibration peaks. The absence of such peaks will be sufficient to determine the acceptability of the fuel assembly design.

2.0 Test Conditions

The test flow conditions were systematically varied in an effort to excite the vibration modes of the fuel assembly. Such a variation consisted of setting the loop at the required temperature of [ ] [ ] [TS] and sweeping the loop flow rate from [ ] [TS] to the maximum achievable flow rate. The flow rate was then returned to [ ] [TS] at a same rate. The maximum achievable flow rate for this test was [ ].[TS] The PLUS7 fuel assembly will be placed at [ ].[TS] The equivalent mechanical design flow in the FACTS test is [ ].[TS] Although the FACTS loop could not reach the elevated test flow rate [ ],[TS] the maximum achievable flow rate does bound all possible operating flow rates, representing over 117% of the best estimate flow [ ],[TS] which is the flow rate at which PLUS7 fuel assembly will be placed. The maximum achievable flow rate is more than adequate to confirm that the PLUS7 design does not exhibit flow-induced resonant fuel assembly vibration.

3.0 Test Results

The flow sweep test was performed at [ ].[TS] In this test, the loop flow rate was increased in a constant manner from [ ] [TS] to the maximum achievable loop flow rate of [ ] [TS] [ ][TS] in six minutes. Because the instrumented rod accelerometers were mounted at mid-grid elevations with as-built cell conditions, the accelerometer outputs represent the fuel assembly vibration.

Figure A.2.1-2 shows that the assembly did not experience the high resonance flow-induced fuel assembly vibration. There was no indication of abnormal flow-induced vibration response throughout the test flow range.

4.0 Summary and Conclusion

A FACTS loop test was conducted to verify that the PLUS7 design did not exhibit high resonance flow-induced fuel assembly vibration. Displacement transducers and instrumented fuel rods at grid locations measured the fuel assembly vibration. There was no indication of abnormal flow-induced vibration response throughout the test flow range.

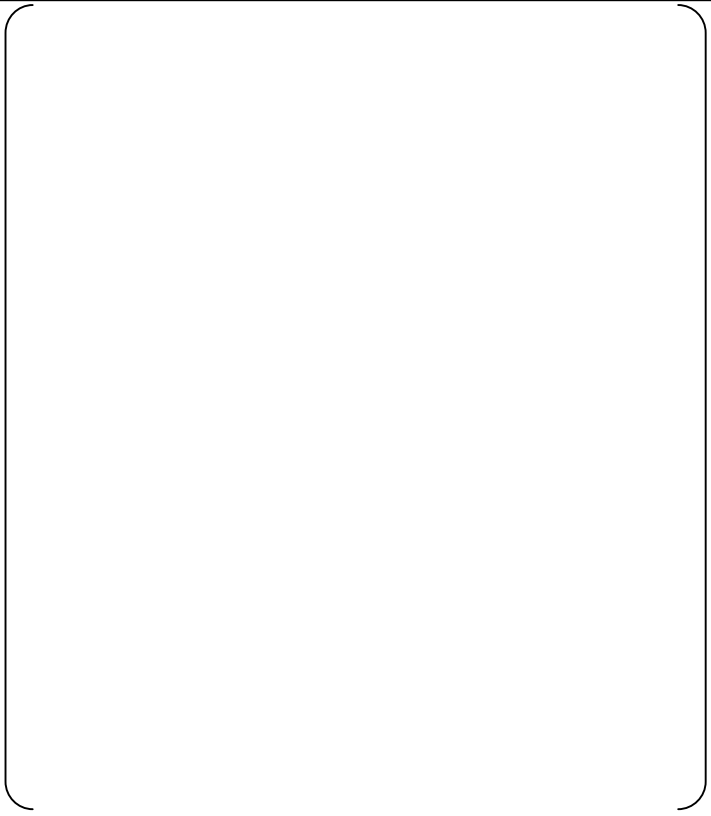

TS

Figure A.2.1-1 Placement of Inductive Displacement Transducers and Flow Housing Accelerometer

TS

Figure A.2.1-2 Results of Vibration Test on PLUS7 Fuel Assembly

A.2.2 VISTA High Frequency Vibration Test: Mid grid Designs

1.0 Introduction and Objectives

The objective of these hydraulic tests is to determine the high frequency vibration (HFV) characteristics of PLUS7 mid grid designs in the Vibration Investigation of Small-scale Test Assemblies (VISTA) test loop. The HFV characteristics are determined by subjecting the mid grid designs to the test conditions.

2.0 Test Conditions

The HFV testing was performed by varying the bundle velocity in a range from [ ].[TS]

For the PLUS7 design, the in-core flow rates would vary from [ ].[TS] The mid grid designs were tested over the [ ] [TS]range to bound the actual in-core flow rates. Loop temperature was maintained at approximately [ ],[TS] using the tank heat exchanger as required. The loop pressure increased with an increasing velocity with a peak pressure of [ ] [TS] at the maximum bundle velocity [ ] [TS] tested.

3.0 Test Results

For each grid design, multiple face 1 cells (See Figure A.2.2-1) of grid #4 were investigated at different locations on each panel. This was done to find the peak panel and point vibrations.
Figure A.2.2-3 shows that the PLUS7 design has an acceptable HFV response since the HFV is significantly low in the operating rage.

4.0 Summary and Conclusion

This test is for high frequency vibration (HFV) testing of PLUS7 mid grid designs. This testing was done in the Vibration Investigation of Small-scale Test Assemblies (VISTA) hydraulic test loop. The following points can be concluded from the results presented in this test:

- The PLUS7 mid grid has significantly low HFV.
- The PLUS7 design has an acceptable HFV response.

TS

Figure A.2.2-1 High Frequency Vibration Measurement Position

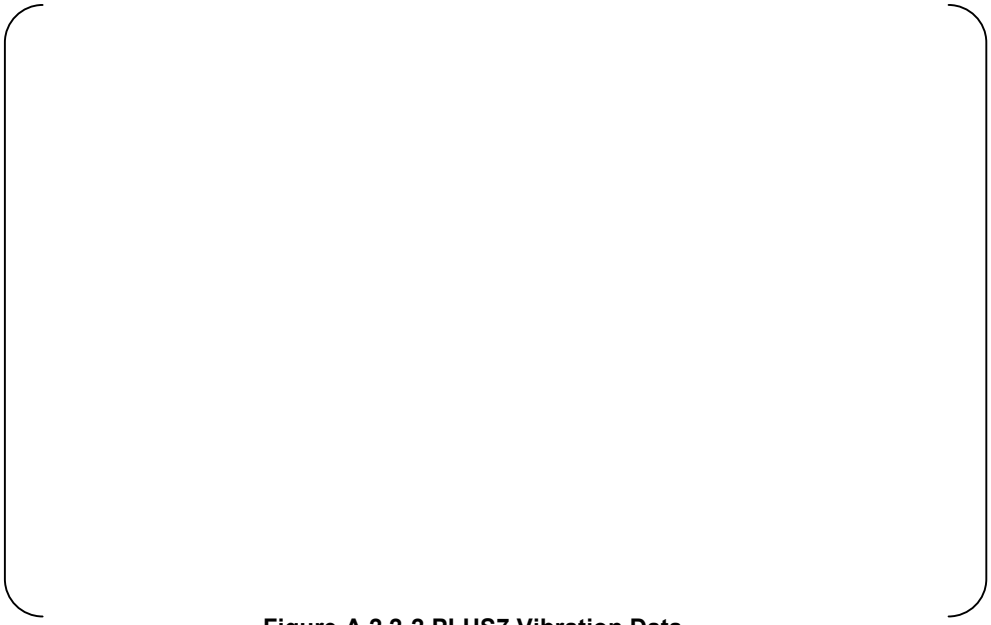

TS

Figure A.2.2-2 PLUS7 Vibration Data

TS

Figure A.2.2-3 PLUS7 Vibrometer Data

A.2.3 VIPER PLUS7 Fuel Assembly Long-Term Wear Test

1.0 Introduction and Objectives

In this test, a PLUS7 fuel assembly with mixing vanes and a Guardian fuel assembly without mixing vanes were placed in the loop side by side. The PLUS7 fuel assembly consists of a reconstitutable top nozzle, a debris filter bottom nozzle, 4 ZIRLO guide thimbles and an instrument tube with a 0.98 inch diameter, 236 ZIRLO fuel rods with a 0.374 inch diameter, Inconel top and bottom grids, 9 ZIRLO mid grids, and an Inconel protective grid. The Guardian fuel assembly consists of a reconstitutable top nozzle, a standard bottom nozzle, 4 Zry-4 guide thimbles and an instrument tube with a 0.98 inch diameter, 236 Zry-4 fuel rods of 0.382 inch diameter, 10 Zry-4 grids, and an Inconel bottom grid. These two assemblies have nearly the same grid spacing. The PLUS7 ZIRLO mid grids have conformal spring and dimple features, while the Guardian Zry-4 mid grids and the top grid have wavy spring and dimple features.

Test objectives:

- To obtain grid-rod fretting wear data for the PLUS7 in a transition core environment and severe flow conditions

The test acceptance criteria for PLUS7 test assembly are as follows:

- Oxidized rods located in realistic gap cells [ ],[TS] when projected to the expected operating life of the assembly, will not result in wear through the cladding

2.0 Test Conditions

The duration of the long-term wear test was 500 hours. The axial flow was intended to remain at [ ].[TS] The average test conditions are listed below.

Table A.2.3-1 Test Loop Conditions

[ ][TS]

3.0 Test Results

The PLUS7 assembly had a combination of pre-oxidized rods and non-oxidized rods in a checkerboard pattern. Figure A.2.3-1 shows the locations of rods with wear in the assembly. The value in a cell is the maximum depth of the worst dimple or spring wear scar on each rod. Figure A.2.3-2 shows the wear scar grid elevations corresponding to Figure A.2.3-1 and the order of the grid number in each cell corresponds to the wear severity up to three grids. A bar chart, Figure A.2.3-3, shows the wear scar distribution along the grid elevation.

Some observations and conclusions are obtained from the PLUS7 assembly wear results.

1. Under the axial flow test conditions and using the normal size flow housing with non-perforated side walls, the PLUS7 assembly wear pattern showed a basic random distribution radially. Since

Guardian assembly and PLUS7 assembly had different pressure drops at local mid grid and mid-span, some local cross flow was generated between two assemblies. Even though the wear at the side facing Guardian assembly was slightly higher, deep wear also occurred in the other side. The effect of local cross flow was not significant.

2. The rods in [ ]^{TS} gap cells showed less wear than those in [ ]^{TS} gap cells. Eight rods showed wear scars in the [ ]^{TS} gap cells. Three rods in [ ]^{TS} gap cells had over [ ]^{TS} deep wear (all three scars were single dimple wears). The maximum wear depth in a [ ]^{TS} gap cell was [ ]^{TS} from a spring wear scar (See Figure A.2.3-1).

3. Non-oxidized rods had less wear resistance than oxidized rods. None of the oxidized rods showed wear while 60 non-oxidized rods showed measurable wear.

Table A.2.3-2 PLUS7 Assembly Measurable Wear Scar

[ ]^{TS}

Figure A.2.3-3 shows the wear distribution along grid elevations. Each mid grid had relatively even wear. Grid 2 has the least wear and Grid 8 has the most wear.

4.0 Summary and Conclusion

This test is for the long-term wear test of the PLUS7 fuel assembly and Guardian fuel assembly. The PLUS7 and Guardian fuel assemblies were tested in the VIPER loop residing side by side for 500 hours. The total loop axial flow was [ ].^{TS}

This test was to verify the adequacy of the PLUS7 design. The vibration signals of the instrumented rods showed that the fuel assembly and fuel rods did not experience any abnormal flow-induced vibration. Every rod in the PLUS7 test assembly (including instrumented rods) was examined for grid-rod fretting wear, and all fretting wear scars were measured using the Accumeasure System 9000 tool to determine the fretting wear depth. Since all oxidized rods in [ ]^{TS} gap cells had no measurable wear, the PLUS7 test assembly met the test acceptance criteria.

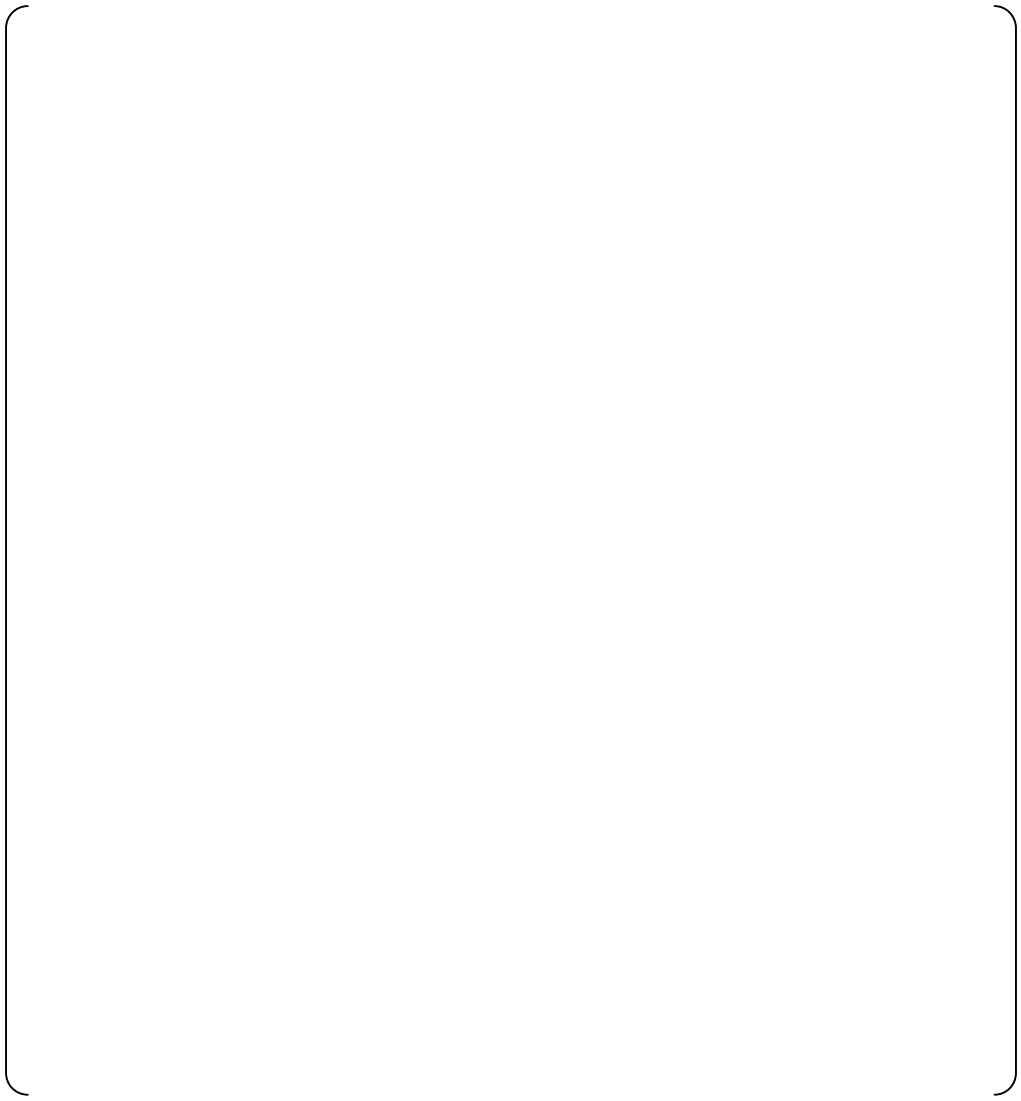

TS

Figure A.2.3-1 Fretting Wear Scar Locations

TS

Figure A.2.3-2 Fretting Wear Scar Elevations

TS

Figure A.2.3-3 PLUS7 Assembly Wear Scar Distribution Along Grid Elevations

A.2.4 Mid Grid Crush Test

1.0 Introduction and Objectives

The dynamic crush strength of the mid grid is required to obtain the structural characteristics to show that both seismic and LOCA loads are met.
The specific test objectives for the dynamic crush test of the PLUS7 ZIRLO mid grid design at elevated temperatures were as follows:

- To obtain the impact force as a function of impact velocity
- To determine the grid ultimate load capability
- To characterize the grid failure mode
- To obtain the data to determine the grid dynamic stiffness

2.0 Test Conditions

The dynamic crush test was performed at operating temperature and the pendulum inertial mass was calculated as the weight of one span of PLUS7 fuel assembly.

The pendulum angle was increased by 1° from 7° until grid crushed.

- Elevated temperature: 600°F±20°F
- Pendulum inertial mass: [ ]^{TS}
- Pendulum initial angle: 7°

3.0 Test Results

Twelve grid crush tests were sequentially performed. The PLUS7 ZIRLO mid grid crush test results are summarized as follows:

Table A.2.4-1 PLUS7 ZIRLO Mid grid Crush Test Results

[ ]^{TS}

4.0 Summary and Conclusion

The crush strength values for the PLUS7 ZIRLO mid grid tested with rod-in-cell are shown in Figure A.2.4-3.

A summary of the dynamic crush test results is as follows:

- Dynamic Crush Strength:

- The lower 95% confidence value of true mean is [ ]. [TS]

- Dynamic Grid Stiffness:
  - The average dynamic stiffness using an impact duration method is [ ]. [TS]

- Impact Performance Factor:
  - The impact performance factor $(P/\sqrt{K})$ for the test sample is [ ]. [TS]

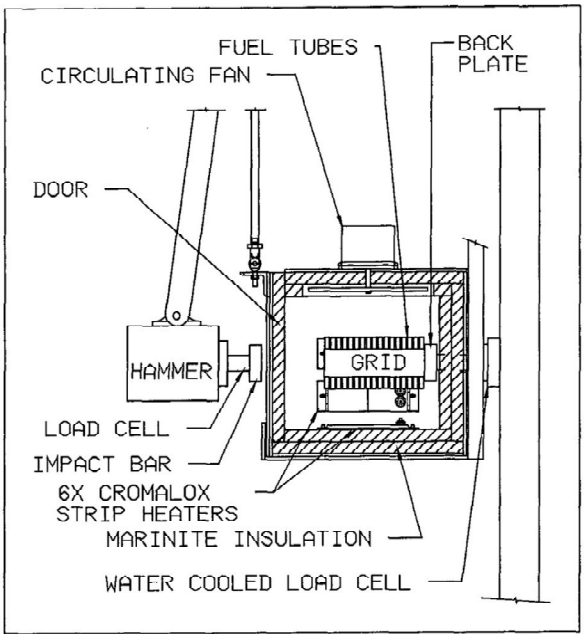

Figure A.2.4-1 Dynamic Crush Test Apparatus Detail

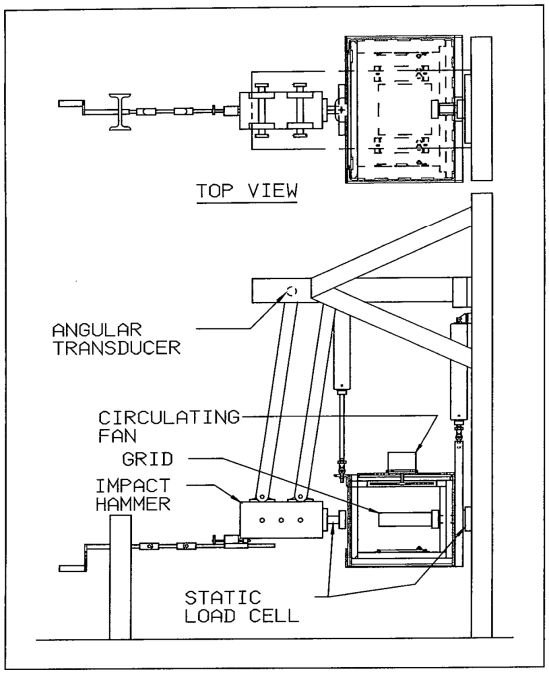

Figure A.2.4-2 Dynamic Crush Test Apparatus

TS

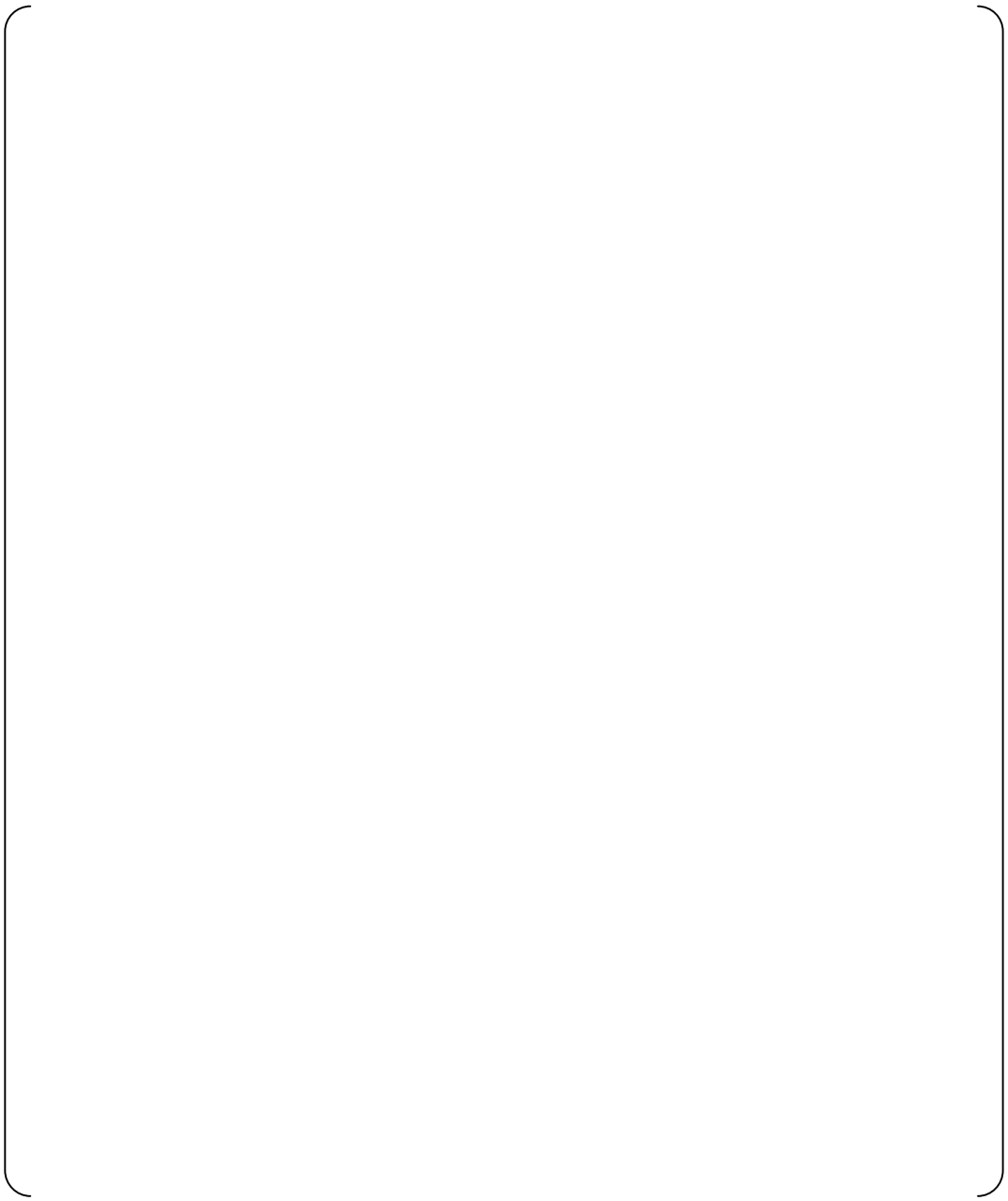

Figure A.2.4-3 Impact Velocity versus Impact Force

A.2.5 Top Nozzle Mechanical Test

1.0 Introduction and Objectives

The objectives of this test were to obtain displacements of the holddown plate as a function of axial loading.

The specific test objectives were as follows:

- To obtain the deflection characteristics of the holddown plate as a function of applied load
- To obtain the stiffness of the holddown spring

Loads applied in the test corresponded to the following:

- Shipping and handling load (> 4g)
- Holddown load (up to 0.05 inch above the holddown spring solid height)

2.0 Test Conditions

The PLUS7 top nozzle was tested in air at room temperature using an Instron Universal Testing Machine. The test arrangements used to perform the PLUS7 top nozzle test are shown in Figures A.2.5-1 through A.2.5-3.

3.0 Test Results

3.1 Shipping Load Test

The [ ]^{TS} load was applied on the top surface of the inner extension. The load was transmitted to directly the guide thimble through the inner extension. The maximum relative deflection on the holddown plate was [ ]^{TS} and the holddown plate elastically returned to its original shape when the loads were removed.

The deflection indication demonstrated that the PLUS7 top nozzle design met the design criterion that the dimensional stability be maintained.

3.2 Handling Load Test

The [ ]^{TS} load was applied on the bottom surface of the holddown plate by the handling tool. The maximum relative deflection on the holddown plate was [ ]^{TS} and the holddown plate elastically returned to its original shape when the loads were removed.

The deflection indication demonstrated that the PLUS7 top nozzle design met the design criterion that the dimensional stability be maintained.

3.3 Holddown Load Test

The holddown spring was deflected by [ ]^{TS} from the as-assembled condition for the first loading cycle. The holddown plate elastically returned to its original location when the loads were removed. The stiffness of the four assembled holddown springs for the first loading and unloading cycles were [ ],^{TS} respectively. The average stiffness per one holddown spring for the first loading and unloading cycle was[ ]^{TS} and these values

met the drawing requirements of [ ].[TS] In the second loading and unloading cycle, the deflection of [ ] [TS]was applied. The stiffness of the four assembled holddown springs for the second loading and unloading cycles were [ ],[TS] respectively. The average stiffness per one holddown spring for the second loading and unloading cycle was [ ] [TS] [ ][TS] and [ ][TS] and these values met the drawing requirements. Figure A.2.5-4 shows the load deflection characteristics of the holddown spring.

4.0 Summary and Conclusion

The mechanical test of the PLUS7 top nozzle was performed to determine if the system met all the test objectives. The material deflections under load and permanent deformation after loading were characterized for load conditions of [ ][TS] shipping and handling and a holddown spring deflection of 0.05 inch above the spring solid height.

For the 4g shipping and handling load conditions, the deflection indications showed that deformation of the top nozzle remained elastic, and the dimensional stability was maintained. The holddown plate was slightly deformed when the [ ][TS] lifting load was applied but elastically returned to its original shape when the load was removed.

For the holddown load condition, the load deflection data and test observations demonstrated that the PLUS7 top nozzle met the design criteria for the structural integrity and holddown spring repeatability.

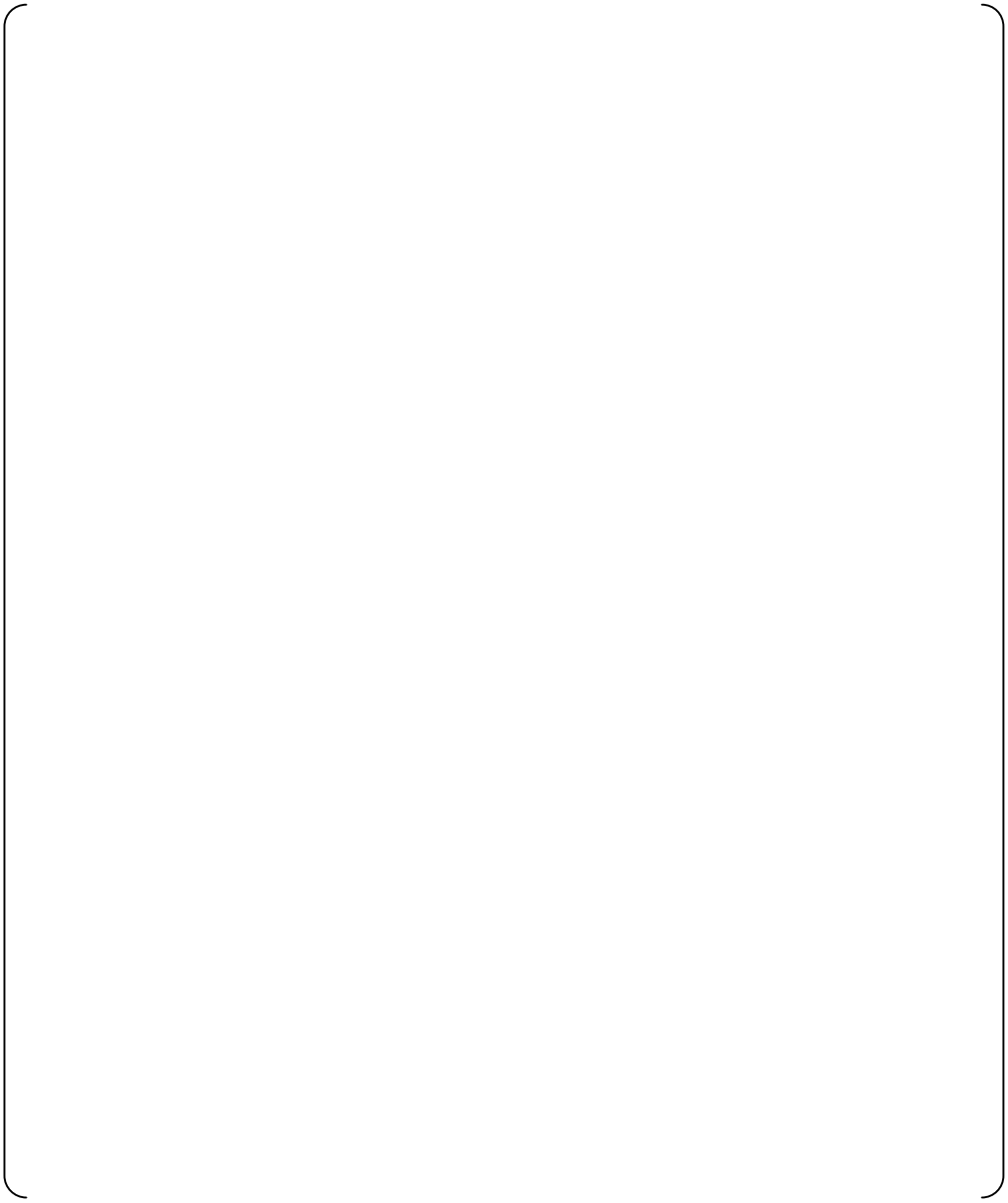

TS

Figure A.2.5-1 Shipping Test Setup

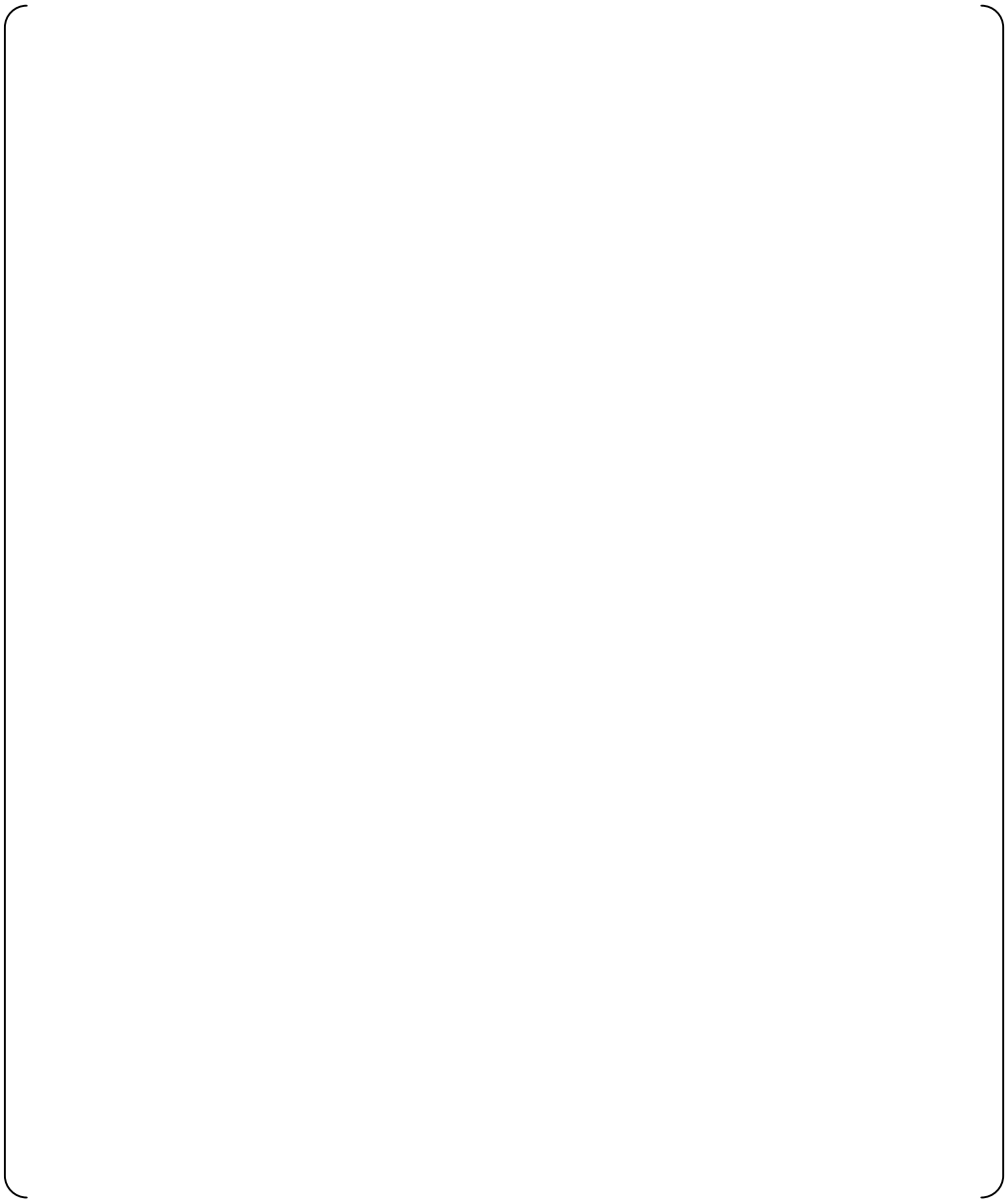

TS

Figure A.2.5-2 Handling Test Setup

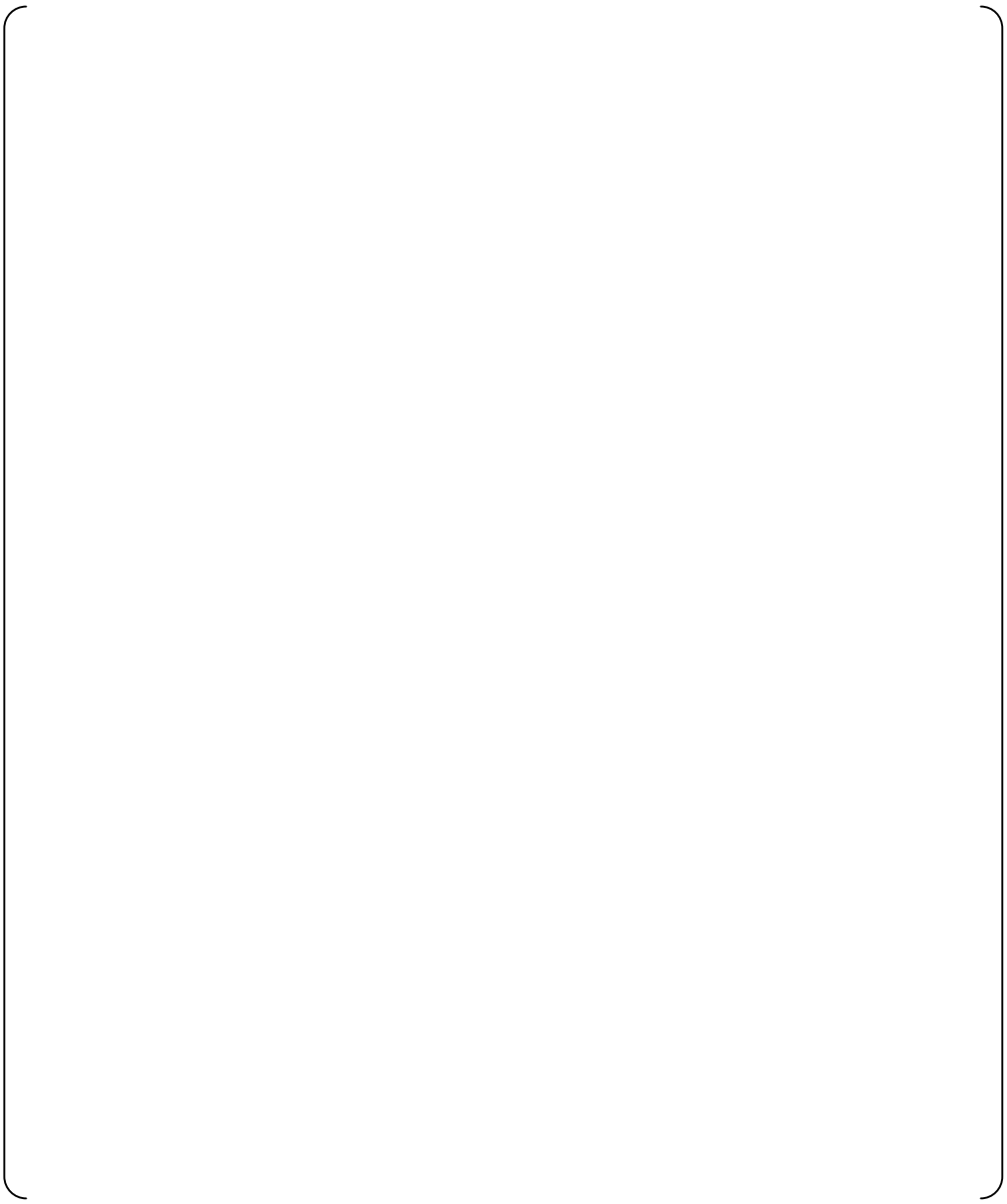

Figure A.2.5-3 Holddown Load Test Setup

TS

Figure A.2.5-4 Holddown Spring Load Deflection Curve

A.2.6 DFBN Mechanical Test

1.0 Introduction and Objectives

The objectives of this test were to obtain displacements of the adapter plate as a function of the axial loading.

The specific test objectives were as follows:

- To obtain the deflection characteristics of the bottom nozzle as a function of the applied load

Loads applied in the test corresponded to the following:

- Shipping and handling load (> 4g)
- LOCA load [ ].[TS]

These axial loads were applied to the adapter plate of the DFBN at the guide thimble locations. The axial loading was applied through a set of Belleville washers to simulate the stiffness of the fuel assembly.

2.0 Test Conditions

The PLUS7 DFBN was tested in air at room temperature using an Instron Universal Testing Machine. The test arrangements used to perform the PLUS7 DFBN test are shown in Figures A.2.6-1 and A.2.6-2.

3.0 Test Results

3.1 Shipping and Handling Load Test

The load cycles to [ ][TS] (> 4g shipping and handling load) was applied on the adapter plate of the DFBN. The largest measured elastic deflection was about [12] [TS] [ ].[TS] Deflection traces for both load/unload cycles were fairly linear, and the distribution of deflections was consistent with the expected plate behavior. The maximum deflection on the DFBN was [ ].[TS] After the load cycles, all deflection indications returned to zero.

The deflection indications and flatness measurements demonstrated that the PLUS7 DFBN design met the design criterion that the dimensional stability be maintained.

3.2 LOCA Load Test

The deflection traces were linear up to a load of [ ].[TS] Residual deflections after the load were from [ ].[TS]

Observation during testing and visual inspection afterwards found no indication of loss of structural integrity (e.g., unrestrained or excessive deformation, cracking) in the DFBN assembly.

4.0 Summary and Conclusion

The material deflections under load and permanent deformation after loading were characterized for load cycles to [ ]^{TS} (> 4g shipping and handling load) and [ ]^{TS} (LOCA load).
For the 4g shipping and handling load, the deflection indications and flatness measurements demonstrated that the PLUS7 DFBN design met the design criterion that the dimensional stability be maintained.

For the LOCA load, the load deflection data, flatness measurements, and test observations demonstrated that the PLUS7 DFBN met the design criterion that the structural integrity be maintained.

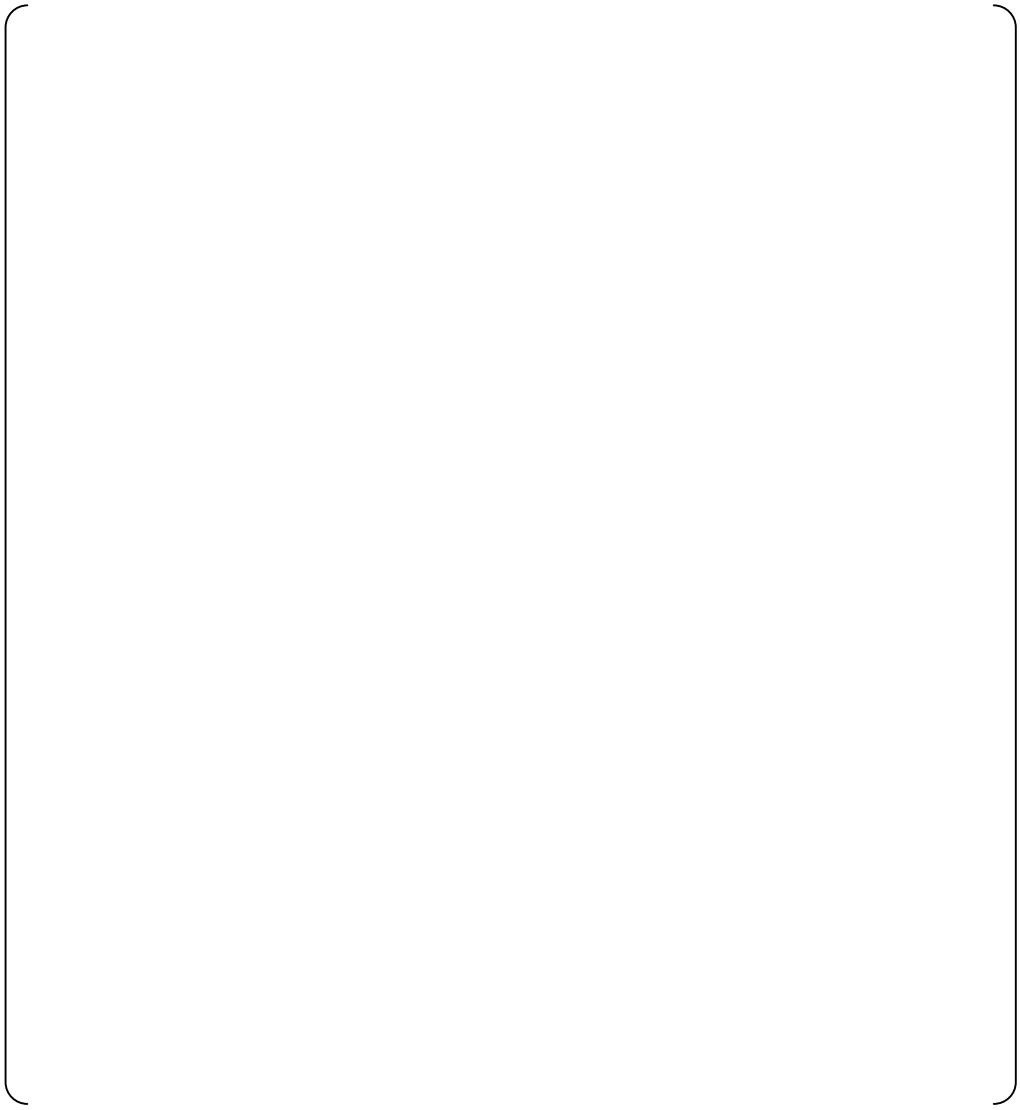

TS

Figure A.2.6-1 Shipping and Handling Load Test Setup

TS

Figure A.2.6-2 LOCA Load Test Setup

A.2.7 Grid Hang-up Test

1.0 Introduction and Objectives

The grid hang-up test was performed as part of the confirmation tests for the PLUS7 fuel assembly grid design. The objective of the test was to perform full scale testing of the PLUS7 test assembly against the same PLUS7 fuel assembly and Guardian assembly it could interact with during fuel handling.

2.0 Test Conditions

A PLUS7 mechanical test assembly was used as the stationary fuel assembly. The stationary fuel assembly was bound on the strong back positioned vertically, and movable assemblies were connected to an overhead crane in turn as shown in Figure A.2.7-1. The top and bottom nozzles of the stationary fuel assembly next to a movable fuel assembly were bound on the strong back using two belts. The movable assemblies were pushed against the stationary assembly to enforce a required side load during the test.

The procedure was to position the grids of the movable assembly between the grids of the stationary assembly, to push the movable assembly against the stationary fuel assembly to enforce the required side load, and to raise or lower the movable assembly.

The location of the stationary assembly and the movable assembly during testing and the test definition are shown in Figure A.2.7-2. During the hang-up test, the movable assembly was raised and lowered three times in 19 cases per Figure 2.7-2. The PLUS7 to PLUS7 test was performed first and the PLUS7 to Guardian test followed. The crane speed was maintained at [ ].[TS] All tests were performed in air at room temperature.

3.0 Test Results

PLUS7 vs. Guardian and PLUS7 vs. PLUS7 hang-up test revealed no irregularity during the raising or lowering of the movable assembly three times for each of the 19 cases.

4.0 Summary and Conclusion

The full scale grid hang-up tests of PLUS7-PLUS7 and PLUS7-Guardian fuel assemblies were performed for grid verification. The PLUS7 to Guardian fuel assemblies did not have any hang-up problems and the PLUS7 to PLUS7 fuel assemblies also did not have any hang-up problems.

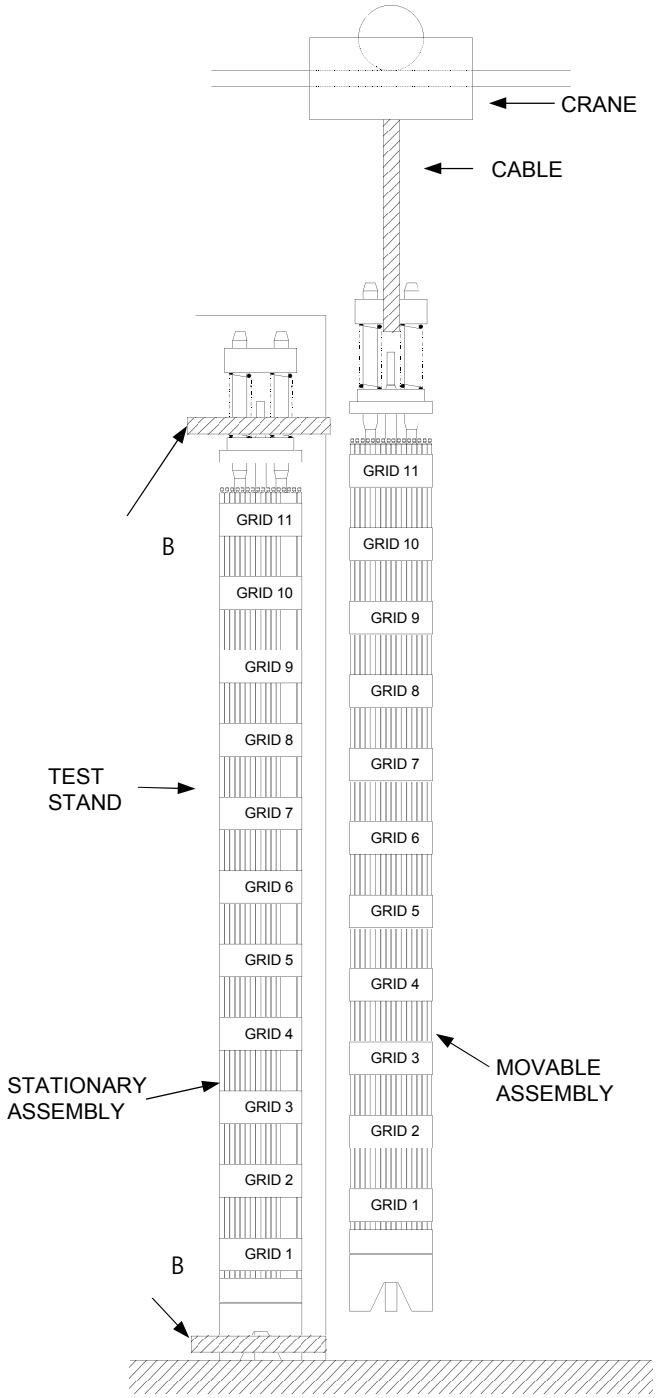

Figure A.2.7-1 Grid Hang-up Test Setup

TS

Figure A.2.7-2 Fuel Assembly Grid Hang-up Test Series

A.2.8 FACTS Hydraulic Test for PLUS7 Fuel Assembly

1.0 Introduction and Objectives

The purpose of this test is to determine the pressure loss coefficient of the PLUS7 fuel assembly. This test was performed by using the Combustion Engineering Nuclear Power (CENP) method based on the PLUS7 fuel assembly hydraulic test at the Westinghouse FACTS (Fuel Assembly Compatibility Test System).

2.0 Test Conditions and Methods

2.1 Conditions

The hydraulic tests were performed by varying the flow rate over a predetermined range at two temperatures, [ ].[TS] For the temperature of [ ], [TS] the flow ranged from [ ] [TS] to the maximum achievable flow rate ([ ][TS] for the fuel assembly with 40/20 DFBN, Debris Filter Bottom Nozzle with a [ ])[TS] with increments of [ ].[TS] At the temperature of [ ], [TS] the flow ranged from [ ] [TS] to the maximum achievable flow rate ([ ][TS] for the fuel assembly with 40/20 DFBN) with increments of [ ].[TS] Given these flow rates and temperatures, the Reynolds number values ranged from approximately [ ].[TS]

2.2 Methods

The CENP method uses the following equation to calculate the pressure loss coefficient from the measured pressure drop test data.

$$\left(\qquad \right)^{TS}$$

The resultant grid loss coefficients do not include the bare rod friction losses. The bare rod friction is predicted by the Colebrook equation shown below, assuming a [ ] [TS] rod surface roughness.

$$\left(\qquad \right)^{TS}$$

The measured pressure loss coefficients are reduced to the form:

$$\left(\qquad \right)^{TS}$$

Where, A and B are constants which describe loss coefficient (K) as a function of the Reynolds number (Re). Additionally, the adjustments on the fitted data were performed to account for geometric differences and thermal expansion effects between the test and the reactor conditions.

3.0 Test Results

The pressure loss coefficients for each fuel assembly component based on the CENP methods are as shown in Table A.2.8-1.

Table A.2.8-1 Pressure Loss Coefficients

[ ] TS

4.0 Summary and Conclusion

The FACTS test result for the PLUS7 fuel assembly was treated using the CENP method and the pressure loss coefficient for the PLUS7 fuel assembly was determined as shown in Table A.2.8-1.

A.2.9 Grid Spring Test

1.0 Introduction and Objectives

The spring tests of grids were performed to determine the cell stiffness and force values for use in the design calculations. Specifically, the objectives of these tests were to determine the load deflection characteristics and the unloading spring stiffness in the inner, outer and adjacent thimble cells of the test grids.

2.0 Test Conditions

A linear stepper motor and a strain gage equipped with an in-cell deflection measuring device (See Figures A.2.9-1and A.2.9-2) were used for cell stiffness measurement. Fuel rod sections were inserted into the grid cells surrounding the specified test cells (See Figures A.2.9-3 through A.2.9-6). A spring force/deflection measurement tool, with a motor and a motor bracket, was used to cyclically load the grid cells. The grids were tested in air at room temperature.

3.0 Test Results

The grid spring load deflection tests of the PLUS7 ZIRLO mid grid, Inconel top/bottom grids and protective grid were performed in air at room temperature. The load deflection results are shown in Table A.2.9-1 and the inner cell load deflection curves are shown in Figure A.2.9-7.

Dashed vertical lines indicating nominal, maximum and minimum deflections are overlaid on the graph and reflect the expected range of deflections due to the manufacturing tolerance. Spring unloading curves are also shown for the adjacent minimum, nominal and maximum spring deflection values. Since some deflection for the grid cell is in the elastic range, its unloading curve follows the deflection curve.

4.0 Summary and Conclusion

The load deflection results for each grid are shown in Table A.2.9-1 and the load deflection curves are shown in Figure A.2.9-7.

Table A.2.9-1 Summary of Grid Spring Load Deflection Test Results

TS

Figure A.2.9-1 Spring Test Apparatus Setup

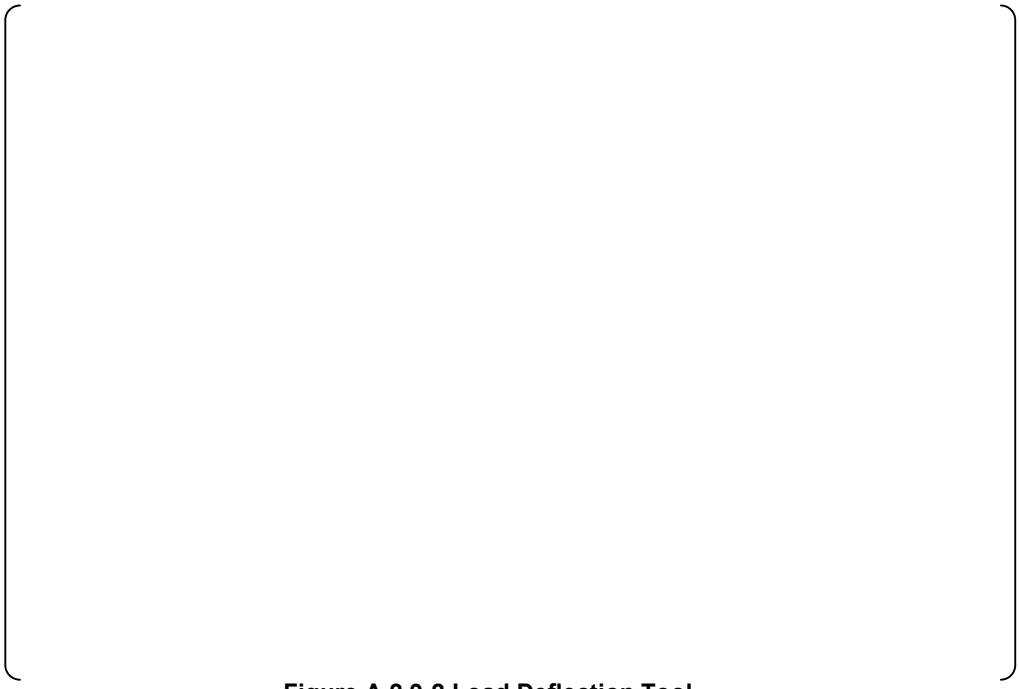

TS

Figure A.2.9-2 Load Deflection Tool

TS

Figure A.2.9-3 ZIRLO Mid Grid Test Locations (Bottom View)

Figure A.2.9-4 Inconel Top Grid Test Locations (Bottom View)

TS

Figure A.2.9-5 Inconel Bottom Grid Test Locations (Top View)

Figure A.2.9-6 Protective Grid Test Locations (Bottom View)

Figure A.2.9-7 ZIRLO Mid and Inconel Top/Bottom/Protective Grid Inner Cell Load Deflection

A.2.10 FACTS Lift-off Test for the PLUS7 Fuel Assembly

1.0 Introduction and Objectives

The objective of the lift-off tests of the PLUS7 fuel assembly is to determine the flow rates at which the fuel assembly lifts off under specified temperatures and holddown spring compressions. The test was performed with the Fuel Assembly Compatibility Test System (FACTS) as shown in Figure A.2.10-1 for the PLUS7 fuel assembly design with 40/20 ([ ] [ ]) Debris Filter Bottom Nozzle (DFBN).

2.0 Test Conditions

To ensure that the fuel assembly would lift off during the tests, the holddown springs were compressed by [ ]. The lift-off tests were performed by increasing the flow rate from [ ] [ ] with increments of [ ]. When the flow rate reached [ ], the flow increased with an increment of [ ] for a better estimate of the flow rate that could lift off the fuel assembly.

Two uni-axial accelerometers were mounted on the base of the pressure vessel to monitor the output impact signal. The output from the accelerometers was amplified and monitored through an oscilloscope and a visicorder.

Table A.2.10-1 Fuel Assembly and Specifications

Component Descriptions	
Top Grid Material	Inconel 718
Protective Grid Material	Inconel 718
Bottom Grid Material	Inconel 718
Protective Grid Inner Strap Heights	[ ]
Bottom Grid Inner Strap Heights	[ ]
Top Grid Inner Strap Heights	[ ]
Mid Grid Material	ZIRLO
Number of Mid grids	9
Mid Grid Inner Strap Heights	[ ]
Number of Rods	236
Rod OD	[ ]
Test Rod Length	[ ]
Number of Guide Thimble	4
Diameter of Guide Thimble Tubes	[ ]
Number of Instrument Tube	1
Diameter of Instrument Tube	[ ]
Dashpot Elevation (Top of Thimble Tube Smaller OD Elevation)	[ ]
Rod-to-Bottom Nozzle Gap	[ ]
Thimble Tube Plugging Device	None. However the flow is blocked by the standoff tubes
Test Condition	

3.0 Test Results

The flow rates required to lift off the PLUS7 fuel assembly with a 40/20 DFBN at temperatures of [ ]^{TS} were determined from the lift-off test. It was expected from similar tests that the fuel assembly would lift off at a flow rate higher than [ ].^{TS} No noticeable signal related to the assembly lift-off was detected until the flow rate reached [ ].^{TS} The first noticeable accelerometer signal was detected at the flow rate of [ ]^{TS} and above this flow rate the signals became more noticeable. To find out the exact flow rate of the lift-off, the tests were performed with several different flow rates around the flow rate at which the first signal was detected. It was confirmed that the fuel assembly began to lift off at [ ].^{TS}

The same test procedure was followed for [ ]^{TS} case and the results confirmed that at a temperature of [ ]^{TS} the fuel assembly was lifted off at [ ].^{TS} The test results are summarized in Table A.2.10-3. Figures A.2.10-2 and A.2.10-3 show the inlet loss coefficients and outlet loss coefficients versus the flow rate, respectively. In these figures, a sudden change in the slope of the loss coefficients indicates a lift-off.

Table A.2.10-2 Results of the Lift-off Tests Based on the Accelerometer Indications

( ) ^{TS}

4.0 Summary and Conclusion

The FACTS lift-off tests confirmed that the PLUS7 fuel assembly with a holddown spring compression of [ ]^{TS} was lifted off at the flow rates of [ ]^{TS} at temperatures of [ ],^{TS} respectively.

TS

Figure A.2.10-1 FACTS Flow Diagram

TS

Figure A.2.10-2 K11 (inlet) from The Lift-off Test

TS

Figure A.2.10-3 K8 (outlet) from The Lift-off Test

A.3.0 CONCLUSION

Hydraulic and Mechanical tests of the PLUS7 fuel assembly were conducted to verify their out-of-pile performance. All the tests were performed to ensure that the system met all the design criteria.

Appendix B

Commercial Operating Experience of KEPCO NF PWR Fuels

November 2012

TABLE OF CONTENTS

LIST OF TABLES

B.1.0 COMMERCIAL OPERATING EXPERIENCE OF KEPCO NF PWR FUEL

In Korea, the first nuclear power plant, Kori unit-1 (PWR), began commercial operation in April 1978. Currently there are 17 PWRs and four PHWRs in operation in Korea. KEPCO Nuclear Fuel (KNF) was established in 1982 and started to supply PWR and PHWR fuels from 1989 and 1997, respectively. PWR fuels supplied by KNF are as follows:

(1) 14x14 Fuel for Kori Unit 1

Kori unit 1 uses the fuel with a 14x14 lattice configuration and KNF has supplied this type of fuel assemblies since the 11th cycle of the unit as shown in Table B.1-1.

Table B.1-1 Fuel Supplied by KNF for Kori Unit 1

Cycle	Date	Fuel Type	FAs	FRs	Clad Material
11	91/01 ~ 92/01	KOFA	48	8,592	Zry-4
12	92/03 ~ 93/05	KOFA	48	8,592	Zry-4
13	93/07 ~ 94/07	KOFA	44	7,876	Zry-4
14	94/09 ~ 96/01	KOFA	44	7,876	Zry-4
15	96/04 ~ 97/03	KOFA	44	7,876	Zry-4
16	97/07 ~ 98/06	KNF-OFA	52	9,308	Zry-4 (W)*
17	98/09 ~ 99/09	KNF-OFA	40	7,160	Zry-4 (W)
18	99/11 ~ 00/10	KNF-OFA	40	7,160	Zry-4 (S)**
19	00/11 ~ 01/11	KNF-OFA	40	7,160	Zry-4 (Z)***
20	01/12 ~ 03/01	KNF-OFA	40	7,160	Zry-4 (Z)
21	03/02 ~ 04/02	KNF-OFA	40	7,160	Zry-4 (Z)
22	04/03 ~ 05/03	KNF-OFA	40	7,160	Zry-4 (Z)
23	05/05 ~ 06/05	KNF-OFA	40	7,160	Zry-4 (Z)
24	06/06 ~ 07/06	KNF-OFA	40	7,160	Zry-4 (Z)
25	08/01 ~ 08/11	KNF-OFA	40	7,160	Zry-4 (Z)
26	08/12 ~ 09/12	KNF-OFA	41	7,339	Zry-4 (Z)
27	10/01 ~ 11/01	KNF-OFA	41	7,339	Zry-4 (Z)
28	11/02 ~ 12/02	KNF-OFA	41	7,339	KNF ZIRLO
29	12/02 ~ 13/03	KNF-OFA	45	8,055	KNF ZIRLO
Total	**91/01 ~ 13/03**	**-**	**808**	**144,632**	**-**

* : Westinghouse – Imp. Zry-4, ** : ANF – PCA-2a
*** : CEZUS – AFA-2G

(2) 16x16 Fuel for Kori Unit 2

Kori unit 2 uses the fuel with a 16x16 lattice configuration and KNF has supplied this type of fuel assemblies since the 7th cycle of the unit as shown in Table B.1-2.

Table B.1-2 Fuel Supplied by KNF for Kori Unit 2

Cycle	Date	Fuel Type	FAs	FRs	Clad Material
7	90/03 ~ 91/04	KOFA	48	11,280	Zry-4
8	91/05 ~ 92/05	KOFA	48	11,280	Zry-4
9	92/07 ~ 93/09	KOFA	50	12,220	Zry-4
12	96/02 ~ 97/02	KNF-STD	44	10,340	Zry-4 (W)*
13	97/04 ~ 98/02	KNF-STD	36	8,460	Zry-4 (W)
14	98/03 ~ 99/03	KNF-STD	44	10,340	Zry-4 (W)
15	99/05 ~ 00/05	KNF-STD	44	10,340	Zry-4 (S)**
16	00/07 ~ 01/05	KNF-STD	40	9,400	Zry-4 (Z)***
17	01/07 ~ 02/08	KNF-STD	48	11,280	Zry-4 (Z)
18	02/09 ~ 03/10	KNF-STD	48	11,280	Zry-4 (Z)
19	03/11 ~ 04/12	KNF-STD	48	11,280	Zry-4 (Z)
20	05/01 ~ 06/02	KNF-STD	40	9,400	Zry-4 (Z)
		16ACE7 (LTA)	4	940	ZIRLO****
21	06/03 ~ 07/04	KNF-STD	52	12,220	Zry-4 (Z)
22	07/05 ~ 08/05	KNF-STD	40	9,400	Zry-4 (Z)
23	08/07 ~ 09/09	16ACE7	48	11,280	ZIRLO
24	09/09 ~ 10/10	16ACE7	48	11,280	ZIRLO
25	10/11 ~ 12/03	16ACE7	56	13,160	KNF ZIRLO
26	12/04 ~ 13/05	16ACE7	40	9,400	KNF ZIRLO
Total	**90/03 ~ 13/05**	**-**	**826**	**194,580**	**-**

* : Westinghouse – Imp. Zry-4, ** : ANF – PCA-2a
*** : CEZUS – AFA-2G, **** : Westinghouse

(3) 17x17 Fuel

Fuel with a 17x17 lattice configuration is used for Kori units 3&4, Yonggwang units 1&2 and Ulchin units 1&2, and the fuels of this type supplied by KNF are shown in Tables B.1-3 through B.1-8.

Table B.1-3 Fuel Supplied by KNF for Kori Unit 3

Cycle	Date	Fuel Type	FAs	FRs	Clad Material
5	90/01 ~ 90/12	KOFA	56	14,784	Zry-4
6	91/02 ~ 91/12	KOFA	48	12,672	Zry-4
7	92/02 ~ 92/12	KOFA	48	12,672	Zry-4
8	93/02 ~ 94/03	KOFA	64	16,896	Zry-4
11	97/04 ~ 98/05	KNF-V5H	56	14,784	Zry-4 (W)*
12	98/07 ~ 99/11	KNF-V5H	64	16,896	Zry-4 (W)
13	00/01 ~ 01/03	KNF-V5H	60	15,840	Zry-4 (S)**
14	01/04 ~ 02/09	KNF-V5H	68	17,952	Zry-4 (Z)***
15	02/10 ~ 04/01	KNF-V5H	60	15,840	ZIRLO****
16	04/03 ~ 05/06	KNF-RFA	60	15,840	ZIRLO
17	05/07 ~ 06/11	KNF-RFA	60	15,840	ZIRLO
		17ACE7 (LTA)	4	1,056	ZIRLO
18	07/01 ~ 08/04	KNF-RFA	64	16,896	ZIRLO
19	08/05 ~ 09/10	KNF-RFA	68	17,952	ZIRLO
20	09/12 ~ 11/04	17ACE7	68	17,952	ZIRLO
21	11/05 ~ 12/09	17ACE7	68	17,952	KNF ZIRLO
22	12/10 ~ 14/01	17ACE7	65	17,160	KNF ZIRLO
Total	**90/01 ~ 14/01**	**-**	**981**	**258,984**	**-**

* : Westinghouse – Imp. Zry-4, ** : ANF – PCA-2a
*** : CEZUS – AFA-2G, **** : Westinghouse

Table B.1-4 Fuel Supplied by KNF for Kori Unit 4

Cycle	Date	Fuel Type	FAs	FRs	Clad Material
5	90/07 ~ 91/04	KOFA	44	11,616	Zry-4
6	91/05 ~ 92/04	KOFA	48	12,672	Zry-4
7	92/06 ~ 93/07	KOFA	64	16,896	Zry-4
8	93/09 ~ 94/12	KOFA	76	20,064	Zry-4
10	96/06 ~ 97/09	KNF-V5H	60	15,840	Zry-4 (W)*
11	97/11 ~ 99/01	KNF-V5H	60	15,840	Zry-4 (W)
12	99/03 ~ 00/07	KNF-V5H	68	17,952	Zry-4 (W)
13	00/09 ~ 01/11	KNF-V5H	60	15,840	Zry-4 (Z)**
14	01/12 ~ 03/04	KNF-V5H	60	15,840	Zry-4 (Z)
15	03/05 ~ 04/09	KNF-V5H	60	15,840	ZIRLO***
16	04/10 ~ 06/02	KNF-RFA	64	16,896	ZIRLO

17	06/04 ~ 07/06	KNF-RFA	64	16,896	ZIRLO
18	07/08 ~ 08/12	KNF-RFA	64	16,896	ZIRLO
19	09/02 ~ 10/05	17ACE7	64	16,896	ZIRLO
20	10/06 ~ 11/09	17ACE7	64	16,896	KNF ZIRLO
21	11/10 ~ 13/01	17ACE7	65	17,160	KNF ZIRLO
Total	**90/07 ~ 13/01**	**-**	**985**	**260,040**	**-**

* : Westinghouse – Imp. Zry-4, ** : CEZUS – AFA-2G
*** : Westinghouse

Table B.1-5 Fuel Supplied by KNF for Yonggwang Unit 1

Cycle	Date	Fuel Type	FAs	FRs	Clad Material
5	90/10 ~ 91/08	KOFA	52	13,728	Zry-4
6	91/10 ~ 92/08	KOFA	48	12,672	Zry-4
7	92/10 ~ 93/11	KOFA	64	16,896	Zry-4
8	93/12 ~ 95/03	KOFA	76	20,064	Zry-4
9	95/06 ~ 96/09	KOFA	76	20,064	Zry-4 (W)*
10	96/11 ~ 98/01	KNF-V5H	60	15,840	Zry-4 (W)
11	98/03 ~ 99/06	KNF-V5H	60	15,840	Zry-4 (W)
12	99/08 ~ 00/10	KNF-V5H	60	15,840	Zry-4 (W)
13	00/11 ~ 02/02	KNF-V5H	60	15,840	Zry-4 (Z)**
14	02/03 ~ 03/05	KNF-V5H	56	14,784	ZIRLO***
15	03/06 ~ 04/10	KNF-V5H	60	15,840	ZIRLO
16	04/11 ~ 06/03	KNF-RFA	60	15,840	ZIRLO
17	06/04 ~ 07/09	KNF-RFA	64	16,896	ZIRLO
18	07/10 ~ 09/03	KNF-RFA	64	16,896	ZIRLO
19	09/04 ~ 10/09	KNF-RFA	68	17,952	ZIRLO
20	10/10 ~ 12/02	17ACE7	68	17,952	KNF ZIRLO
21	12/03 ~13/08	17ACE7	69	18,216	KNF ZIRLO
Total	**90/10 ~ 13/08**	**-**	**1,065**	**281,160**	**-**

* : Westinghouse – Imp. Zry-4, ** : CEZUS – AFA-2G
*** : Westinghouse

Table B.1-6 Fuel Supplied by KNF for Yonggwang Unit 2

Cycle	Date	Fuel Type	FAs	FRs	Clad Material
4	90/06 ~ 91/02	KOFA	48	12,672	Zry-4
5	91/04 ~ 92/03	KOFA	48	12,672	Zry-4
6	92/05 ~ 93/03	KOFA	48	12,672	Zry-4
7	93/04 ~ 94/05	KOFA	64	16,896	Zry-4
10	97/05 ~ 98/09	KNF-V5H	64	16,896	Zry-4 (W)*
11	98/12 ~ 00/04	KNF-V5H	60	15,840	Zry-4 (W)

12	00/05 ~ 01/09	KNF-V5H	60	15,840	Zry-4 (S)**
13	01/10 ~ 03/01	KNF-V5H	60	15,840	ZIRLO***
14	03/02 ~ 04/05	KNF-V5H	56	14,784	ZIRLO
15	04/07 ~ 05/11	KNF-RFA	60	15,840	ZIRLO
16	05/12 ~ 07/04	KNF-RFA	64	16,896	ZIRLO
17	07/05 ~ 08/09	KNF-RFA	64	16,896	ZIRLO
18	08/10 ~ 10/03	KNF-RFA	64	16,896	ZIRLO
19	10/04 ~ 11/08	17ACE7	68	17,952	ZIRLO
20	11/10 ~ 13/01	17ACE7	65	17,160	KNF ZIRLO
Total	**90/06 ~ 13/01**	**-**	**893**	**235,752**	**-**

* : Westinghouse – Imp. Zry-4, ** : ANF – PCA-2a
*** : Westinghouse

Table B.1-7 Fuel Supplied by KNF for Ulchin Unit 1

Cycle	Date	Fuel Type	FAs	FRs	Clad Material
3	91/01 ~ 92/02	KOFA	48	12,672	Zry-4
4	92/04 ~ 93/02	KOFA	44	11,616	Zry-4
5	93/03 ~ 94/01	KOFA	44	11,616	Zry-4
6	94/03 ~ 95/03	KOFA	64	16,896	Zry-4
7	95/05 ~ 96/04	KOFA	56	14,784	Zry-4
8	96/06 ~ 97/10	KNF-V5H	60	15,840	Zry-4 (W)*
9	97/12 ~ 98/12	KNF-V5H	56	14,784	Zry-4 (W)
10	99/02 ~ 00/06	KNF-V5H	60	15,840	Zry-4 (W)
11	00/08 ~ 01/10	KNF-V5H	60	15,840	Zry-4 (Z)**
12	01/10 ~ 03/05	KNF-V5H	64	16,896	ZIRLO***
13	03/07 ~ 04/10	KNF-V5H	60	15,840	ZIRLO
14	04/11 ~ 06/04	KNF-RFA	56	14,784	ZIRLO
15	06/05 ~ 07/09	KNF-RFA	64	16,896	ZIRLO
16	07/10 ~ 09/02	KNF-RFA	64	16,896	ZIRLO
17	09/03 ~ 10/08	KNF-RFA	68	17,952	ZIRLO
18	10/10 ~ 12/02	KNF-RFA	68	17,952	ZIRLO
19	12/05 ~ 13/09	17ACE7	65	17,160	KNF ZIRLO
Total	**91/01 ~ 13/09**	**-**	**1,001**	**264,264**	**-**

* : Westinghouse – Imp. Zry-4, ** : CEZUS – AFA-2G
*** : Westinghouse

Table B.1-8 Fuel Supplied by KNF for Ulchin Unit 2

Cycle	Date	Fuel Type	FAs	FRs	Clad Material
2	90/11 ~ 91/10	KOFA	44	11,616	Zry-4
3	91/12 ~ 92/11	KOFA	48	12,672	Zry-4

4	92/12 ~ 93/10	KOFA	48	12,672	Zry-4
5	93/11 ~ 94/09	KOFA	48	12,672	Zry-4
6	94/11 ~ 95/12	KOFA	64	16,896	Zry-4
7	96/01 ~ 97/04	KOFA	76	20,064	Zry-4
8	97/06 ~ 98/08	KNF-V5H	60	15,840	Zry-4 (W)*
9	98/10 ~ 00/01	KNF-V5H	60	15,840	Zry-4 (W)
10	00/03 ~ 01/05	KNF-V5H	60	15,840	Zry-4 (S)**
11	01/06 ~ 02/09	KNF-V5H	60	15,840	Zry-4 (Z)***
12	02/11 ~ 04/05	KNF-V5H	64	16,896	ZIRLO****
13	04/06 ~ 05/10	KNF-RFA	60	15,840	ZIRLO
14	05/12 ~ 07/04	KNF-RFA	64	16,896	ZIRLO
15	07/05 ~ 08/09	KNF-RFA	64	16,896	ZIRLO
16	08/10 ~ 10/03	KNF-RFA	64	16,896	ZIRLO
17	10/04 ~ 11/09	KNF-RFA	68	17,952	KNF ZIRLO
18	11/11 ~ 13/04	17ACE7	65	17,160	KNF ZIRLO
Total	**90/11 ~ 13/04**	**-**	**1017**	**268,488**	**-**
* : Westinghouse – Imp. Zry-4, ** : ANF – PCA-2a, *** : CEZUS – AFA-2G, **** : Westinghouse					

(4) 16x16 Fuel for OPR1000

Fuel with a 16x16 lattice configuration is used for OPR1000's including Yonggwang units 3 through 6, Ulchin units 3 through 6 and Shin-Kori unit 1. The fuels of this type supplied by KNF are shown in Tables B.1-9 through B.1-17.

Table B.1-9 Fuel Supplied by KNF for Yonggwang Unit 3

Cycle	Date	Fuel Type	FAs	FRs	Clad Material
1	94/10 ~ 96/02	KSFA	177	41,772	OPTIN*
2	96/04 ~ 97/02	KSFA	48	11,328	OPTIN
3	97/05 ~ 98/03	KSFA	60	14,160	OPTIN
5	99/07 ~ 00/09	KSFA	64	15,104	OPTIN
6	00/11 ~ 02/03	KSFA	64	16,896	OPTIN
7	02/04 ~ 03/05	K-Guardian	56	13,216	ZIRLO**
8	03/06 ~ 04/10	K-Guardian	60	14,160	ZIRLO
9	04/11 ~ 06/01	K-Guardian	60	14,160	ZIRLO
10	06/02 ~ 07/04	K-Guardian	64	15,104	ZIRLO
11	07/06 ~ 08/10	PLUS7	64	15,104	ZIRLO
12	08/11 ~ 10/02	PLUS7	64	15,104	ZIRLO
13	10/03 ~ 11/05	PLUS7	60	14,160	KNF ZIRLO
14	11/07 ~ 12/10	PLUS7	69	16,284	KNF ZIRLO
Total	**94/10 ~ 12/10**	**-**	**910**	**216,552**	**-**

* : Maunfactured by SANDVIK, ** : ZIRLO manufactured by Westinghouse
*** : ZIRLO manufactured by KNF

Table B.1-10 Fuel Supplied by KNF for Yonggwang Unit 4

Cycle	Date	Fuel Type	FAs	FRs	Clad Material
1	95/07 ~ 96/11	KSFA	177	41,772	OPTIN*
2	97/01 ~ 97/10	KSFA	48	11,328	OPTIN
4	99/02 ~ 00/02	KSFA	56	13,216	OPTIN
5	00/03 ~ 01/05	KSFA	56	13,216	OPTIN
6	01/06 ~ 02/10	K-Guardian	60	14,160	ZIRLO**
7	02/11 ~ 04/04	K-Guardian	72	16,992	ZIRLO
8	04/05 ~ 05/08	K-Guardian	64	15,104	ZIRLO
9	05/09 ~ 07/01	K-Guardian	60	14,160	ZIRLO
10	07/02 ~ 08/05	PLUS7	64	15,104	ZIRLO
11	08/06 ~ 09/10	PLUS7	64	15,104	ZIRLO
12	09/11 ~ 11/01	PLUS7	64	15,104	M5***
13	11/03 ~ 12/06	PLUS7	64	15,104	KNF ZIRLO
14	12/07 ~ 13/10	PLUS7	64	15,104	KNF ZIRLO
Total	**95/07 ~ 13/10**	**-**	**913**	**215,468**	**-**

* : SANDVIK, ** : Westinghouse, *** : CEZUS

Table B.1-11 Fuel Supplied by KNF for Yonggwang Unit 5

Cycle	Date	Fuel Type	FAs	FRs	Clad Material
1	02/04 ~ 03/03	KSFA	177	41,772	OPTIN*
2	03/05 ~ 04/01	K-Guardian	48	11,328	ZIRLO**
3	04/04 ~ 05/05	K-Guardian	64	15,104	ZIRLO
4	05/06 ~ 06/11	KSFA	4	944	OPTIN
		K-Guardian	60	14,160	ZIRLO
5	06/12 ~ 08/04	PLUS7	68	16,048	ZIRLO
6	08/05 ~ 09/08	PLUS7	64	15,104	ZIRLO
7	09/09 ~ 10/12	PLUS7	64	15,104	M5***
8	11/01 ~ 12/04	PLUS7	64	15,104	KNF ZIRLO, HANA-4, 6
9	12/05 ~ 13/09	PLUS7	69	16,284	KNF ZIRLO
Total	**02/04 ~ 13/09**	**-**	**682**	**160,952**	**-**
* : SANDVIK, ** : Westinghouse, *** : CEZUS					

Table B.1-12 Fuel Supplied by KNF for Yonggwang Unit 6

Cycle	Date	Fuel Type	FAs	FRs	Clad Material
1	02/12 ~ 03/11	KSFA	177	41,772	OPTIN*
2	04/04 ~ 05/01	K-Guardian	48	11,328	ZIRLO**
3	05/02 ~ 06/02	K-Guardian	64	15,104	ZIRLO
4	06/03 ~ 07/07	K-Guardian	64	15,104	ZIRLO
5	07/07 ~ 08/11	PLUS7	64	15,104	ZIRLO
6	08/12 ~ 10/03	PLUS7	64	15,104	ZIRLO
7	10/04 ~ 11/06	PLUS7	60	14,160	KNF ZIRLO
8	11/07 ~ 12/11	PLUS7	69	16,284	KNF ZIRLO
Total	**02/12 ~ 12/11**	**-**	**610**	**143,960**	**-**
* : SANDVIK, ** : Westinghouse					

Table B.1-13 Fuel Supplied by KNF for Ulchin Unit 3

Cycle	Date	Fuel Type	FAs	FRs	Clad Material
1	98/01 ~ 99/06	KSFA	177	41,772	OPTIN*
2	99/08 ~ 00/05	KSFA	48	11,328	OPTIN
3	00/07 ~ 01/07	KSFA	64	15,104	OPTIN
4	01/07 ~ 02/11	KSFA	64	15,104	ZIRLO**
5	02/12 ~ 04/04	K-Guardian	60	14,160	ZIRLO
		PLUS7	4	944	ZIRLO
6	04/05 ~ 05/09	K-Guardian	68	16,048	ZIRLO
7	05/10 ~ 07/01	K-Guardian	68	16,048	ZIRLO

8	07/03 ~ 08/07	PLUS7	64	15,104	ZIRLO
9	08/07 ~ 09/10	PLUS7	64	15,104	ZIRLO
10	09/11 ~ 11/02	PLUS7	64	15,104	M5***
11	11/03 ~ 12/06	PLUS7	64	15,104	KNF ZIRLO
12	12/07 ~ 13/11	PLUS7	69	16,284	KNF ZIRLO
Total	**98/01 ~ 13/11**	**-**	**878**	**207,208**	**-**
* : SANDVIK, ** : Westinghouse, *** : CEZUS					

Table B.1-14 Fuel Supplied by KNF for Ulchin Unit 4

Cycle	Date	Fuel Type	FAs	FRs	Clad Material
1	98/10 ~ 00/03	KSFA	177	41,772	OPTIN*
2	00/05 ~ 01/02	KSFA	48	11,328	OPTIN
3	01/03 ~ 02/04	KSFA	64	15,104	OPTIN
4	02/05 ~ 03/08	K-Guardian	60	14,160	ZIRLO**
5	03/09 ~ 05/01	K-Guardian	68	16,048	ZIRLO
6	05/02 ~ 06/05	K-Guardian	68	16,048	ZIRLO
7	06/06 ~ 07/09	PLUS7	64	15,104	ZIRLO
8	07/11 ~ 09/02	PLUS7	64	15,104	ZIRLO
9	09/02 ~ 10/05	PLUS7	64	15,104	M5***
10	10/06 ~ 11/09	PLUS7	64	15,104	M5, KNF ZIRLO
11	12/04 ~ 13/07	PLUS7	69	16,284	KNF ZIRLO
Total	**98/10 ~ 13/07**	**-**	**810**	**191,160**	**-**
* : SANDVIK, ** : Westinghouse, *** : CEZUS					

Table B.1-15 Fuel Supplied by KNF for Ulchin Unit 5

Cycle	Date	Fuel Type	FAs	FRs	Clad Material
1	03/12 ~ 05/06	K-Guardian	177	41,772	ZIRLO*
2	05/08 ~ 06/09	K-Guardian	60	14,160	ZIRLO
3	06/10 ~ 07/11	K-Guardian	64	15,104	ZIRLO
4	07/12 ~ 09/05	PLUS7	60	14,160	ZIRLO
5	09/05 ~ 10/09	PLUS7	60	14,160	M5**
			4	944	ZIRLO
6	10/10 ~ 11/12	PLUS7	60	14,160	KNF ZIRLO
7	11/12 ~ 13/05	PLUS7	69	16,284	KNF ZIRLO
Total	**03/12 ~ 13/05**	**-**	**554**	**130,744**	**-**
* : Westinghouse, ** : CEZUS					

Table B.1-16 Fuel Supplied by KNF for Ulchin Unit 6

Cycle	Date	Fuel Type	FAs	FRs	Clad Material

1	04/11 ~ 06/03	K-Guardian	177	41,772	ZIRLO*
2	06/05 ~ 07/06	K-Guardian	60	14,160	ZIRLO
3	07/06 ~ 08/09	PLUS7	64	15,104	ZIRLO
4	08/10 ~ 10/02	PLUS7	64	15,104	ZIRLO
5	10/03 ~ 11/06	PLUS7	64	15,104	KNF ZIRLO
6	11/06 ~ 12/10	PLUS7	61	14,396	KNF ZIRLO
		HIPER	8	1,888	KNF ZIRLO, HANA-6
Total	**04/11 ~ 12/10**	**-**	**498**	**117,528**	**-**
* : Westinghouse					

Table B.1-17 Fuel Supplied by KNF for Shin-Kori Unit 1

Cycle	Date	Fuel Type	FAs	FRs	Clad Material
1	10/07 ~ 12/01	K-Guardian	177	41,772	ZIRLO*
2	12/02 ~ 13/03	PLUS7	60	14,160	KNF ZIRLO
Total	**10/17 ~ 13/03**	**-**	**237**	**55,932**	**-**
* : Westinghouse					

Appendix C

PLUS7 Scram Data Verification

November 2012

TABLE OF CONTENTS

LIST OF TABLES

LIST OF FIGURES

C.1.0 PURPOSE

The purpose of this analysis is to verify that the CEA (Control Element Assembly) SCRAM analysis provides reasonable and conservative predictions of the CEA insertion time for the 90% insertion criterion during reactor operating conditions.

C.2.0 INTRODUCTION

The SCRAM analysis was developed to describe the CEA position, velocity and acceleration as a function of time and applicable reactor geometry during the rapid insertion of the CEAs into the reactor core to obtain a reactor “shutdown” condition.

C.3.0 DESIGN CRITERIA

Both full and part strength CEAs must be capable of traveling from a fully withdrawn position to the 90% insertion position within the time limits (4.0 seconds) as shown in Figure C.3-1. This criterion assures that the CEAs can be reliably inserted to shut down the reactor within the time limits.

TS

Figure C.3-1 CEA Position Requirements during Reactor Scram

C.4.0 VERIFICATION

Emphasis in this verification analysis is primarily directed towards comparison of the predicted insertion times with the actual test data. SCRAM analysis data were based on the OPR1000 plants loaded with PLUS7 fuel assemblies and the actual test data were collected at YGN-5 (an OPR 1000 plant) Cycle7 with PLUS7 full core as shown in Table C.4-2 and Figure C.4-3.

As indicated in Table C.4-1, Figure C.4-1 and Figure C.4-2 below, the actual test data do not exceed the data predicted from the SCRAM analysis. Therefore, it can be generally concluded that the SCRAM analysis provides a reasonably conservative prediction on the 90% insertion time.

TS

Figure C.4-1 Distribution of Actual Test Data

Table C.4-1 Summary of CEA Actual Test Data

TS

TS

Figure C.4-2 Histogram of Actual Test Data

TS

Figure C.4-3 Actual Test Raw Data from YGN-5

Table C.4-2 Actual Test Data (CEA Types)

TS

C.5.0 CONCLUSION

The results of the analysis show that the SCRAM analysis provides reasonably conservative predictions of the CEA insertion time for the 90% insertion criterion, compared with the actual test data from an operating plant.

Appendix D

PLUS7 Wear Performance Analysis

November 2012

TABLE OF CONTENTS

LIST OF FIGURES

D.1.0 INTRODUCTION

PLUS7 mid grids introduced conformal springs and dimples in order to minimize damage to fuel rods caused by fretting wear. A long-term wear test was performed to evaluate the fuel rod wear performance of PLUS7 grids that have area contact with fuel rods. The cells of the grids were adjusted to have some gaps between them and the fuel rods, and the wear test was performed for 500 hours in the VIPER (Vibration Investigation and Pressure-drop Experimental Research) hydraulic test facility of Westinghouse Co. in the USA. Based on the wear scar data from the wear test, fuel rods, springs, and dimples were modeled using the Solidworks to calculate wear volumes relative to wear depths. The required time to reach the critical wear volume which is related to its wear depth was predicted.

The cladding wear evaluation is summarized as follows:

(1) Out-of-pile tests

- Results of the VIPER long-term wear tests (See Appendix A.2.3)

  - All fretting wear scars of the PLUS7 assembly were measured using the Accumeasure System 9000 tool to determine the fretting wear depth.
  - No measurable wear scars were found in the pre-oxidized rods.

(2) Analysis

- Wear volume-to-depth calculations

  - Fretting wear performance was evaluated by wear mark inspection.
  - Analytical calculation based on geometric configuration.

D.2.0 TEST CRITERIA

Fuel rod wear of the test assembly, projected using the standard linear wear volume extrapolation, should not exceed a depth of [ ]. [TS]

- The depth of [ ][TS] clad thickness is conservatively calculated considering fuel failure.

D.3.0 WEAR CALCULATION AND EVALUATION

The measurable wear scars were extrapolated to the critical volume (at [ ][TS]clad thickness) appropriate for the grid support feature. This extrapolation assumed that the wear rate determined from the VIPER wear scars would be constant throughout the life of the assembly. This relative fretting performance of assembly grid designs were compared in the days to the critical wear volume. With a constant work rate, the following relationship exists:

$$\frac{\text{Days to Critical Wear Volume}}{\text{Critical Wear Volume}} = \frac{\left(500/24\right)\ \text{days}}{\text{Wear Volume at } \left(500/24\right)\text{days}}$$

Therefore, the days to the critical wear volume for each spring and dimple wear scar can be calculated by the following.

$$\text{Days to Critical Wear Volume} = \text{Critical Wear Volume} \times \frac{\left(500/24\right)\ \text{days}}{\text{Wear Volume at } \left(500/24\right)\text{days}}$$

For a 0.374 inch diameter fuel rod, with the [ ][TS] nominal cladding thickness, the critical wear volume occurs at a wear depth equal to [ ][TS]([ ][TS] of the nominal cladding thickness).

D.4.0 CONCLUSION

- Since all oxidized rods had no measurable wear, the PLUS7 test assembly met the design criteria. Fretting wear did not occur when a realistic [ ] [TS] gap existed between fuel rods and grids.

- Figure D.4-1 shows the days to the critical wear volume relative to wear depths that occurred during 500 hours of non-oxidized fuel rod. The conservatively evaluated time for the first fuel rod to reach the initial critical volume is [ ].[TS] Thus the PLUS7 test assembly meets the internal design criteria.

TS

Figure D.4-1 Days to the Critical Wear Volume Relative to Wear Depths